British Geological Survey
NATURAL ENVIRONMENT RESEARCH COUNCIL

Micromorphology of the Quaternary sediments from the Solway area, Southern Uplands, Scotland

Integrated Geological Survey (North)

Internal Report IR/02/140

BRITISH GEOLOGICAL SURVEY

INTERNAL REPORT IR/02/140

Micromorphology of the Quaternary sediments from the Solway area, Southern Uplands, Scotland

Dr Emrys Phillips

Key words

Micromorphology, Quaternary sediments, Solway area, Scotland.

Bibliographical reference

E. R. PHILLIPS. 2002. Micromorphology of the Quaternary sediments from the Solway area, Southern Uplands, Scotland. *British Geological Survey Internal Report*, IR/02/140. 42pp.

Keyworth, Nottingham British Geological Survey 2002

BRITISH GEOLOGICAL SURVEY

The full range of Survey publications is available from the BGS Sales Desks at Nottingham and Edinburgh; see contact details below or shop online at www.thebgs.co.uk

The London Information Office maintains a reference collection of BGS publications including maps for consultation.

The Survey publishes an annual catalogue of its maps and other publications; this catalogue is available from any of the BGS Sales Desks.

The British Geological Survey carries out the geological survey of Great Britain and Northern Ireland (the latter as an agency service for the government of Northern Ireland), and of the surrounding continental shelf, as well as its basic research projects. It also undertakes programmes of British technical aid in geology in developing countries as arranged by the Department for International Development and other agencies.

The British Geological Survey is a component body of the Natural Environment Research Council.

Keyworth, Nottingham NG12 5GG

☎ 0115-936 3241 Fax 0115-936 3488
e-mail: sales@bgs.ac.uk
www.bgs.ac.uk
Shop online at: www.thebgs.co.uk

Murchison House, West Mains Road, Edinburgh EH9 3LA

☎ 0131-667 1000 Fax 0131-668 2683
e-mail: scotsales@bgs.ac.uk

London Information Office at the Natural History Museum (Earth Galleries), Exhibition Road, South Kensington, London SW7 2DE

☎ 020-7589 4090 Fax 020-7584 8270
☎ 020-7942 5344/45 email: bgslondon@bgs.ac.uk

Forde House, Park Five Business Centre, Harrier Way, Sowton, Exeter, Devon EX2 7HU

☎ 01392-445271 Fax 01392-445371

Geological Survey of Northern Ireland, 20 College Gardens, Belfast BT9 6BS

☎ 028-9066 6595 Fax 028-9066 2835

Maclean Building, Crowmarsh Gifford, Wallingford, Oxfordshire OX10 8BB

☎ 01491-838800 Fax 01491-692345

Parent Body

Natural Environment Research Council, Polaris House, North Star Avenue, Swindon, Wiltshire SN2 1EU

☎ 01793-411500 Fax 01793-411501
www.nerc.ac.uk

Foreword

This report is the published product of a study by the British Geological Survey (BGS) as part of their regional geological mapping programme. It describes the micromorphology of a suite glacial sediments from the Solway area, southern Scotland. The work forms part of a multidisciplinary Southern Scotland Quaternary Project.

Acknowledgements

Jon Merritt, Nick Golledge and Clive Auton are thanked for their assistance in the field whilst collecting the samples. David Oates is acknowledged for his expertise in making high quality large format thin sections, even of out the most poorly consolidated of materials.

Contents

FIGURES

TABLES

PLATES

Plate 1. (a) Recumbent fold deforming laminated silt and clay. Overturned limb of fold is truncated by a small-scale thrust fault (Sample N2840, plane polarised light, scale bar = 4 mm). (b) Recumbent, rootless fold deforming silt within partially fluidised silt and clay (Sample N2840, plane polarised light, scale bar = 4 mm). (C) Disrupted laminated silt and clay deformed by small-scale crenulation-style folds and thrust faults (Sample N2840, plane polarised light, scale bar = 4 mm).

Plate 2. (a) Water escape feature filled by distinctive orange-brown clay cutan. Also note presence of graded micro-scale channel lag at the base of this feature (Sample N2840, plane polarised light, scale bar = 1 mm). (B) Water escape feature filled by clay cutan which possesses a well developed concentric plasmic fabric (Sample N2840, crossed polarised light, scale bar = 1 mm). (C) Lower magnification view of water escape conduit showing that it occurs immediately above a low permeability clay layer and is elongate parallel to bedding (Sample N2840, plane polarised light, scale bar = 4 mm).

Plate 3. (a) Fe-staining cross cutting lamination in silt and clay (Sample N2841, plane polarised light, scale bar = 4 mm). (b) Normally graded silt and clay with reverse grading of included sand grade material (Sample N2841, crossed polarised light, scale bar = 4 mm). (c) and (d) Well developed bedding parallel plasmic fabric in clay laminae. Also note the presence of dark coloured mud-rip up clasts (Sample N2841, plane and crossed polarised light, scale bar = 4 mm).

Plate 4. (a) Rounded to irregular till pebbles within a clay matrix (Sample N2842, plane polarised light, scale bar = 1 mm). (b) Rounded to irregular till pebbles within a clay matrix which possess a well developed plasmic fabric (Sample N2842, crossed polarised light, scale bar = 1 mm). (c) Lower magnification view of water escape conduit cross cutting diamicton layer rich in rounded till pebbles. Late-stage fluid flow concentrated into distinct pathways resulting in the deposition of orange-brown clay cutan (Sample N2842, plane polarised light, scale bar = 4 mm).

Plate 5. (a) Rounded to irregular till pebbles within a clay matrix. Also note presence of cutan filled late-stage water escape features within the matrix (Sample N2842, plane polarised light, scale bar = 4 mm). (b) Rounded to irregular till pebbles within a clay matrix which possess a well developed plasmic fabric. Also note presence of cutan filled late-stage water escape features within the matrix (Sample N2842, crossed polarised light, scale bar = 4 mm). (c) Fractured, elongate lithic clast enclosed within a clay cutan coating (Sample N2842, plane polarised light, scale bar = 4 mm).

Plate 6. (a) Rounded to irregular till pebbles within a clay matrix (Sample N2842, plane polarised light, scale bar = 1 mm). (b) Rounded to irregular till pebbles within a clay matrix which possess a well developed plasmic fabric (Sample N2842, crossed polarised light, scale bar = 1 mm). (c) recumbent fold structure in hanging wall of thrust fault deforming laminated clay and silt (Sample N2842, plane polarised light, scale bar = 1 mm).

Plate 7. (a) sandy diamicton containing rounded lithic clasts. These lithic clasts locally represent broken fragments of larger pebbles (Sample N2843, plane polarised light, scale bar = 4 mm). (b) Rounded wacke sandstone rock fragment containing detrital blue amphibole (Sample N2843, crossed polarised light, scale bar = 1 mm). (c) Small-scale grading in cutan filled water escape feature (Sample N2843, plane polarised light, scale bar = 1 mm).

Plate 8. (a) irregular clay-rich layer within sandy diamicton. Also note rounded clast of altered olivine basalt (Sample N2843, plane polarised light, scale bar = 4 mm). (b) geopetal-like partial infill to water escape features (Sample N2843, plane polarised light, scale bar = 1 mm). (c) fractured mudstone lithic clast in sandy diamicton (Sample N2843, plane polarised light, scale bar = 1 mm).

Plate 9. (a) low-angle faults deforming laminated silt and clay (Sample N2844, plane polarised light, scale bar = 4 mm). (b) low-angle faults deforming laminated silt and clay (Sample N2844, plane polarised light, scale bar = 4 mm). (c) fluidised sand forming discrete layer within laminated sediments. This layer is fed by a sand filled hydrofracture (Sample N2844, plane polarised light, scale bar = 4 mm).

Plate 10. (a) patch of fluidised sand cross cutting laminated silt resulting in localised disruption of bedding (Sample N2846, plane polarised light, scale bar = 4 mm). (b) clay cutan filling late-stage water escape features (Sample N2846, plane polarised light, scale bar = 4 mm). (c) poorly sorted clast-rich diamicton (Sample N2848, plane polarised light, scale bar = 4 mm). (d) rounded bioclastic limestone clast in diamicton (Sample N2848, plane polarised light, scale bar = 4 mm).

Plate 11. (a) variably developed circular and arcuate structures developed in matrix of diamicton (Sample N2848, plane polarised light, scale bar = 4 mm). (b) clay cutan cement in diamicton composed of angular to subangular mudstone rock fragments (Sample N2849, plane polarised light, scale bar = 4 mm). (c) highly birefringent clay cutan cement (Sample N2849, crossed polarised light, scale bar = 4 mm).

Plate 12. (a) lithic-rich diamicton in which the clasts are mainly composed of cleaved mudstone. Also note local development of clay cutan cement in areas lacking in matrix (Sample N2849, plane polarised light, scale bar = 4 mm). (b) geopetal-like clay cutan developed in pore spaced in lithic-rich diamicton (Sample N2850, plane polarised light, scale bar = 1 mm). (c) poorly sorted, lithic-rich diamicton (Sample N2850, plane polarised light, scale bar = 4 mm).

Plate 13. (a) and (b) poorly sorted gravelly diamicton composed almost entirely of material derived from the granitic to granodioritic Criffle-Dalbeattie granite intrusion (Sample N2851, plane and crossed polarised light, scale bar = 4 mm). (c) silty caps developed upon large lithic clasts (Sample N2851, plane polarised light, scale bar = 4 mm). (D) silty caps developed upon large lithic clasts (Sample N2851, plane polarised light, scale bar = 1 mm).

Summary

This report describes the micromorphology of the Quaternary sediments exposed in the Solway area of southern Scotland. The work forms part of the Southern Scotland Quaternary Project of the Integrated Geological Survey (North) Programme.

The report provides detailed descriptions of the micromorphology of twelve large format thin sections of the Quaternary sediments exposed at several locations within the project area.

1 Introduction

This report describes the micromorphology of a suite of Quaternary sediments exposed in the Solway area of southern Scotland. Micromorphology is a relatively new and still developing technique and refers to the examination of Quaternary and other glacial sediments in thin section. (see van der Meer 1987, 1993; Menzies 2000). A total of five large format thin sections of unconsolidated sediment from Westend sand and gravel quarry have been examined. The results are used to develop a model for the emplacement of a very coarse, laterally persistent mass flow deposit which forms a distinctive unit within these glaciofluvial sediments.

Twelve samples of a variety of unconsolidated Quaternary sediments were collected from the following locations: Plumpe Farm, near Gretna [NY 3344 6813] (four samples); Small Holms Farm [NY 29732 73398] (four samples); Kelhead Quarry, Cumbertrees [NY 1511 6932] (one sample); North Corbelly, near New Abbey [NX 9853 6337] (two samples); and Townhead Saw Mill, New Abbey [NX 9600 6620] (one sample). The lithostratigraphy of the Quaternary sediments exposed in the Gretna area is shown in Table 1.

Table 1. Quaternary lithostratigraphy in the Gretna area

Gretna Till Formation (GRET)	Plumpe Bridge Till Member (Presently WCDR)		Irish Sea Glacigenic Sub-group (Presently WCDR)	'Scottish Readvance' of Main Late Devensian
	Plumpe Sand and Gravel Formation PLSG	Plumpe Farm Sand Member PFS		Distal glaciofluvial to glaciolacustrine, possibly partly glacio-estuarine
		Loganhouse Gravel Member LOGG		Glaciofluvial
	Chapelknowe Till Member CHAK			Main Late Devensian or older glaciation

The samples were collected using 10 cm square, aluminium kubiena tins which were either cut or pushed into the face of the exposure (Plate 1). The samples were then removed and sealed into two plastic bags and stored within the BGS cold store at Murchison House (Edinburgh) to prevent the material from drying out prior to sample preparation.

2 Analytical techniques

A total of twelve samples were prepared by Mr D. Oates at the British Geological Survey, Thin Sectioning Laboratory (Keyworth) as large format covered thin sections following the procedures for sample preparation of unconsolidated or poorly lithified materials. The thin sections were examined using a standard Zeiss petrological microscope and Zeiss projector enabling the analysis of both large and small scale microscopic textures and fabrics. A photomicrograph and detailed, annotated scanned images of each thin section have been used to describe the main microscopic features developed within these Quaternary deposits.

3 Terminology

The description and interpretation of the micromorphology and deformation structures developed within glacial deposits is a relatively recent and still developing technique (see van der Meer 1987, 1993; Seret 1993; van der Meer *et al*. 1990; van der Meer *et al*. 1992; van der Meer *et al*. 1994, Phillips & Auton 2001; Menzies 2000; Rose & Harte 2001). Although repetitive features have been recognised by several workers (see van der Meer 1987, 1993 and references therein) no standard nomenclature has yet to be formalised. The terminology used in this report is that proposed by van der Meer (1987, 1993) (also see Menzies 2000) and is based upon nomenclature developed by pedologists (for references see van der Meer 1993). A definition of the terms used for the various textures and fabrics, and their proposed mode of formation is given below and summarised in Fig. 1 (also see the glossary at the end of this report).

Plasmic fabric - The arrangement of high birefringent clay plasma/domains which are visible under the microscope (under cross polars) because of the similar extinction of similarly orientated domains. These fabrics are only observed when the diamicton is clayey. Diamictons which contain a limited amount of fines or relatively high proportion of carbonate within the matrix do not exhibit a well developed plasmic fabric.

Unistrial plasmic fabric - A planar plasmic fabric defined by relatively continuous domains which is typically observed defining discrete shears (Fig. 1). Interpreted as developing in response to planar movement (van der Meer 1993).

Skelsepic plasmic fabric - A plasmic fabric in which the orientated domains occur parallel to the surface of large grains (Fig. 1). Interpreted as developing in response to rotational movement (van der Meer 1993).

Lattisepic plasmic fabric - A plasmic fabric defined by short orientated domains in two perpendicular directions. In many cases this fabric is found associated with a skelsepic plasmic fabric (Fig. 1). Therefore, lattisepic plasmic fabrics are also interpreted as having developed in response to rotational movement (van der Meer 1993).

Omnisepic plasmic fabric - A plasmic fabric in which all the domains have been reoriented (Fig. 1). Interpreted as developing in response to rotational movement (van der Meer 1993).

Till 'pebbles' - Formed by rotational movement (van der Meer 1993). They are subdivided into three types: Type (1) consists of till which lack an internal plasmic fabric. They are defined by encircling voids and the shape of the 'pebbles' becomes progressively angular and flatter with depth; Type (2) is characterised by 'pebbles' of fine-grained material which were part of the original sediment host. They are recognised by an internal plasmic structure and are not defined by voids; Type (3) form isolated 'pebbles' of either till or fine-grained sediments and are usually interpreted as having formed by reworking of the till. They may or may not contain internal plasmic fabrics.

Other microscopic features - Include: the circular arrangement of clasts (skeleton grains) with or with out a 'core stone' (Fig. 1), interpreted as having formed in response to rotation (van der Meer 1993); pressure shadows (Fig. 1) which are also interpreted as having formed in response to rotation (van der Meer 1993); dewatering structures associated with shearing; microboudinage; microscopic scale primary sedimentary structures (lamination, cross lamination……etc.); water escape structures associated with forceful dewatering; and crushing of clastic grains (Fig. 1).

4 Thin section descriptions

Detailed descriptions of each thin section examined during this study are presented below.

4.1 SAMPLE N2840

Sample Number: ERP 1. **Registered Number:** N2840. **Location:** Plumpe Farm, near Gretna [NY 3344 6813]. **Location Number:** NY36NW ME263. **Lithology:** laminated silt, sand and clay from the lowest part of the silty clay unit, Plumpe Farm Sand Member (see Table 1).

Description: This thin section is of a finely bedded and laminated silt and clay with very fine-grained sand at the base of some graded layers. For ease of description the sample is divided into 8 units (Fig. 2).

Unit 1 **–** occurs at the base of the thin section (Fig. 2) and comprises finely laminated silt and clay in which the individual laminae range from 0.3 to 1.3 mm in thickness. Small-scale, normal grading within these laminae clearly indicates that the sediments are, in general, the right way up. However, the lamination is deformed by a recumbent, tight fold which results in the localised overturning of bedding on the upper limb of this structure (Plate 1a). The upper limb of this fold structure is truncated against a low-angle to sub-horizontal reverse fault (thrust) (Plate 1a) which exhibits an apparent dextral (top-to-right) sense of displacement. This thrust fault also forms the upper boundary between Unit 1 and the overlying sediments of Unit 2. Thrusting also resulted in the minor imbrication of the laminated silt and clay. The asymmetry of the deformed lamination within these small-scale thrust slices yields a dextral sense of displacement.

The lower limb of the fold is deformed by a number of small-scale (wave length 1.5 to 2.5 mm) upright to steeply inclined, symmetrical to weakly asymmetrical, open folds (Plate 1a) as well as a small-scale reverse fault. The sequence of events recorded by these deformation structures is: (1) recumbent folding (F1) and localised overturning of bedding; (2) small scale up-right folding (F2); and (3) thrust faulting leading to the truncation of the earlier developed fold structures. A very weak plasmic fabric is developed within the clay laminae with this foliation being approximately axial planar to the recumbent fold. The plasmic fabric is partially overprinted or obscured by later reddening/hematisation of the sediment.

Unit 2 – is approximately 20 mm thick and composed of massive fine-silt to silty clay (Fig. 2). Detrital grains within this silty unit are angular to subangular in shape with a low sphericity. These fine elongate clasts may locally exhibit a weak preferred shape alignment both parallel to, and at a high-angle bedding, the latter possibly represent fluid pathways/flow zones through the sediment. No obvious plasmic fabrics have been noted associated with these zones. The detrital assemblage is dominated by monocrystalline quartz with minor to accessory opaque minerals, white mica/muscovite, plagioclase, chloritised biotite and rare chloritic/bowlingite pseudomorphs after olivine and/or pyroxene.

The most distinctive feature of Unit 2 is a network of bands or zones of reddened silt/silty clay (Fig. 2 and Plate 3a). There are no obvious fractures or dislocations associated with these reddened zones (Plate 3a) which are interpreted as having formed due to Fe oxidation due to intergranular flow of pore water. These zones cut across bedding, which can locally be seen passing straight through (i.e. no off-set) these features (Plate 3a). The reddened zones thin upwards and appear to terminate at or just above the boundary between Unit 2 and the overlying Unit 3. Several these zones appear to originate from the thrust separating Units 1 and 2. This detachment may have provided the main focus for fluid migration with subtle variations within the overlying massive silt allowing localised upward, intergranular migration of pore water through these sediments.

Unit 3 – is approximately 12 to 13 mm thick and composed of variably disrupted (soft sediment deformation) and fluidised, laminated silt and clay (Fig. 2). These originally laminated sediments are compositionally similar to those of Unit 1. The lower boundary of the unit is deformed by a series of asymmetrical, arcuate flame-like structures (Fig. 2) which yield an apparent dextral sense of displacement (top-to-right). Immediately above the base of the unit the clays and silts are finely laminated with individual laminae ranging up to 0.3 mm in thickness. These laminae are deformed by small-scale, upright to steeply inclined folds, small scale shears and rare recumbent fold structures (Plates 1b and c). The laminated silt and clay are bound by a prominent thrust (dextral) which truncates both the lamination and fold structures.

The remainder of Unit 3 is composed of similar laminated material in which this primary sedimentary feature has been partially overprinted or locally destroyed by soft sediment deformation and accompanying fluidisation of the silty laminae. Soft sediment deformation structures present include rootless fold, low-angle thrusts, disharmonic folds and narrow diffuse shears in which the asymmetry of the foliation yields a dextral sense of shear. Although deformed no obvious plasmic fabrics have been recognised within the clay laminae. Soft sediment deformation is essentially confined to Unit 3 and may have been lithologically controlled. This lithological control may resulted in the partitioning (focusing) of deformation into this particular horizon. Alternatively, this deformed horizon may simply represent a fine-grained mass-flow deposit. However, a monoclinal-like fold structure which deforms the upper part of Unit 3 also deforms the overlying sediments of Unit 4 (Fig. 2), indicating that deformation post dated the deposition of at least this part of the sedimentary sequence.

Occasional clay cutan filled voids are present near the top of Unit 3. The cutan is orange-brown in colour with a distinctive bright birefringence under crossed polarised light. The formation of this clay infilling appears to have post-dated all the soft sediment deformation.

Unit 4- this unit is approximately 10 mm thick and is composed of laminated silt (individual laminae 0.5 to 1.0 mm thick) which locally preserve a low-angle cross lamination (Fig. 2). The base of the unit is marked by a 0.3 to 0.4 mm thick sandy layer or lag which contains coarser grained fine- to coarse-sand grade clasts. These detrital grains are angular to subangular in shape with a low to moderate sphericity. They are mainly composed of monocrystalline quartz and mud rip-up clasts (intraclasts). Other minor to accessory detrital components include polycrystalline quartz, plagioclase, opaque minerals, chlorite, white mica and chloritic pseudomorphs after a ferromagnesian mineral (pyroxene and/or olivine). The silt within this unit is lithologically similar to that of Unit 2. Detrital micas and other elongate grains may exhibit a preferred shape-alignment parallel to bedding.

Deformation is restricted to a monoclinal fold and associated open synformal warp-like structure (Fig. 2). This monocline also deforms the upper part of the underlying unit, but dies out upwards through Unit 4 (see Fig. 2).

The laminated silts of Unit 4 contain a number of irregular, rounded to occasionally eye-shaped voids or water escape conduits which are variably filled by a distinctive orange-brown clay cutan (Plate 2). The circular to irregular plasmic fabric developed within this highly birefringent clay is locally disrupted and/or fragmented (Plate 2b). This fabric is thought to have formed due to the plating of the clay plasma against the margins of the conduit during fluid flow. The subsequent disruption of this fabric may have occurred during either: a later phase of fluid flow due to an increase in pore water pressure which exceeded the cohesive strength of the clay cutan; or as a result of partial collapse of the void due to compaction of the sediment. The largest of these cutan lined fluid pathways is approximately 6.0 mm across and contains 4 or 5 small-scale graded units (Plate 2). The graded units fine upwards and comprise a coarser base containing silt to very fine sand grade clasts overlain by orange-brown clay (Plate 2a). These sequences clearly represent microscopic “channel-fills” and record several phases “high” discharge followed by decreasing flow. The fining of these deposits upward means that the magnitude of these flow events decreased with time. Furthermore, this complex record of infilling means that the conduit was stable enough to remain open for a prolonged period. It is possible that the earliest formed cutan layer formed a lining which stabilised the walls of the conduit. These graded fills to the water escape conduits may also be used as way up indicators, comparable to geopetal infills. In general these cutan filled features are associated with prominent bedding surfaces indicating that these primary sedimentary features may, in some cases, control subsequent pore water flow through the sediment. These bedding surfaces denote changes in sediment composition (clayey sediments retarding water flow), porosity and permeability all of which will effect the migration of water.

The silty sediments of Unit 4 are also cut by an irregular network of reddened zones which cross-cut the sedimentary lamination. As in the underlying units, no obvious fractures have been recognised associated with reddened zones which appear to have formed due to Fe oxidation during intergranular water flow.

Unit 5 – comprises an undeformed sequence of finely laminated silt with thin darker coloured clayey partings (Fig. 2). Occasional clay cutan filled voids and Fe-oxide stained (reddened) zones are also present within this unit.

Unit 6 – is comparable to the underlying silty sediments of Unit 5. The base of the unit is sharp and immediately overlain by an approximately 5.0 mm thick layer of finely laminated, slightly darker brown clayey silt (Fig. 2). This basal layer is overlain by a 10.0 to 12.0 mm thick graded silt to silty clay layer which possess a low-angle cross lamination (Fig. 2). The upper part of this cross laminated layer grades upward into the overlying silty sediments of Unit 7.

Unit 7 – is composed of thinly laminated package of silty sediment (Fig. 2)which is lithologically similar to the underlying Unit 6. As with the underlying unit, Unit 7 composed a slightly darker coloured finely laminated basal layer overlain by more massive, normal-graded silt to silty clay. This graded layer possesses a coarse silt to very fine sand lag at its base.

Unit 8 – this unit consists of weakly laminated silt and clay (Fig. 2). It is distinguished from the underlying units by the more diffuse nature of the lamination and the presence of sand-grade mud rip-up clast. These clasts are angular to rounded in shape with a low sphericity, and exhibit a preferred shape-alignment parallel to bedding. At the top of the unit is a large (12.0 to 14.0 mm long) irregular void filled by orange-brown, birefringent clay. This cutan filled void is elongate parallel to the sedimentary lamination within Unit 8.

Units 4 to 8 within this sample represent individual packages of sedimentation comprising a finely laminated, more clay-rich layer at the base over lain by massive to cross-bedded normally graded silt. These sediment packages represent quiet water conditions resulting in the deposition of the laminated clays. The overlying graded packages may represent distal turbiditic deposits which were deposited during increased sediment discharge.

4.2 SAMPLE N2841

Sample Number: ERP 2. **Registered Number:** N2841. **Location:** Plumpe Farm, near Gretna [NY 3344 6813]. **Location Number:** NY36NW ME263. **Lithology:** laminated silt, sand and clay from the middle to upper part of the silty clay unit, Plumpe Farm Sand Member (see Table 1).

Description: This thin section is of a finely interlaminated sand, silt and clay. For ease of description the sample is divided into 3 units (Fig. 3).

Unit 1 – is approximately 25.0 mm thick and is composed of laminated, poorly sorted, open-packed, matrix-rich, immature fine-grained sand (Fig. 3). The lamination is defined by the variation in the modal proportions of the clay matrix, with thin clay partings occurring near the base of the unit. Clastic grains are typically ≤ 0.2 mm in size, but may occasionally range up to 0.5 mm in diameter. They are angular, subangular to occasionally subrounded in shape with a low to moderate sphericity. The clasts are mainly composed of monocrystalline quartz with minor to accessory plagioclase, mudstone rock fragments, polycrystalline quartz, opaque minerals, siltstone, apatite, allanite, white mica/muscovite, chlorite, amphibole, biotite microcline and felsite rock fragments.

The clay-grade matrix to this sandy unit is reddened due to hematitic staining. No obvious plasmic fabric(s) have been recognised within the clay matrix. The high proportion of clay matrix within this sandy unit results in an open to very open packed, matrix supported texture in which the clastic grains appear to ‘float’ within the surrounding matrix. Inter-grain contacts are only locally developed within the matrix-rich sand.

Localised water migration along bedding/lamination surfaces is recorded by the present of impersistant clay cutan filled fractures or veinlets. The clay infill is orange-brown in colour with a well developed optical alignment of the clay plasma and strong birefringence. Irregular spots or patches of opaque oxide were also noted.

Unit 2 **–** comprises 3 packages of normally graded silt to clay, with the central package being much thinner than the upper and lower layers (Fig. 3). An increase in included coarse-silt to sand-grade clasts towards the clayey tops of these packages gives then an overall reverse graded appearance (Plate 3b). The base of the unit is sharp and overlain by a 15.0 mm thick unit of parallel laminated to cross laminated silt. The basal silty part of the packages grades upward into a more clay-rich sediment; the grading being highlighted by a gradual colour change.

The coarse silt to sand grade clastic grains are angular to subangular in shape with a low to moderate sphericity, and mainly composed of monocrystalline quartz. Rare rounded clasts are also present. The composition of the detrital assemblage within this sandy component is similar to the sandy sediments of the underlying Unit 1. The modal proportion of the included coarse silt to sand grade clasts increases upward through Unit 2, with the upper part of the unit being lithologically similar to the underlying Unit 1 (see Fig. 3). The sandy upper parts to the sediment packages within Unit 2 possess an open to very open packed, matrix supported texture. This texture suggests that the sand grains were deposited due to the rain-out of fine-grained material from melting ice, i.e. drop stones. The normal graded silt and clay would represent the main background sedimentation.

Rounded to irregular clay cutan filled voids are elongate parallel to the lamination and are mainly concentrated within the silty parts of the unit.

Unit 3 **–** this unit is general lithologically similar to Unit 2. It comprises 2 to 3 packages of normal graded silt and clay which containing coarse silt to sand grade clasts within the finer upper parts (Fig. 3). In contrast to the underlying unit, these sediment packages may also comprise a basal layer containing elongate angular to very angular mud rip-up clasts (Plates 3c and d). The clay-rich part of the graded units locally possess a bedding-parallel plasmic fabric which is distorted around the included coarse silt and sand grains (Plate 3d); possibly due to differential compaction. This microtextural relationship suggests that the bedding parallel fabric developed early (? syn-sedimentary) and was distorted/deformed during compaction of the sediments.

The sediments at the base of Unit 3 are disrupted. This disrupted layer varies in thickness and appears to have resulted from the mixing of the underlying sandy sediment with more clay-rich material (see Fig. 3). This disrupted layer contains fragments of highly deformed (folded) laminated silt and clay. Deformation occurred prior to the incorporation of these intra clasts within this deposit.

4.3 SAMPLE N2842

Sample Number: ERP 3. **Registered Number:** N2842. **Location:** Plumpe Farm, near Gretna [NY 3344 6813]. **Location Number:** NY36NW ME263. **Lithology:** laminated silt, clay and diamicton from the lower, stratified part of a till unit exposed in the upper part of the section, Plumpe Bridge Till Member (see Table 1).

Description: This thin section is of a coarse-grained, poorly sorted, stratified diamicton which contains discrete layers of internally disrupted, finely laminated silt and clay. For ease of description the sample is divided into 5 units (Fig. 4).

Unit 1 **–** (approximately 15.0 to 17.0 mm thick) occurs at the base of the thin section and is composed of originally laminated silt and clay (Fig. 4). The lamination has been disrupted and locally overprinted by the variable fluidisation and mobilisation of the silt laminae. The boundaries between the individual laminae are diffuse and are locally deformed by complex, small-scale disharmonic folds. This silt and clay dominated unit also contains occasional lithic clasts and rounded to irregular till pebbles (Type 1 of van der Meer 1993). The till pebbles posses sharp to diffuse margins and range from being internally massive to locally possessing a circular arrangement of finer included grains. However, the clayey matrix to these till pebbles lacks any obvious plasmic fabric. The margins of the till pebbles are slightly paler in colour, possibly reflecting a decrease in clay content of the matrix towards the rim of the clast. The irregular shape of some of the till pebbles suggests that they have undergone plastic deformation and were not over-consolidated when incorporated into the silt and clay. The lamination within the host silt and clay is clearly wrapped/deflected around these included till pebbles and lithic clasts.

The lithic clasts are subangular to subrounded in shape with a low sphericity. They are composed of very fine-grained quartz arenite and coarse siltstone (Plate 5c) which may have been derived from the Carboniferous or Permo-Triassic sandstone sequences exposed in the Solway area. One large, elongate clast (approximately 20 mm in length) composed of a weakly laminated, very fine-grained quartz-arenite is fractured with the fracture filled by fluidised silty clay. This fracture is interpreted as having been a pre-existing structure within the rock fragment rather than evidence of crushing due to subglacial deformation.

The complex disharmonic folding and distortion of the lamination within Unit 1 are closely associated with clay cutan lined or filled veinlets and voids. These cutan filled features represent fluid pathways and developed due to the deposition of fine, argillaceous material as pore water was concentrated into discrete flow zones during water escape/apparently late-stage fluid migration. This infill is composed of a distinctive orange-brown coloured (under plane polarised light), highly birefringent clay which possesses a well developed circular or disrupted plasmic fabric.

The incorporation of the till pebbles within Unit 1, disharmonic folding and disruption of the lamination within this layer are interpreted as having occurred simultaneously. Soft sediment deformation was accompanied by the fluidisation of the silty laminae, with water flow through the sediment being concentrated into discrete flow zones during the later stages of deformation and dewatering; these zones being preserved as clay cutan filled veinlets and voids.

Unit 2 **–** is a distinctive clay-rich layer containing rounded to elongate till pebbles (Fig. 4 and Plates 4, 5a and 5). The boundary between this unit and the underlying laminated silt and clay of Unit 1 is sharp but irregular in form. The till pebbles within Unit 2 exhibit a preferred shape alignment parallel to bedding and are all composed of the same pale grey to yellow-brown (under plane polarised light), fine-grained clayey diamicton (Plate 4). These till pebbles mainly contain fine-sand to coarse silt grade included grains. However, coarse sand and granule sized fragments are present within the larger pebbles (Plate 4c). The clastic grains are angular to subangular in shape with a low sphericity. They are mainly composed of monocrystalline quartz with minor to accessory mudstone/siltstone, opaque minerals, very fine-grained sandstone, polycrystalline quartz, quartz-arenite, hematised fine-grained sandstone, hematised siltstone, cleaved mudstone, mud, diamicton (i.e. till pebbles within the clasts of diamicton), garnet, plagioclase and altered biotite.

Internally the till pebbles are typically massive (Plates 4, 5a and b) (*c.f.* Type 1 till pebbles of van der Meer 1983). However, variably developed circular and/or galaxy structures are present in some pebbles. A weak planar plasmic fabric was also noted in a few till pebbles, with the intensity of this foliation being proportional to the clay content of the diamicton. Although the matrix to the diamicton is of clay-grade, the modal proportion of clay minerals is highly variable and, in some cases, is a relatively minor constituent. The till pebbles are locally embayed against neighbouring more rigid grains. However, flattening and/or folding of the till pebbles is restricted to thin, wispy-looking clasts; in particular where these thin elongate clasts are wrapped around larger, apparently more rigid, till pebbles. A number of the till pebbles possess variably developed 'tails' which extend away from the main body of the clast. In contrast to these plastically deformed or flattened clasts, the majority of the till pebbles are undeformed and range from irregular to rounded in shape.

The matrix to Unit 2 is composed of a brown to orange-brown, strongly birefringent clay which possesses a well developed plasmic fabric (Plates 5a, 5b, 6a and 6b). This plasmic fabric is deformed or locally disrupted by later kink-style folds and clearly wraps around the included till pebbles. The apparent intensity of this plasmic fabric is in marked contrast to the lack deformation within the till pebbles. Localised plastic deformation of these pebbles, including embayment of clasts against neighbouring relatively more rigid pebbles, indicates that the till pebbles were not over consolidated at the time of the deposition/formation of Unit 2. Consequently, it is unlikely that the plasmic fabric present within the matrix was imposed as a result of deformation. The morphology of this plasmic fabric is comparable to the clay cutan present within the spatially related water escape conduits/flow zones. The matrix is locally observed grading into clay cutan structures (Plates 5a and b). It is possible, therefore, that the matrix to Unit 2 was also deposited from clay suspended in actively flowing pore water.

The deposition of the clay matrix is thought to be intimately linked to till pebble formation. Both of these features may have formed during fluidisation and the initial stages of mixing of two rheologically distinct sediments. The relatively more cohesive diamicton retained its integrity, forming irregular to rounded till pebbles contained within water saturated/fluidised clay. The less competent of these till pebbles began to plastically deform. The resultant texture is reminiscent of load structures (e.g. sand balls), in which the originally overlying diamicton has been fully dissected and included within the underlying water saturated clay.

Unit 2 is cut by a subvertical water escape conduit (Fig. 4 and Plate 4c) which appears to have initially developed within the laminated silts and clay of the underlying Unit 1. The boundary between Unit 2 and the overlying argillaceous sediments of Unit 3 is sharp.

Unit 3 – is lithologically similar to Unit 1 and is composed of finely laminated silt and clay (Fig. 4). The silty laminae within this unit have undergone varying degrees of liquefaction and mobilisation, which accompanied disharmonic folding and localised boudinage of the more clay-rich laminae. Other deformation structures present include the nose of a recumbent, small-scale fold which occurs in the hanging wall of a low-angle thrust fault (Plate 6c) and a small number of rootless recumbent folds which exhibit a pronounced thickening of the laminae in the hinge area. A weakly to moderately developed bedding-parallel plasmic fabric occurs within the more clay-rich laminae. This plasmic fabric is deformed by the disharmonic folds and becomes highly disrupted in the cores of these small-scale structures. The bedding-parallel fabric is also deformed by a number of narrow shears, defined by a unistrial plasmic fabric and associated with small-scale thrust faults. These microstructural relationships indicate that the bedding-parallel foliation developed prior to deformation and liquefaction. This fabric may have formed during initial compaction and de-watering of the laminated silt and clay prior to its incorporation within the stratified diamicton.

Liquefaction of the silty laminae appears to be partially controlled by the clay content. The presence of clay cutan lined fissures and veinlets within the laminated silt and clay, which

locally cross cut the earlier developed soft sediment deformation features, indicate that pore water movement became focused into particular flow zones during the later stages of this liquefaction/deformation event.

The laminated silt and clay of Unit 3 contains a small number of rounded to irregular till pebbles and rock fragments. The lithic clasts are subrounded in shape with a low sphericity. They are mainly composed of fine-grained quartz-arenite and contain shape aligned detrital muscovite and muscovite. These rock fragments were possibly derived from the Carboniferous or Permo-Triassic sedimentary sequences exposed in the Solway area.

The upper boundary of Unit 3 is irregular in nature, with evidence of the injection of the variably fluidised laminated silt and clay into the overlying diamicton-rich sediments of Unit 4. Later clay cutan filled water escape features are also focused within these flame-like injection structures.

Unit 4 – comprises a layer of poorly sorted, immature, matrix supported, sandy to silty diamicton (Fig. 4) which contains occasional coarse sand, granule and pebble sized clasts. These large, low sphericity clasts are angular to rounded in shape and mainly composed of rock fragments including: fine-grained quartzose sandstone, hematised mudstone or siltstone, hematised quartzose sandstone, siltstone, mudstone, and altered basaltic volcanic rock. The basaltic rock fragments are probably derived from the Carboniferous in age Birrenswark Volcanic Formation. The sandstone and siltstone lithic fragments also include lithic-rich, occasionally weakly metamorphosed (sub-greenschist facies) sedimentary detritus which was probably derived from the Ordovician-Silurian strata which dominate the pre-Quaternary geology of the Southern Uplands terrane. The more quartzose sandstone rock fragments were probably derived from the Carboniferous or Permo-Triassic strata exposed in the Solway area.

The finer grained detrital grains are angular, subangular to subrounded in shape with a low to occasionally moderate sphericity. These clasts are mainly composed of monocrystalline quartz, polycrystalline quartz and subordinate rock fragments. The fine grained lithic clasts include the same range of lithologies as the larger rock fragments. Other minor to accessory detrital components include opaque minerals, plagioclase, felsite and chloritic pseudomorphs after ferromagnesian minerals (olivine and/or pyroxene). The silt to sand grade clasts locally occur in arcuate, circular or galaxy-like aggregates which may, in some cases, surround larger clastic grains.

The diamicton is cut by a number of irregular veinlets or fissures which are filled by brown silty clay or orange-brown coloured clay cutan; the latter is highly birefringent and possesses a well developed plasmic fabric. The veinlets of silty clay can locally be traced into silt and clay filled flame structures which extent from the underlying laminated silt and clay of the underlying unit. The silty clay within the veinlets may also possess a variably developed plasmic fabric which occurs parallel to the vein margin. Both the clay and cutan filled features are interpreted as being related to the injection of partially fluidised sediment upward into the diamicton and subsequent concentration of pore water migration into discrete flow zones. The injection of the clay-rich material resulted in hydrofracturing and localised fragmentation of the diamicton into irregular to rounded till pebbles (Type 1 till pebbles of van der Meer 1983). This process of hydrofracturing and clay injection may lead to the detachment of till pebbles which are incorporated into the underlying silt and clay. Similar clay and silt injection features were also noted extending downward from the overlying laminated silt and clay horizon (see Fig. 4). The continued ‘intermixing’ by this injection/fluidisation process may lead to the formation of the complex till pebble-rich deposit represented by Unit 2.

Unit 5 – is dominated by laminated clay and silt which contains irregular to rounded clasts of diamicton (Fig. 4). These till pebbles are compositionally similar to the diamicton of Unit 4. The lamination within Unit 5 is highly deformed/distorted in adjacent to the till pebbles with the

complexity of this soft-sediment deformation being consistent with the partial fluidisation of the clay-silt. The silty laminae are more susceptible to liquefaction than the associated clay laminae. This soft-sediment deformation probably accompanied the incorporation of the till pebbles into the laminated clay and silt. Irregular flames and elongate tails developed upon the till pebbles indicate that the diamicton was poorly consolidated during deformation. The lower boundary of this unit is sharp, but highly irregular in nature. A number of partially formed till pebbles were noted along this contact. These pebbles are partially included within the laminated silt and clay of Unit 5, but are still connected/attached to the underlying diamicton (Unit 4) by a thin 'tail'.

The laminated silts and clay of Unit 5 also contain rounded, low sphericity granule to small pebble sized clasts of very fine-grained wacke sandstone. These rock fragments were probably derived from the Ordovician-Silurian strata of the Southern Uplands. The lamination within the host silts and clay is wrapped/distorted around these large lithic clasts. A weakly developed plasmic fabric present within the clay-rich laminae locally defines an anastomosing network of narrow high-strain zones or shears. Displacement along these shears results in the dissection and disruption of the clay laminae.

4.4 SAMPLE N2843

Sample Number: ERP 4. **Registered Number:** N2843. **Location:** Plumpe Farm, near Gretna [NY 3344 6813]. **Location Number:** NY36NW ME263. **Lithology:** red diamicton exposed at top of section, Plumpe Bridge Till Member (see Table 1).

Description: This thin section is of a weakly laminated, matrix supported, poorly sorted, immature, sandy diamicton which contains occasional very coarse sand to small pebble sized lithic clasts (Fig. 5 and Plate 7). These large clasts are subangular, subrounded to rounded in shape with a low sphericity. The elongate clasts also exhibit a weakly developed preferred shape orientation (see section 5). The lithic clasts are mainly composed of sandstone and siltstone (Plates 7 a and b). Recognisable lithologies include: chloritised wacke sandstone, very fine-grained quartz arenite, hematised mudstone (Plate 8c), mudstone, hematised sandstone, altered basalt (Plate 8a), hematised siltstone and granite. The majority of the sedimentary rock fragments are derived from the Ordovician-Silurian sequence of the Southern Uplands. One of these wacke sandstone clasts contains a fragment of Na-rich amphibole (glaucophane or crossite) (plate 7b) indicating that this rock fragment was derived from the Ordovician in age Portpatrick Formation which is exposed within the northern belt of the Southern Uplands terrane. This clast and a number of the other wacke sandstone lithic fragments are well-rounded indicating that they have undergone a prolonged period of transport prior to their incorporation within this diamicton. The clasts composed of altered olivine basalt (Plate 8a) were probably derived from the Carboniferous in age Birrenswark Volcanic Formation. These basaltic lithic clasts are enclosed within a red-brown coating of a hematitic clay. Hematitic coatings have also been noted on a number of other clasts within this diamicton indicative secondary remobilisation and oxidation of Fe.

The matrix to the diamicton possesses a distinctive sandy to silty texture (Plate 7c). It is poorly to very poorly sorted and mainly composed of angular to subangular, low sphericity silt to sand grade clasts set in a red-brown (under plane polarised light) silt/clay. Occasional rounded sand grains are also present. These rounded grains are locally broken and are clearly polycyclic in origin. The clasts are mainly composed of monocrystalline quartz with subordinate to minor lithic fragments. The lithic clasts are composed of a similar range of lithologies to the larger granule to pebbles sized fragments present within the diamicton. Other minor to accessory detrital components include polycrystalline quartz, plagioclase, basalt, chlorite, opaque minerals and chloritic pseudomorphs after a ferromagnesian mineral (olivine and/or pyroxene). The

matrix also contains irregular to rounded voids and fissures which are partially filled by a distinctive orange-brown (under plane polarised light) clay cutan.

The diffuse layering present within the diamicton is marked by a gradual, but relatively rapid, increase in the modal proportion of silt/clay grade material within the matrix (Plate 8a). This increase in argillaceous material is accompanied by a decrease in the modal proportions of included sand grains. The silt-clay layers are irregular to wispy in nature (Fig. 5) with flame-like projections extending into the adjacent diamicton. A fine-scale lamination and anastomosing/disrupted plasmic fabric are locally developed/preserved within these silt/clay layers. The lamination is locally deformed by small-scale disharmonic folds. Circular to arcuate arrangement/aggregates of sand grade clasts have been recognised within the silt/clay layers; such textures are less obvious within the more sandy parts of the diamicton.

4.5 SAMPLE N2844

Sample Number: ERP 5. **Registered Number:** N2844. **Location:** Small Holmes Farm [NY 29732 73398]. **Location Number:** NY27SE. **Lithology:** laminated clay and silt collected from northern end of section, trend of section 029°.

Description: This thin section is mainly composed of finely laminated silt and clay which contains two discrete layers of matrix-poor, fine-grained sand (Fig. 6). For ease of description the sample has been subdivided into four main units.

Unit 1 **–** is composed of finely laminated silt with thin silty clay partings (Fig. 6). Individual laminae range from 0.3 to 1.5 mm thick and may possess a weakly developed normal grading. Silt grade clastic grains present within the coarser grained fraction are angular to subangular in shape with a low sphericity. These detrital grains are mainly composed of monocrystalline quartz with minor to accessory opaque minerals, chlorite, white mica/muscovite, feldspar, altered biotite and chloritic pseudomorphs after altered ferromagnesian minerals. Detrital phyllosilicate may exhibit a weak to moderately developed preferred shape alignment parallel to the lamination.

Unit 1 is divided in two by a prominent layer of red-brown clay, overlain by matrix-poor silt to very fine-grained sand (Fig. 6 and Plates 9a and b). The laminated silt and clay above and below this horizon can be further subdivided into a number of sediment packages based upon the spacing of the lamination (see Fig. 6). The red-brown clay band possesses a well-developed bedding-parallel plasmic fabric which is disrupted immediately adjacent to a set of low-angle normal faults which deform the lamination within Unit 1 (Fig. 6 and Plates 9a and b). These curved to planar faults downthrow towards the south or south-southwest and resulted in the localised tilting of bedding (Fig. 6). In detail, the individual fault planes are diffuse, lacking an obvious discrete plane of dislocation. Minor drag folding and rare small-scale reverse faulting has been recognised associated with these normal faults. Extension which occurred during faulting resulted in the opening of these low-angle normal faults allowing the migration of pore water along these brittle structures. Although, the normal faults deform the boundary between Units 1 and 2, resulting in the stepped nature of this contact, they do not appear to have effected the silty sediments of this overlying unit. It is possible that normal faulting pre-dated the deposition and/or disruption of Unit 2.

Unit 2 **–** is approximately 10.0 mm thick and is composed of a disrupted sequence of laminated clay and silt which contains a 4.0 to 5.0 mm thick layer of matrix-poor sand (Fig. 6). The

lamination within the lower part of the unit is best preserved within the footwall, adjacent to the scarp formed by the normal faults present within the Underlying Unit 1. The lamination above this basal zone is deformed by small-scale rootless, tight to isoclinal recumbent folds. Where the deformation is more intense the clayey laminae are dissected into a number of lenticular fragments. The clay within these disrupted laminae possesses a well developed plasmic fabric.

The fine-grained matrix-poor, weakly laminated sand layer (Plate 9c) within Unit 2 is weakly reverse graded and contains elongate, angular mud rip-up clasts which possess a variably deformed/distorted plasmic fabric. This microtextural relationship indicates that the plasmic fabric formed prior to the deposition of the matrix-poor sand which may have been injected into the laminated silt and clay. The injection of this fluidised sand accompanied hydrofracturing (see Plate 9c) and soft-sediment deformation and led to the localised disruption of the laminated silt and clay. The lamination with the sand layer is defined by the variation in a dusty clay matrix and/or a orange-brown coloured clay cutan cement. The clay cutan mainly occurs towards the base of the sand layer where the sand possesses an open packed, locally cement supported texture. The sand is mainly composed of angular to subangular, low sphericity monocrystalline quartz clasts. Minor to accessory detrital components present within the sand also include plagioclase, opaque minerals, chlorite, muscovite/white mica and microcline.

This apparently fluidised sand layer is overlain by variably deformed, laminated silt and clay. The boundary between Unit 2 and the overlying sediments is marked by a 1.0 to 2.0 mm thick band of clay (see Fig. 6).

Unit 3 **–** is composed of a single layer of weakly laminated, matrix-poor, moderately sorted, fine- to very fine-grained sand (Fig. 6) which possesses a moderate to closely packed grain supported texture. This sand layer is lithologically similar to the sand present within Unit 2. The lamination within Unit 3 is defined by a variation in the modal proportion of a orange-brown clay cutan cement (see Fig. 6). The occurrence of this cement is accompanied by a variation in the packing of the sand. In the laminae which possess the clay cement the sand possesses an dilated, open packed, cement supported texture. The clay cement is highly birefringent and possesses a variably developed plasmic fabric. A similar clay cutan was also noted infilling rounded to irregular voids and veinlets. Occasional spots or patches of a hematitic cement have also been recorded within this sand layer. The top of Unit 3 grades into the overlying laminated sediments.

Unit 4 **–** is composed of finely laminated silt and clay (Fig. 6) in which the individual laminae may possess a fine-scale, normal grading. Small-scale, 2.0 to 3.0 mm thick thinning and apparently fining upward sequences have also been recognised. Similar packages of sediment have also been recognised within Unit 1 and may represent fluctuations in clastic sediment input.

4.6 SAMPLE N2845

Sample Number: ERP 6. **Registered Number:** N2845. **Location:** Small Holmes Farm [NY 29732 73398]. **Location Number:** NY27SE. **Lithology:** laminated clay and silt collected from northern end of section, trend of section 029°.

Description: This thin section is mainly composed of finely laminated silt and clay which contains a layer of matrix-poor, fine-grained sand (Fig. 7). This sample is lithologically similar to sample N2844 and occurs at a similar structural/stratigraphical level within the exposed sequence. For ease of description sample N2845 has been subdivided into four main units.

Unit 1 **–** is composed of titled and faulted, laminated silt and clay (Fig. 7). Individual laminae range from 0.4 to 2.0 mm thick and possess a variably developed normal grading defined by a change in colour of the sediment. The top of the unit is marked by a lens of red-brown clay which is off-set by a number of small-scale normal faults which downthrow to the south to south-southeast. The clay band possesses a well-developed bedding-parallel plasmic fabric which is disrupted immediately adjacent to the faults. The laminated silt and clay which dominate the remainder of this unit can be divided into several packages of sedimentation which exhibit an overall thickening and coarsening upward of the laminae (see Fig. 7). Silt grade clastic grains present within the coarser grained fraction are angular to subangular in shape with a low sphericity. These detrital grains are mainly composed of monocrystalline quartz.

The curved to planar normal faults downthrow towards the south or south-southwest and resulted in the tilting of bedding (Fig. 7). In detail, the individual fault planes are relatively diffuse and lack an obvious plane of dislocation. Minor drag folding and slightly larger scale warping of the sedimentary has been recognised associated with the faults. Extension which occurred during faulting resulted in the opening of these gently to moderately dipping normal faults allowing the migration of pore water along these brittle structures. The migration of water along some of the structures resulted in the localised staining of the sediment within the adjacent hanging wall and footwall. However, zones of reddening are also present which are not associated with any faulting or fracturing. These zones cross-cut bedding, but the lamination can be seen to pass straight through the zone without any obvious off-set. Water migration within these zones is, therefore, considered to have been intergranular.

Irregular to rounded clay cutan filled water escape conduits are also present.

Unit 2 **–** is composed of a variably disrupted and fluidised layer of clay and silt (Fig. 7). The silty laminae have undergone varying degrees of liquefaction and mobilisation. This accompanied soft-sediment deformation and fragmentation of the clay laminae. Small-scale deformation structures present include disharmonic convolute-style folds and flame structures. The clay laminae possess a locally well-developed bedding-parallel plasmic fabric which is deformed by the later deformation structures. This microtextural relationship indicates that the plasmic fabric developed prior to deformation, possibly in response to loading/compaction. Compaction would have resulted in the dewatering of the clay leading to its more brittle response to deformation. The laminated silts and clays are cut by an irregular layer or veinlet of variably mixed silt, coarse silt and very fine-grained sand which was injected into Unit 2 during the later stages of soft-sediment deformation.

Unit 3 **–** is composed of weakly laminated, matrix-poor, moderately sorted, fine-grained sand which possesses a moderate to open packed, grain supported texture (Fig. 7). This sand layer is lithologically similar to, and correlated with the sand (Unit 3) present within sample N2844. The lamination within the sand is defined by a variation in the modal proportion of a orange-brown clay cutan cement. These cemented layers possess an dilated, open to very open packed, cement supported texture. The clay cement is highly birefringent and is similar to the clay cutan observed elsewhere within the sample.

Unit 4 **–** is composed of finely laminated silt and clay which record an overall thickening and weakly coarsening upward sequence (Fig. 7). Individual laminae are normally graded with the grading being reflected by a slight change in colour from pale brown silt at the base, to darker brown more clay-rich sediment at the top. The lamination at the base of the Unit is deformed by

rare normal faults and broad, open warp-like folds. Minor drag-folding was noted associated with the faults.

4.7 SAMPLE N2846

Sample Number: ERP 7. **Registered Number:** N2846. **Location:** Small Holmes Farm [NY 29732 73398]. **Location Number:** NY27SE. **Lithology:** laminated clay and silt collected from southern end of section, trend of section 029°.

Description: This thin section is mainly composed of laminated silt and clay (Fig. 8). For ease of description the sample has been subdivided into two main units.

***Unit 1* –** is approximately 50 mm thick and is composed of laminated coarse silt (Fig. 8). The lamination is defined by the variation in modal clay and the occurrence of a orange-brown (under plane polarised light) clay cement. The clay cement is highly birefringent and is similar to the clay cutan observed filling water escape conduits and fissures. In general the silts contain only a small proportion of clay minerals and possess a closely packed, clast supported texture. Clastic grains are angular to subangular in shape with a low sphericity. The clasts are mainly composed of monocrystalline quartz within minor to accessory plagioclase, opaque minerals, muscovite/white mica, tourmaline, chlorite and biotite. Occasional fine sand-grade clasts are also present within the coarser grained laminae. These are composed of basalt rock fragments and occasional clasts of polycrystalline quartz. The basalt lithic clasts were possibly derived from the Birrenswark Volcanic Formation.

Irregular patches of red-brown hematitic stain have been noted within the silty laminae. Unit 1 also contains an irregular pocket of sandy material (Plate 10a and Fig 8). The sand is mainly composed of monocrystalline quartz with occasional lithic fragments of fine-grained quartz arenite. This sandy material also contains broken, coarse sand to granule sized clasts of basalt (Plate 10a). The lamination within the adjacent silts is disrupted indicating that the sand was probably forcefully injected into these sediments. This conclusion is supported by the presence of irregular patches of red-brown, highly birefringent clay cutan within the sand.

***Unit 2* –** is composed of laminated silt which contains broken fragments of laminated to massive clay (Fig. 8). The silts are compositionally/lithologically similar to the underlying sediments of Unit 1. The lamination is defined by a slight variation in the clay content of the sediment, with the units containing two relatively discrete, relatively clay-rich horizons (Fig. 8). The fragments of clay within the silt are angular to very angular in shape with a low sphericity. These clasts possess sharp to locally diffuse margins and have undergone very little obvious plastic deformation. This evidence suggests that these clay rip-up clasts acted as relatively rigid blocks during erosion and transport.

These laminated silts are cut by two prominent water escape features (Fig. 8) which are filled by massive, fluidised silt which contains lenticular to elongate veinlets of clay cutan (Plate 10b).

4.8 SAMPLE N2847

Sample Number: ERP 8. **Registered Number:** N2847. **Location:** Small Holmes Farm [NY 29732 73398]. **Location Number:** NY27SE. **Lithology:** mottled clay and silt, trend of section 118°.

Description: This thin section is composed of highly disrupted, originally laminated silt and clay (Fig. 9) which is lithologically similar to Unit 2 within sample N2846. The lamination within this sample is diffuse and has been distorted/disrupted resulting in a distinctive mottled appearance to the sample at very low magnifications. Two distinct relatively clay-rich laminae (see Fig. 9) present within the sample are internally disrupted. Soft-sediment deformation resulted in the formation of flame and load structures along the base of these clay-rich layers. The lamination within the silts is deformed by a set of diffuse disharmonic folds. The sample is cut by a number of water escape structures which appear to have formed during disruption and soft-sediment deformation. The complexity of deformation and disruption of the unit is consistent with it having occurred in repose to liquefaction. These sediments may, therefore, represent a fine-grained mass-flow deposit.

4.9 SAMPLE N2848

Sample Number: ERP 9. **Registered Number:** N2848. **Location:** Kelhead Quarry, Cummertrees [NY 1511 6932]. **Location Number:** NY16NW ME267. **Lithology:** red diamicton, sample taken approximately 2.0 m down from top of unit.

Description: This thin section is of a poorly sorted, immature, very open packed, matrix supported, massive diamicton with a reddened silty sand matrix (Fig. 10 and Plates 10c and d). Large clasts within the diamicton are angular to rounded in shape, with a low sphericity and range from very coarse sand to small pebble in size (Fig. 10). Rare to occasional moderate sphericity clasts are also present These coarse grained clasts are mainly composed of sedimentary and igneous rock fragments. Recognisable lithologies present include: quartzose litharenite; variably carbonate replaced litharenite and feldspathic litharenite; altered olivine microporphyritic alkali basalt; siltstone; quartz arenite, quartz arenite with a replacive hematitic cement, altered basaltic rock; polycrystalline quartz, mudstone; hematised mudstone, plagioclase-olivine-microporphyritic alkali basalt; sandy limestone; carbonate replaced siltstone, cherty rock; bioclastic (crinoidal) limestone (Plate 10d); polycrystalline carbonate hematised basalt;; shelly/ostracod-rich Fe-stained limestone or ironstone. The litharenites, siltstones and wacke sandstone rock fragments were probably derived from the Silurian in age Hawick and/or Riccarton groups of the Southern Uplands. In contrasts, the limestones and quartz arenites were probably derived from the much younger Carboniferous strata, with the basaltic volcanic rocks having come from the Birrenswark Volcanic Formation. A number of the quartz arenite lithic clasts are very irregular in shape, with a number of these large clasts representing broken fragments of much larger grains.

There is a clear break in the grain size distribution between the large clasts and the finer grained detritus present within the sandy matrix. These coarse silt to sand grade clasts are angular to subangular in shape with a low to moderate sphericity. Rare rounded, moderate sphericity detrital grains were also noted. The detrital assemblage is dominated by monocrystalline quartz and subordinate to minor lithic fragments. These lithic fragments are composed of the same range of lithologies as the coarser grained clasts. Other minor to accessory detrital components present include plagioclase, mudstone, polycrystalline quartz, chlorite, muscovite/white mica, carbonate, cleaved mudstone/siltstone, opaque minerals and microcline. No granitic lithic clasts have been recognised within this diamicton.

The matrix to the diamicton is massive and lacks any obvious plasmic fabric. However, the subsequent hematitic staining of the matrix and/or the presence of finely disseminated carbonate within the matrix may mask any plasmic fabric, if developed. Circular and arcuate arrangements

of silt and sand grade clasts have been noted (Plate 11a). These locally form crudely concentric shells around the larger lithic fragments. These larger clasts may also be enclosed within a haloe or coating of clay-rich material. Rare clay-lined fissures and fractures have been noted within the matrix of the diamicton.

A weak preferred orientation of elongate detrital grains has been recognised at low magnifications (see section 5).

4.10 SAMPLE N2849

Sample Number: ERP 10. **Registered Number:** N2849. **Location:** North Corbelly, near New Abbey [NX 9853 6337]. **Location Number:** NX96SE(N) CA1417. **Lithology:** middle part of till containing occasional rounded granite boulders.

Description: This thin section is of a poorly sorted, clast-rich, lithic-rich, high porosity, immature, essentially monolithic to very weakly heterolithic diamicton which possesses a moderate to open packed, matrix to locally clast supported texture (Fig. 11). The rock fragments range in size from sand grade up to pebble sized (*c*. 6.0 to 7.0 mm, to occasionally 10.0 mm in length). They are very angular to subangular in shape and possess a low sphericity Plate 11b and c). Minor rounding of the lithic clasts has been noted. The majority of the clasts (*c*. 90 to 95%) are composed of cleaved mudstone, siltstone and laminated siltstone (Plate 11b), and were derived from the underlying Silurian bed rock; the latter is exposed at the base of the section. The cleavage within these predominantly argillaceous rocks is defined by very fine-grained, shape-aligned white micas. The presence of this well-developed cleavage and, in some cases, sedimentary lamination partially controls the elongate shape of these lithic clasts. Other minor to accessory detrital components present within the diamicton include polycrystalline quartz, opaque minerals, very fine-grained sandstone or low-grade (sub-green schist facies) metasandstone, monocrystalline quartz, cataclastic fault rock and quartz-hematite vein material.

The elongate lithic clasts exhibit a variably developed preferred shape alignment. A number of fractured lithic clasts are present within this diamicton with cataclasis occurring due to the presence of pre-existing fractures within the rock fragments. Fragmentation of the larger lithic clasts also occurred along the tectonic cleavage present within these deformed low-grade metamorphic rocks. The very open packing of the diamicton suggests that fracturing/grain crushing was not caused by the pressure of the over-riding ice. Alternatively, cataclasis may have occurred due to freeze-thaw within a polythermal glacial environment and/or high pore water pressure resulting in localised failure of pre-existing planes of weakness. Minor rounding of the mudstone rock fragments has been recognised, indicative of at least some transport of this locally derived detritus.

The matrix to the diamicton is composed of green to grey-green clay to fine silt grade material (Plate 12a). The matrix appears to have been derived from degraded lithic clasts (rock flour) and is lacking in clay minerals. The siltstone and very fine-grained sandstone lithic clasts appear to have been more prone to disaggregation, grain reduction and incorporation into the matrix than the more common mudstone rock fragments. The matrix is only patchily developed within this diamicton and locally forms coating upon the lithic clasts. The limited amount of matrix, coupled with the open packing of the coarse-grained clasts results in a high porosity and permeability (see Fig. 11). These pore spaces are locally filled or partially filled by a bright orange-brown, highly birefringent clay cutan (Plate 11b). This clay possesses a well-developed plasmic fabric which mimics the shape of the void (Plate 11c). This fabric is, therefore, considered to have formed due to the plating of the clay plasma to the margins of the void during water flow. Locally the cutan forms a thin coating to voids with a thicker ‘geopetal-like’ in-fill (Plate 12a) at

the base of these water conduits. The initial 'plastering' of clay around the void during higher pore water flow may have resulted in the stabilisation of the voids and initiated cementation of the diamicton. Minor to trace amounts of a hematitic rim cement was noted developed upon some of the lithic clasts. The formation of this hematitic cement clearly pre-dated the deposition of the clay cutan.

4.11 SAMPLE N2850

Sample Number: ERP 11. **Registered Number:** N2850. **Location:** North Corbelly, near New Abbey [NX 9853 6337]. **Location Number:** NX96SE(N) CA1417. **Lithology:** lower part of till, sample taken from just above interface with bedrock.

Description: This thin section is of a poorly sorted, clast-rich, lithic-rich, high porosity, immature, essentially monolithic to very weakly heterolithic diamicton which possesses a moderate to open packed, matrix to locally clast supported texture (Fig. 12). This sample is lithologically similar to N2849, but contains few exotic clasts with the clast assemblage being dominated by fragments of the local bed rock. The rock fragments range in size from sand grade up to pebble sized and are very angular to subangular in shape with a low sphericity (Fig. 12 and Plates 12b and c). Minor rounding of the lithic clasts has been noted. The majority of the clasts (*c*. 90 to 95%) are composed of cleaved mudstone, siltstone and laminated siltstone, and were derived from the underlying Silurian bedrock. The cleavage within these predominantly argillaceous rocks is defined by very fine-grained, shape-aligned white mica. The presence of this well-developed cleavage and, in some cases, sedimentary lamination partially controls the elongate shape of these lithic clasts.

The elongate lithic clasts exhibit a variably developed preferred shape alignment (see section 5). A number of fractured lithic clasts are present within this diamicton with cataclasis occurring due to the presence of pre-existing fractures within the rock fragments. As in sample N2849, there is no evidence to suggest that fragmentation was caused by grain crushing due to the pressure of the over-riding ice. Consequently, cataclasis is thought to have occurred due to either freeze-thaw within a polythermal glacial environment and/or high pore water pressure resulting in localised failure of pre-existing planes of weakness.

The matrix to the diamicton is composed of green to grey-green clay to fine silt grade material (Plate 11c) and was primarily derived from degraded lithic clasts (rock flour). This silty material was also noted forming caps upon a number of the lithic clasts. These caps are indicative of water movement through the sediment and in some cases have been associated with periglacial activity. The limited amount of matrix, coupled with the open packing of the coarse-grained clasts results in a high porosity (see Fig. 12). These pore spaces are lined or partially filled by a bright orange-brown, highly birefringent clay cutan (Plate 12b). This clay possesses a well-developed plasmic fabric which mimics the shape of the void.

4.12 SAMPLE N2851

Sample Number: ERP 12. **Registered Number:** N2851. **Location:** Townhead Saw Mill, New Abbey [NX 9600 6620]. **Location Number:** NX96NE(S) CA1416. **Lithology:** gravely diamicton, sample taken from just above lower boulder pavement.

Description: This thin section is of a coarse-grained, immature, poorly sorted, high porosity, feldspar and lithic-rich, gravely diamicton which possess a matrix supported, open packed

texture (Fig. 13). The diamicton is mainly composed of detritus which has been derived from granodioritic to granitic source (Plate 13), represented by the near-by Criffle-Dalbeattie granite intrusion.

Clasts are angular, subangular to occasionally subrounded in shape with a low to rarely moderate sphericity (Plate 13). They typically equant in shape and range from fine sand to granule in size, with occasional small pebble (*c*. 7.0 to 8.0 mm in length) sized clasts also present. The lithic clasts are mainly composed of medium- to coarse-grained biotite-granite and hornblende-biotite-granodiorite (Plates 13a and b). The granodioritic rock fragments may possess a moderately to well developed pre-full crystallisation fabric. This foliation developed during the emplacement of the granite intrusion and is defined by shape aligned plagioclase and/or biotite and amphibole crystals. The presence of this foliation within the granodioritic lithic clasts suggests that they were derived from the foliated outer part of the Criffle-Dalbeattie granite. The finer grained detritus is mainly composed of fragmented granitic material which is dominated by plagioclase, K-feldspar, monocrystalline quartz and polycrystalline quartz. Other minor to accessory detrital phases present include biotite, amphibole, rounded mudstone rock fragments, fine sandstone, siltstone, opaque minerals, titanite, apatite and microcline.

Detrital plagioclase exhibits varying degrees of alteration to sericitic white mica (± epidote). Alteration of feldspar occurred prior to its incorporation within the diamicton and is probably associated with hydrothermal activity during the later stages of granite emplacement. The grain size of the diamicton appears to be partially controlled by the original grain size of the source granitic material. The latter appears to have been disaggregated during glaciation into individual crystals of its constituent minerals. This has also resulted in the overall ‘gravely’ texture of this diamicton.

Finer grained silt and clay grade matrix is a minor component within the diamicton and appears to have been derived from degraded mudstone lithic clasts. It typically occurs as diffuse patches or forming domed caps upon the tops of the larger detrital clasts (Plates 13c and d). These caps are formed in response to water movement through the sediment, which, in some cases, has been used to indicator subsequent periglacial activity. No plasmic fabrics have been recognised within this diamicton, possibly due to the limited amounts of matrix and/or absence of clay minerals.

5 Clast Shape Analysis

The clast-rich diamictons from the Solway area have also been used as part of a preliminary study to investigate the development of a preferred clast orientation within glacigenic sediments. The approach used here is similar to the Rf/θ method (Ramsay 1967) of strain analysis used by structural geologists and till clast macrofabric analysis used by glaciologists and Quaternary geologists (see Benn & Evans 1998). However, unlike the Rf/θ method the approach used her can not be used to estimate strain as in many cases the markers (i.e. clastic grains) are undeformed and acted as rigid bodies during deposition/deformation. Any preferred alignment of these markers is, therefore, considered to be due to the passive rotation of these clasts within an actively deforming matrix. Alignment of clasts may occur as a result of either primary sedimentary processes and/or subsequent deformation. The role of inheritance of a preferred shape alignment within diamictons has been largely overlooked in studies of till macrofabrics, with such fabrics being interpreted as having developed in response to an imposed deformation rather than resulting from an earlier sedimentary process (*c.f.* imbrication of pebbles in a fluvial deposit).

The aspect ratio (Rf) and orientation (θ in degrees) of coarse sand to pebble sized clasts within three samples (N2848, N2849, N2850) of diamicton have been measured in thin section under low magnification. Rf is the ratio of the short axis and long axis of the clast and θ the angle between the long axis and a datum (e.g. bedding or horizontal). The data obtained is displayed graphically (Figs. 14 to 18) and on a series of diagrammatic representations of the thin sections (Figs. 19 to 21). If a preferred shape alignment of elongate clasts is developed then the data should form a cluster on a plot of aspect ratio (Rf) versus long axis orientation (θ) (e.g. see fig 14a). The degree of clustering of the data broadly reflects the intensity of the this preferred alignment. The greater the spread or scatter in the data on the Rf/θ plot (e.g. Fig. 15a) records either a weakly developed or no fabric. The preferential alignment of clasts can also be established using histograms of long axis orientation (e.g. Fig. 14d) and/or rose diagrams (Fig. 18). These graphical methods will also show if the clasts exhibit more than one direction of long axis orientation (e.g. Fig 18b).

Sample N2848 is of a poorly sorted, immature, very open packed, matrix supported, apparently massive diamicton (see Fig. 10). Data obtained for this sample shows that the clasts in general possess an aspect ratio of < 2.5 (Figs. 14a and b), with a mean Rf of 1.96 (Table 2).

Table 2. Statistical data calculated for the aspect ratio of coarse sand to pebble sized clasts included within Sample N2848.

Mean	1.96
Standard Error	0.06
Median	1.75
Mode	2.00
Standard Deviation	0.68
Sample Variance	0.46
Kurtosis	3.95
Skew	1.76
Range	3.69
Minimum	1.11
Maximum	4.80
Count	126
Confidence Level (95.0%)	0.12

The data show a moderately developed cluster at a value of θ of approximately 45° to 50° (Fig. 14a) with this moderately well-developed preferred shape alignment also clearly seen on Figs. 14d and 18a. Importantly, the bulk of the clasts exhibit a positive value of θ (see Figs. 14c and d). This is consistent with the clasts dipping in an up ice direction and hence having been rotated towards the direction of ice movement. A second weakly developed alignment has also been recognised at approximately 80° to 85° (Fig. 14d and 18a). The relationship between these two preferred alignment fabrics is shown in Fig 19. Figure 19a shows the orientation and length of both the long and short axes of the clasts measured in sample N2848 and there relationship to a horizontal datum. Orientation data for the long axes of these clasts were then extracted in order to establish if there is a consistent pattern of long axis orientation within the sample (Fig. 19b). The resultant pattern (dotted lines of Fig. 19b) clearly shows the main preferred alignment at

approximately 45° to 50°. This fabric appears to have a crudely domainal appearance consisting of discrete zones in which the clasts show a pronounced alignment. In the domains were this main fabric is less pronounced the clasts appear to preserve a ?earlier fabric at approximately 80° to 85° (Fig. 19b). This apparently earlier alignment has been largely overprinted by the main foliation. The first fabric is now preserved within domains where the second fabric is apparently less well developed and immediately adjacent to a larger lithic clast (Fig. 19b).

In the lower right hand quadrant of the thin section the clasts define a foliation which wraps around a large lithic clast (Fig. 19b). This large rock fragment is orientated antithetic to the direction of ice movement (i.e. dipping in adown-ice direction) and probably formed a rigid object within the deforming finer grained matrix of the diamicton.

The domainal nature of the dominant shape alignment fabric within this sample may be interpreted as either recording the partitioning of either deformation or flow within the diamicton either after or during deposition. No obvious plasmic fabric or other deformation related microstructures have been noted in this thin section, suggesting that alignment of the clasts may be a primary depositional feature of this deposit. Consequently, the development of clasts alignments within diamictons may record flow rather than subsequent solid state deformation.

Sample N2849 is of a poorly sorted, clast-rich, lithic-rich, high porosity, immature, essentially monolithic to very weakly heterolithic diamicton which possesses a moderate to open packed, matrix to locally clast supported texture (see Fig. 11). Data obtained for this sample shows that the clasts in general possess an aspect ratio of < 2.5 (Figs. 15a and b), with a mean Rf of 1.86 (Table 3).

Table 3. Statistical data calculated for the aspect ratio of coarse sand to pebble sized clasts included within Sample N2849.

Mean	1.89
Standard Error	0.05
Median	1.75
Mode	2.00
Standard Deviation	0.61
Sample Variance	0.37
Kurtosis	2.65
Skew	1.34
Range	3.33
Minimum	1.00
Maximum	4.33
Sum	299.03
Confidence Level(95.0%)	0.09

The data shows two weakly developed clusters on Fig 15a at a value of θ of approximately - 20° and + 25° to 30°. The presence of two weakly to moderately developed preferred shape alignment fabrics can also be seen on Figs. 15c, 15d and 18ab. Both positive and negative values of θ have been recorded (see Figs. 15c, 15dand 18b) suggesting that the clasts do not exhibit a single relationship to the direction of ice movement in this sample. A weakly developed sub-

vertical fabric (θ = 75° to 80°) can also be seen on Fig. 18b. The relationship between the main preferred alignment fabrics is shown in Fig 20. Figure 20a shows the orientation and length of both the long and short axes of the clasts measured in sample N2848 and there relationship to the horizontal datum. Orientation data for the long axes of the clasts within the sample indicates that the two preferred alignment fabrics show an apparent cross cutting relationship (Fig. 20b).

Sample N2850 is of a poorly sorted, clast-rich, lithic-rich, high porosity, immature, essentially monolithic to very weakly heterolithic diamicton which possesses a moderate to open packed, matrix to locally clast supported texture (see Fig. 12). Visual examination of this thin section at low magnification revealed that the clasts in the upper part of the sample exhibit a different direction of preferred shape alignment (see Fig. 21). Consequently, the thin section was divided into two and clast orientation data for these two areas considered independently. Data obtained for lower part of the sample show that, in general, the clasts possess an aspect ratio of < 2.8 (Figs. 16a and b), with a mean Rf of 2.4 (Table 4). Clasts from the upper part of the thin section possess a mean Rf of 2.0 (Figs. 17a and b, and Table 5). The elongate nature of the clasts is partially controlled by the presence of a well-developed cleavage within the low-grade metasedimentary rock fragments which dominate the clast assemblage within this diamicton. The slight decrease in aspect ratio in the upper part of the thin section may possibly related to the onset of abrasion of the clasts, leading to a modification in shape and aspect ratio. This is tentatively supported by the slightly more rounded nature of these typically angular clasts within the upper part of the sample (see Fig 12).

Table 4. Statistical data calculated for the aspect ratio of coarse sand to pebble sized clasts included within lower part of Sample N2850.

Mean	2.40
Standard Error	0.09
Median	2.16
Mode	2.00
Standard Deviation	0.96
Sample Variance	0.93
Kurtosis	0.46
Skew	0.98
Range	4.30
Minimum	1.08
Maximum	5.38
Sum	278.78
Confidence Level(95.0%)	0.18

Table 5. Statistical data calculated for the aspect ratio of coarse sand to pebble sized clasts included within upper part of Sample N2850.

Mean	2.00
Standard Error	0.09
Median	1.80

Mode	2.00
Standard Deviation	0.79
Sample Variance	0.63
Kurtosis	3.52
Skew	1.53
Range	4.38
Minimum	1.00
Maximum	5.38
Sum	156.11
Confidence Level(95.0%)	0.18

The data for the lower part of the thin section exhibits a moderately developed cluster at a value of θ of approximately 30° to 40° on Fig. 16a. This moderately well-developed preferred shape alignment also clearly seen on Figs. 16d and 18c, with the bulk of the clasts exhibit a positive value of θ (see Figs. 16c and d). The slight spread in the orientation data is possibly due to nearest neighbour effects within this clast-rich diamicton. In contrast to the lower part of the sample, orientation data for the upper part of the thin section reveals that the clasts define two alignment fabrics; one at approximately 40° to 50°, and a send low-angle fabric at c. 10° (Figs. 16c, 16d and 18d). The steeper of the two fabrics is comparable to that developed within the lower part of the sample.

The relationship between the fabrics in both the upper and lower parts of the sample is shown in Fig 21. Figure 19a shows the orientation and length of both the long and short axes of the clasts measured in sample N2850 and there relationship to a horizontal datum. The long axes of these clasts and the pattern of alignment (dotted lines of Fig. 21b) clearly highlights the marked contrast in clast orientation between the upper and lower parts of the thin section. The boundary between these two areas is sharp, but is deflected by the presence of a large lithic clast in the lower part of the sample (see Figs 12 and 21b).

The lower half of the thin section is dominated by a single fabric occurring at an angle of 30° to 40°. Importantly, sample N2850 was collected form just above the interface with the underlying bedrock and the angle of dip of this fabric is comparable to that of the regional tectonic cleavage developed within these Lower Palaeozoic sedimentary rocks. Consequently, this alignment fabric is interpreted as having been controlled by the underlying bedrock. Furthermore, it indicates that there has been very little rotation of the clasts during fragmentation of the substrata and their incorporation into the overlying diamicton. This fragmentation process may have occurred in response to freeze-thaw processes and/or high pore water pressure; the latter leading to hydrofracturing along the cleavage which represents a pre-existing plane of weakness within the bedrock. The low-angle fabric within the upper part of the sample clearly post-dates this ‘inherited’ alignment fabric and is, therefore, interpreted as having been imposed due to displacement within the diamicton leading to clast rotation. This second fabric is crudely domainal in nature with the earlier bedrock related fabric being preserved between these domains. The presence of a domainal fabric within sample N2850 indicates that clast rotation may not occur throughout the diamicton, but is focused into discrete zones of displacement.

The identification of alignment fabrics within this clast-rich diamicton has potentially important implications for the processes involved in the incorporation of bedrock fragments into sub-glacially formed diamictons. The presence of an alignment fabric which preserves the original orientation of the tectonic cleavage within bedrock indicates that fragmentation may not involve rotation and may simply result in the expansion of the bed rock due to fracturing along pre-existing planes of weakness. The clearly ‘inherited’ nature of this clast fabric also means that

even if a diamicton possesses a clast macrofabric it does note necessarily infer that this fabric was formed as a result of deformation.

6 Conclusions and Interpretations

A number of conclusions/interpretations can be made based upon the detailed examination of these large forma thin sections of the Quaternary sediments exposed in the Solway area:

1. Sample N2840 and N2841 are lithologically similar and are composed of finely bedded or laminated silt, clay and very fine-grained sand. Small-scale deformation structures, where present, occur in discrete horizons and may be related to soft sediment deformation during slumping or as a result of partitioning of deformation during the subsequent overriding of the sediments by glacier ice. Soft sediment deformation was accompanied by the variable fluidisation of the silty laminae.
2. The network of bands or zones of Fe-staining within sample N2840 and N2841 are not related to discrete fractures. These features are interpreted as having formed due to Fe oxidation during intergranular flow of pore water.
3. The normally graded silt to clay layers within sample N2841 also contain coarse silt to sand grade clasts which increase towards the clayey tops of these packages resulting in an overall reverse graded appearance. The presence of these coarser grained clasts within the clayey tops of these laminated sediments may possibly have been deposited as ‘rain-out’ from decaying floating ice.
4. A bedding-parallel plasmic fabric present within the clay-rich laminae is interpreted as having developed at an early stage during compaction and dewatering of these sediments.
5. Clay cutan filled water escape conduits and related structures are present in all the samples examined from Plumpe Farm. The well developed plasmic fabric(s) within the cutan is thought to have formed due to the plating of the clay plasma against the margins of the conduit during fluid flow. The subsequent disruption of this fabric may have occurred during either: a later phase of fluid flow due to an increase in pore water pressure which exceeded the cohesive strength of the clay cutan; or as a result of partial collapse of the void due to compaction of the sediment. A number of these microscopic “channel-fills” record several phases of water discharge/flow indicating that such features were relatively stable and active for a period of time. The age of these structures is unknown, but it is possible that they may have developed during the later stages of dewatering of the sediment in a subglacial environment.
6. The stratified till from Plumpe Farm (N2842) is composed of laminated silt and clay layers interbedded with diamicton layers containing rounded to elongate till pebbles (Type 1 till pebbles of van der Meer 1983). The till pebbles are essentially undeformed, but are contained within a clay matrix which possesses a well developed plasmic fabric. This matrix locally grades into recognisable water escape features with morphology of the plasmic fabric being comparable to that present within the clay. Consequently, the formation of the till pebbles is thought to have occurred during fluidisation and mixing of two rheologically distinct sediments. The presence of these mixing textures near the base of the diamicton unit at Plumpe Farm suggests that the glacier was overriding water saturated sediments. The water-rich nature of these sediment may also explain the very

little evidence of deformation within the underlying laminated silts and clay represented by samples N2840 and N2841.

7. In contrast to sample N2842, the overlying diamicton, represented by N2843, possesses a weak stratification defined by diffuse clay-rich layers. This more massive till is compositionally similar to the underlying diamicton and may, therefore, have undergone a greater degree of mixing.
8. Coarse sand to small pebble sized lithic clasts within the diamicton (N2842 and N2843) exposed at Plumpe Farm are mainly composed of sandstone and siltstone rock fragments derived from the Ordovician-Silurian sequence of the Southern Uplands. Importantly, one of these wacke sandstone lithic clasts contains detrital Na-amphibole indicating that it was derived from the Portpatrick Formation which is exposed within the Ordovician northern belt of the Southern Uplands terrane. Detrital glaucophane is unique to the Portpatrick Formation. Other rock fragments were derived from the Carboniferous in age Birrenswark Volcanic Formation (altered olivine basalt) and Carboniferous or Permo-Triassic strata (quartzose sandstone) exposed in the Solway area.
9. The laminated silts and clay (N2844 and N2845) exposed at Small Holmes Farm are locally deformed by a set of low-angle, curved to planar normal faults which downthrow towards the south or south-southwest. Microtextural relationships suggest that normal faulting was syn-sedimentary in nature and was clearly associated with extension possibly as a result of localised gravity induced sliding. The faulted units are immediately overlain by a unit which has undergone soft sediment deformation and is injected by fluidised matrix-poor sand. This sand locally possesses a cement composed of clay cutan and may contain fragments of the adjacent clay/silt laminae.
10. Sample N2846 and N2847 occur above and are lithologically similar to the laminated silts and clay. In sample N2847, however, these originally laminated sediments have been distorted/disrupted resulting in a distinctive mottled appearance. The complexity of deformation and disruption of the unit is consistent with it having occurred in repose to liquefaction. These sediments may, therefore, represent a fine-grained mass-flow deposit.
11. The poorly sorted, matrix supported diamicton (N2848) exposed at Kelhead Quarry, Cummertrees contains angular to rounded coarse sand to small pebble sized clasts composed of sedimentary and igneous rock fragments. The litharenites, siltstones and wacke sandstone rock fragments were probably derived from the Silurian in age Hawick and/or Riccarton groups of the Southern Uplands. In contrasts, the limestones and quartz arenites were derived from the younger Carboniferous strata, with the basaltic volcanic rocks having come from the Birrenswark Volcanic Formation.
12. Samples N2849 and N2850 are lithologically similar and are composed of poorly sorted, lithic-rich, diamicton which possesses a moderate to open packed, matrix to locally clast supported texture. The rock fragments which dominate these samples are composed of cleaved mudstone, siltstone and laminated siltstone which were derived from the underlying Silurian bedrock. The matrix to the diamicton is composed of green to grey-green clay to fine silt grade material, derived from degraded lithic clasts (rock flour). Voids within these high porosity deposits spaces are variably filled by clay cutan; the later having been deposited by percolating pore water.
13. The coarse-grained, feldspar and lithic-rich, gravely diamicton exposed at Townhead Saw Mill, New Abbey is mainly composed of detritus which has been derived from the near-by Criffle-Dalbeattie granite intrusion. The presence of an igneous foliation within the granodioritic lithic clasts suggests that they were derived from the foliated outer part of this intrusion. Fine grained silt and clay grade material within the diamicton typically forms domed caps upon the tops of the larger detrital grains. These caps are formed in

response to water movement through the sediment, which, in some cases, has been used to indicator subsequent periglacial activity.

Glossary

Cleavage – A fabric developed within a metamorphic rocks defined by a sub-parallel set of closely spaced approximately planar surfaces produced during rock deformation. Defined by the preferred alignment of platy or elongate mineral grains (usually phyllosilicate minerals such as muscovite, biotite, chlorite).

Cement supported – Describes a fragmentary deposit where the detrital grains are, to varying degrees, isolated/supported within the cement.

Cement – The material bonding the fragments of clastic sedimentary rocks together and which was precipitated between the grains after deposition.

Clast supported – Describes a fragmentary deposit where all the detrital grains are in contact.

Detritus – A general term for fragmentary material, such as gravel, sand, clay, worn from rock by disintegration. Detrital grains in clastic sedimentary rocks may be composed of single mineral grains (e.g. monocrystalline quartz, plagioclase), polycrystalline mineral grains (e.g. polycrystalline quartz) or lithic fragments including sedimentary, igneous and metamorphic rock fragments.

Grain size – Refers to the size of fragmentary material present in unconsolidated sediments and sedimentary rocks: (a) clay < 0.0039 mm in size; (b) silt, 0.0039 to 0.0625 mm in size; (c) fine sand, 0.0625 to 0.25 mm in size; (d) medium sand, 0.25 to 0.5 mm in size; (e) coarse sand, 0.5 to 1.0 mm in size; (f) very coarse sand, 1.0 to 2.0 mm in size; (g) granules 2.0 to 4.0 mm in size; (h) pebbles 4.0 to 64 mm in size.

Lattisepic plasmic fabric – A term used to describe a plasmic fabric developed within an unconsolidated sediment defined by short orientated domains in two perpendicular directions (van der Meer 1993).

Matrix – Material, usually clay minerals or micas, forming a bonding substance to grains in a clastic sedimentary rock. The matrix material was deposited with the other grains or developed authogenically by diagenesis or slight metamorphism. Also used more generally for finer grained material in any rock in which large components are set.

Matrix supported – Describes a fragmentary deposit where the detrital grains are, to varying degrees, isolated/supported within a finer grained matrix.

Micromorphology – A term used to describe the study of unconsolidated glacial sediments in thin section using a petrological microscope.

Omnisepic plasmic fabric – A term used to describe a plasmic fabric developed in an unconsolidated sediment in which all the domains have been reoriented (van der Meer 1993).

Packing – Describes, as the term suggests, how closely the individual detrital grains are packed together within a fragmentary deposit. The term closely packed is used where all the grains are in contact and there is very little obvious matrix or cement; moderately packed and open packed are used with an increase in the porosity, matrix and/or cement.

Plasmic fabric – A term used to describe the optical arrangement of high birefringent clay plasma/domains within an unconsolidated sediment which are visible under crossed polarised light using a petrological microscope.

Porosity – The volume of voids expressed as a percentage of the total volume of the sediment or sedimentary rock.

Phyllite – A well-cleaved metamorphosed mudstone characterised by a distinctive sheen on foliation surfaces; generally of intermediate grain size and metamorphic grade between slate and schist.

Pressure shadow – A region of low strain developed immediately adjacent to a rigid or competent object in a rock (e.g. a garnet porphyroblast).

Pseudomorph – A mineral or aggregate of minerals having taken the form/shape of another mineral phase that it/they have replaced.

Rounded – Describes the smoothness of the surface of a detrital grain present within a sediment or sedimentary rock. The terms *well-rounded*, *rounded*, *subrounded*, *subangular*, *angular*, *very angular* are used to describe the increasingly angular/irregular/rough nature of the surface of detrital grains.

Skelsepic plasmic fabric – A term used to describe a plasmic fabric developed within an unconsolidated sediment in which the orientated domains occur parallel to the surface of large grains (van der Meer 1993).

Sorting – Well sorted describes a fragmentary deposit in which all the detrital grains are of approximately uniform size. In reality most fragmentary deposits contain a range of grain sizes and can be described as moderately sorted, poorly sorted or in extreme cases unsorted.

Sphericity – Describes the how closely a detrital grains present within a sediment or sedimentary rock approximates to a sphere. The terms low sphericity, moderate sphericity and high sphericity are used to describe how spherical (ball-like) the detrital grains are.

Schist – A metamorphic rock of broadly pelitic composition (i.e. a metamorphosed mudstone) with a well-developed schistosity.

Schistosity – A planar structure developed in a metamorphic rock defined by the alignment of elongate minerals such as micas and amphibole.

Unistrial plasmic fabric – A term used to describe a planar plasmic fabric developed with an unconsolidated sediment defined by relatively continuous domains which is typically observed defining discrete shears (van der Meer 1993).

References

Most of the references listed below are held in the Library of the British Geological Survey at Edinburgh and in Keyworth, Nottingham. Copies of the references may be purchased from the Library subject to the current copyright legislation.

BENN, D. I., EVANS, D. J. A. 1998. *Glaciers and Glaciation*. (London: Arnold).

MENZIES, J. 2000. Micromorphological analyses of microfabrics and microstructures indicative of deformation processes in glacial sediments. *In* Maltman, A. J., Hubbard, B. & Hambrey, J. M. (eds) *Deformation of Glacial Materials*. Geological Society, London, Special Publication. **176**, 245-257.

OSTRY, R. C. & DEANE, R. E. 1963. Microfabric analyses of till. *Geological Society of America Bulletin.* **74**, 165-168.

PASSCHIER, C. W. & TROUW, R. A. J. 1996. *Microtectonics*. Springer.

PHILLIPS E. R. & AUTON C. A. 1998. *Micromorphology and deformation of a Quaternary glaciolacustrine deposit, Speyside, Scotland.* British Geological Survey Technical Report**. WG/98/15**.

VAN DER MEER, J. J. M. 1987. Micromorphology of glacial sediments as a tool in distinguishing genetic varieties of till. In *INQUA Till Symposium*, Finland 1985. KUJANSUU, R. & SAARNISTO, M (editors). Geological Survey of Finland, Special Paper **3**, 77-89.

VAN DER MEER, J. J. M. & LABAN, C. 1990. Micromorphology of some North Sea till samples, a pilot study. *Journal of Quaternary Science*. **5**, 95-101.

VAN DER MEER, J. J. M., RABASSA, J. O. & EVENSON, E. B. 1992. Micromorphological aspects of glaciolacustrine sediments in northern Patagonia, Argentina. *Journal of Quaternary Science*. **7**, 31-44.

VAN DER MEER, J. J. M. 1993. Microscopic evidence of subglacial deformation. *Quaternary Science Reviews*. **12**, 553-587.

VAN DER MEER, J. J. M. & VEGERS, A. L. L. M. 1994. The micromorphological character of the Ballycroneen Formation (Irish Sea Till): a first assessment. *In* WARREN & CROOT (eds.) *Formation and Deformation of Glacial Deposits*. Balkema, Rotterdam. 39-49.

RAMSAY, J. G. 1968. *Folding and Fracturing of rock.* (McGraw & Hill.).

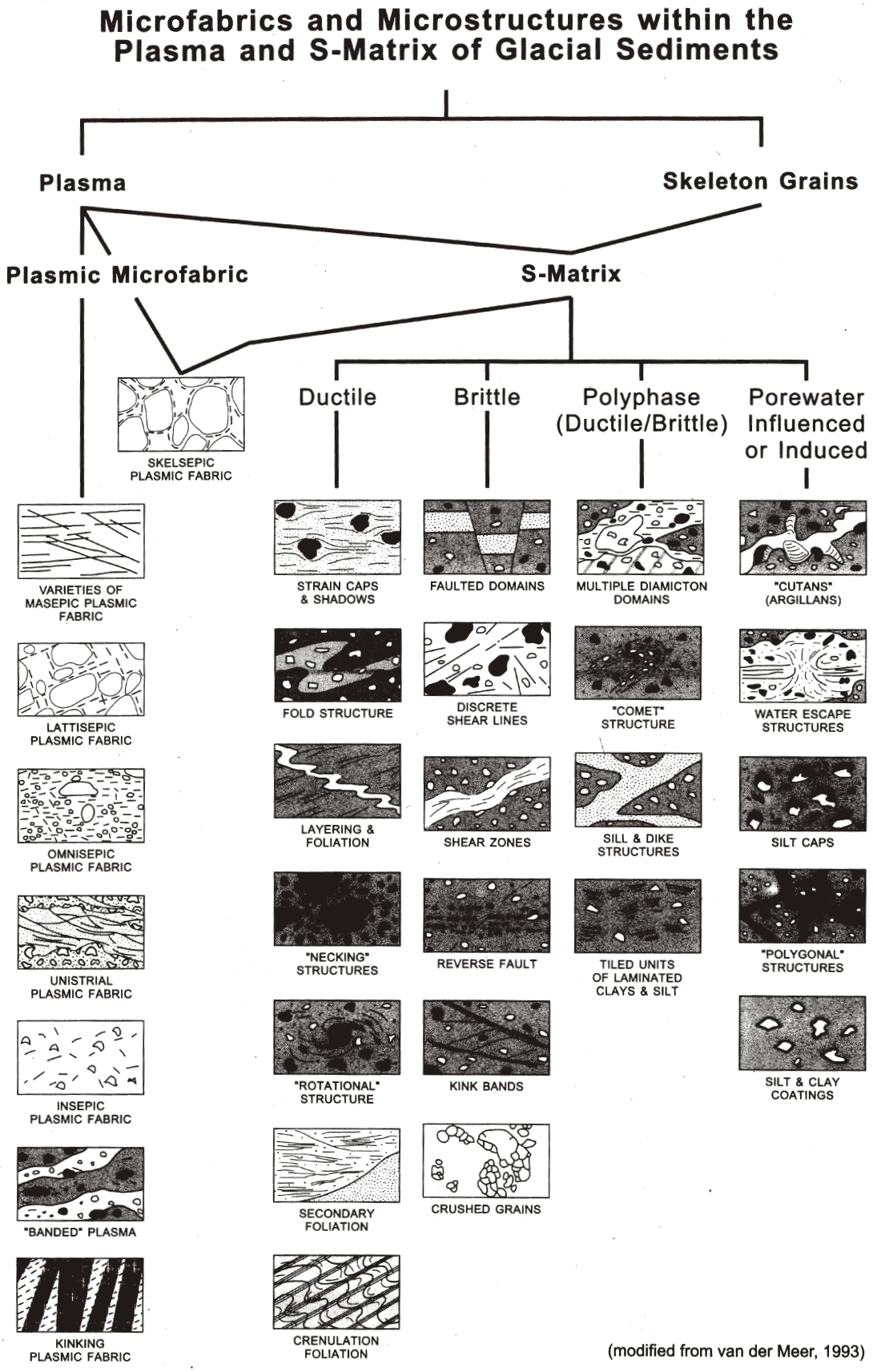

Fig. 1. Microfabrics and microstructures developed within glacial deposits (taken from Menzies 2000).

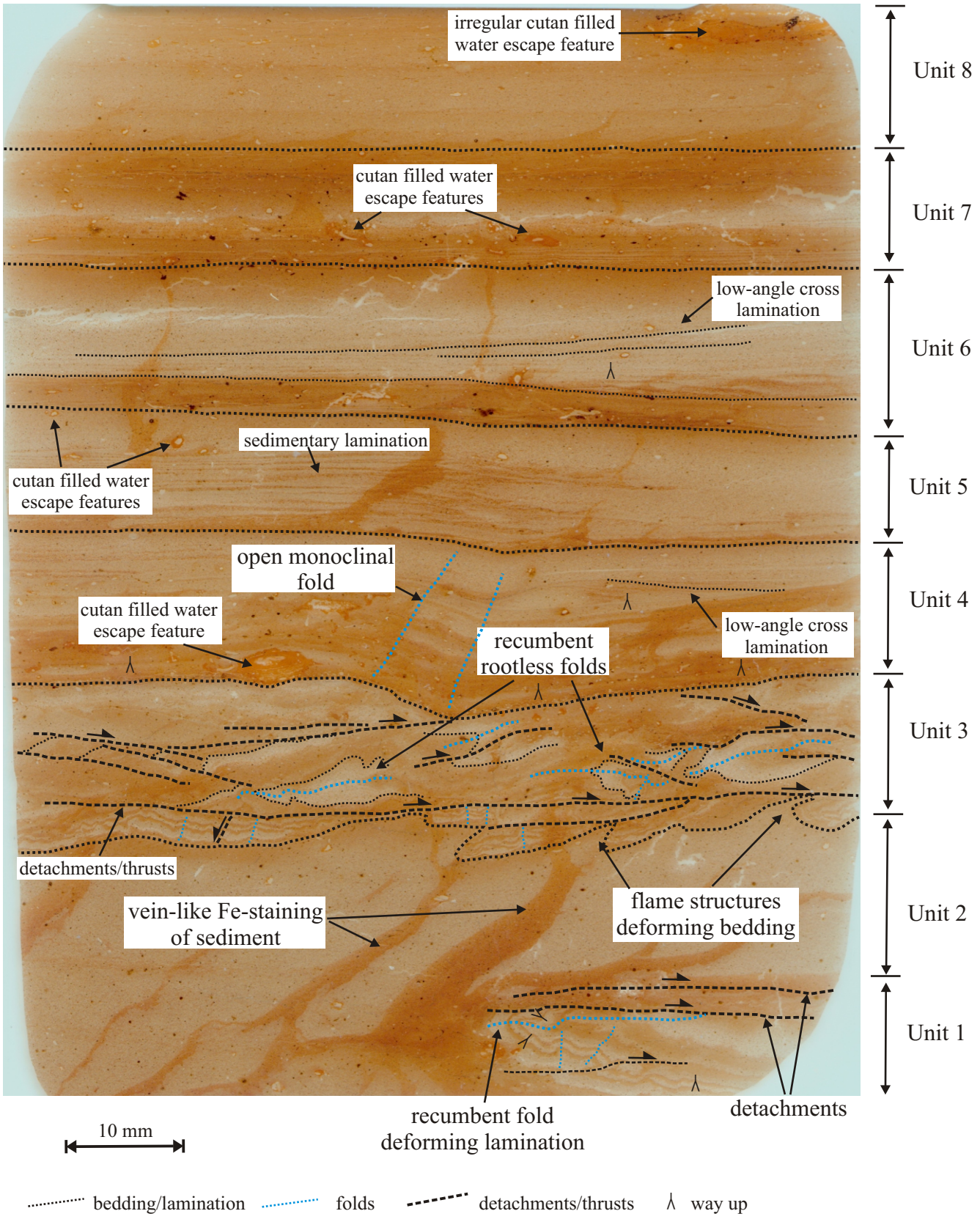

Fig. 2. Annotated scanned image of sample N2840.

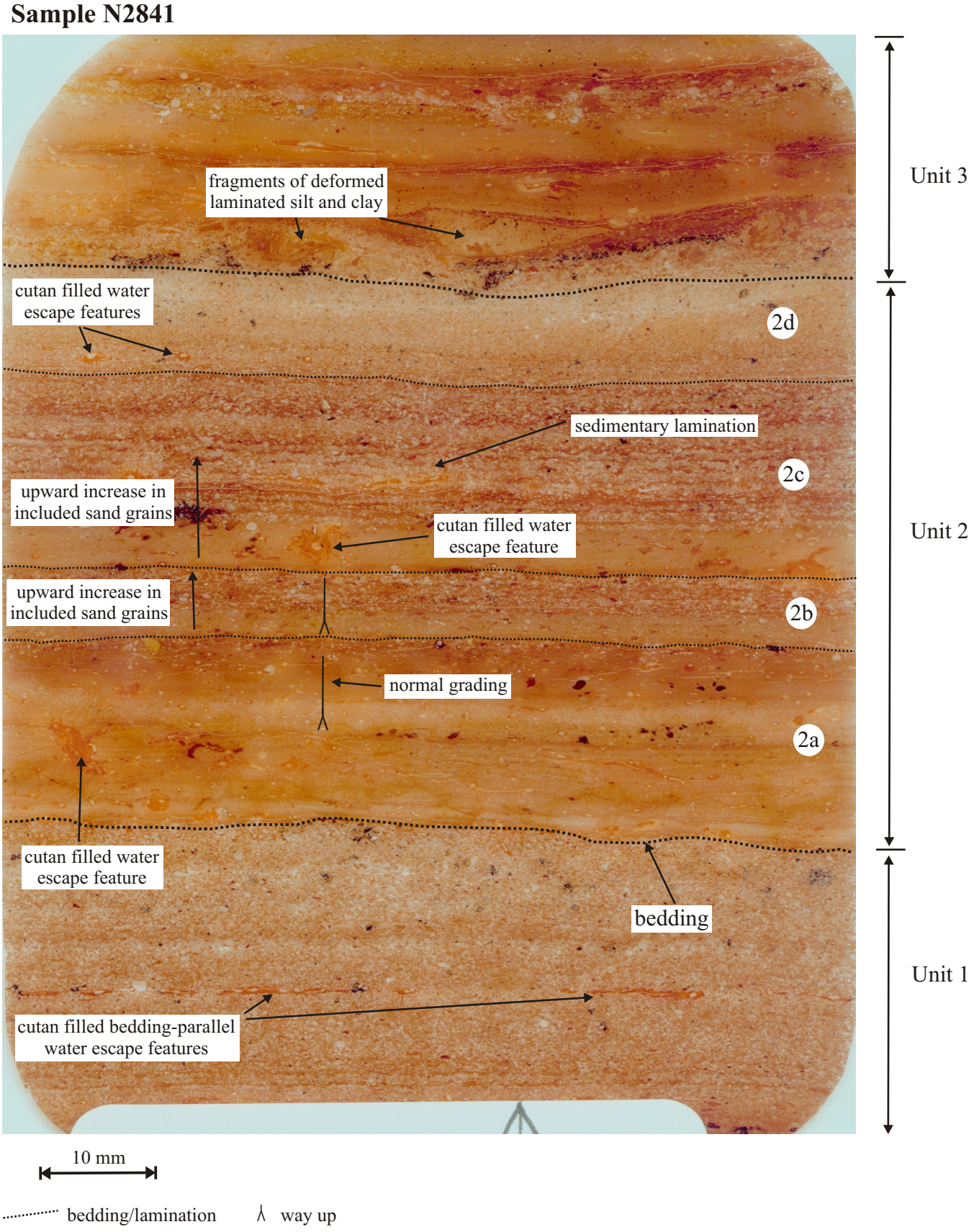

Fig. 3. Annotated scanned image of sample N2841.

Sample N2842

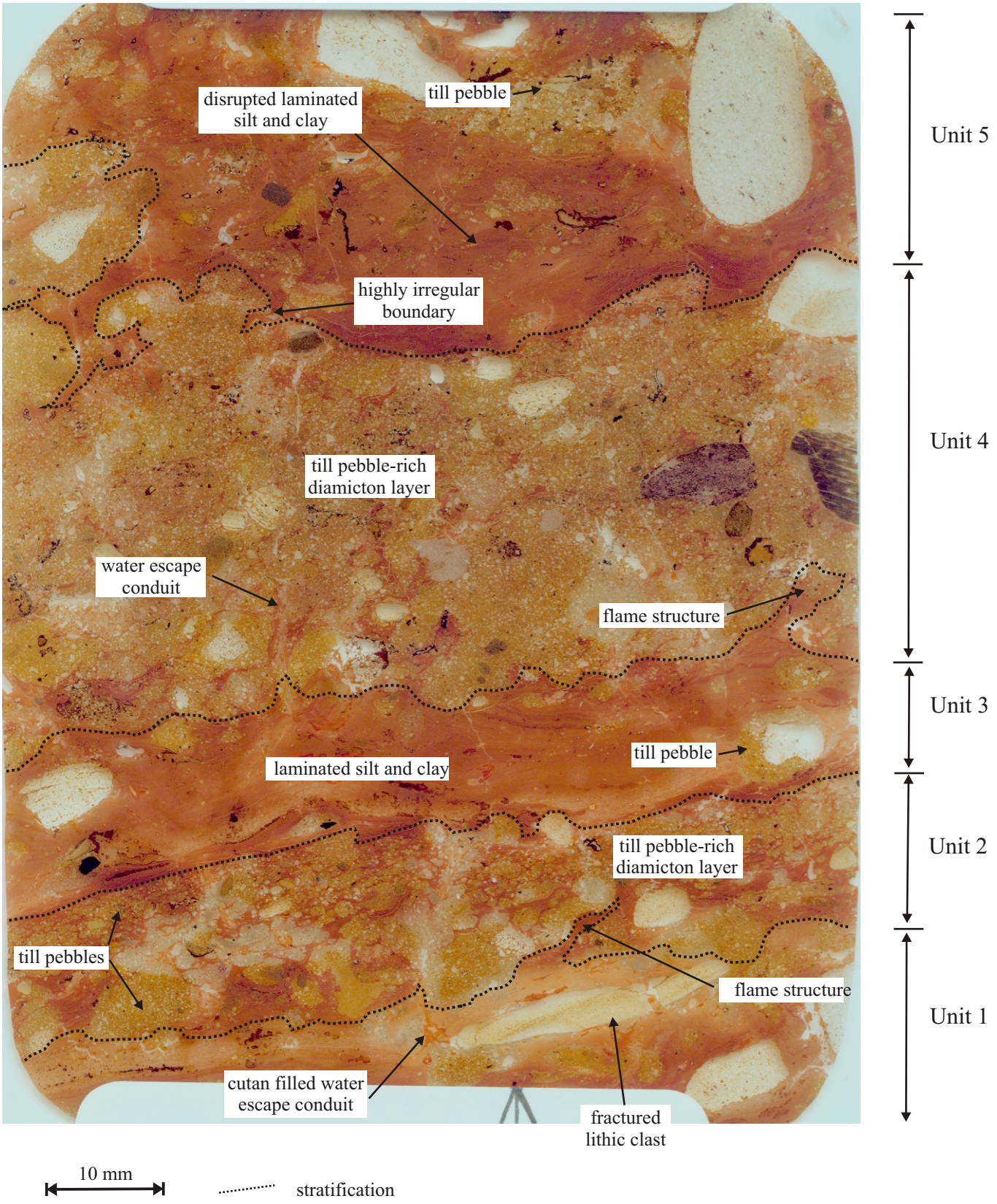

Fig. 4. Annotated scanned image of sample N2842.

Sample N2843

Fig. 5. Annotated scanned image of sample N2843.

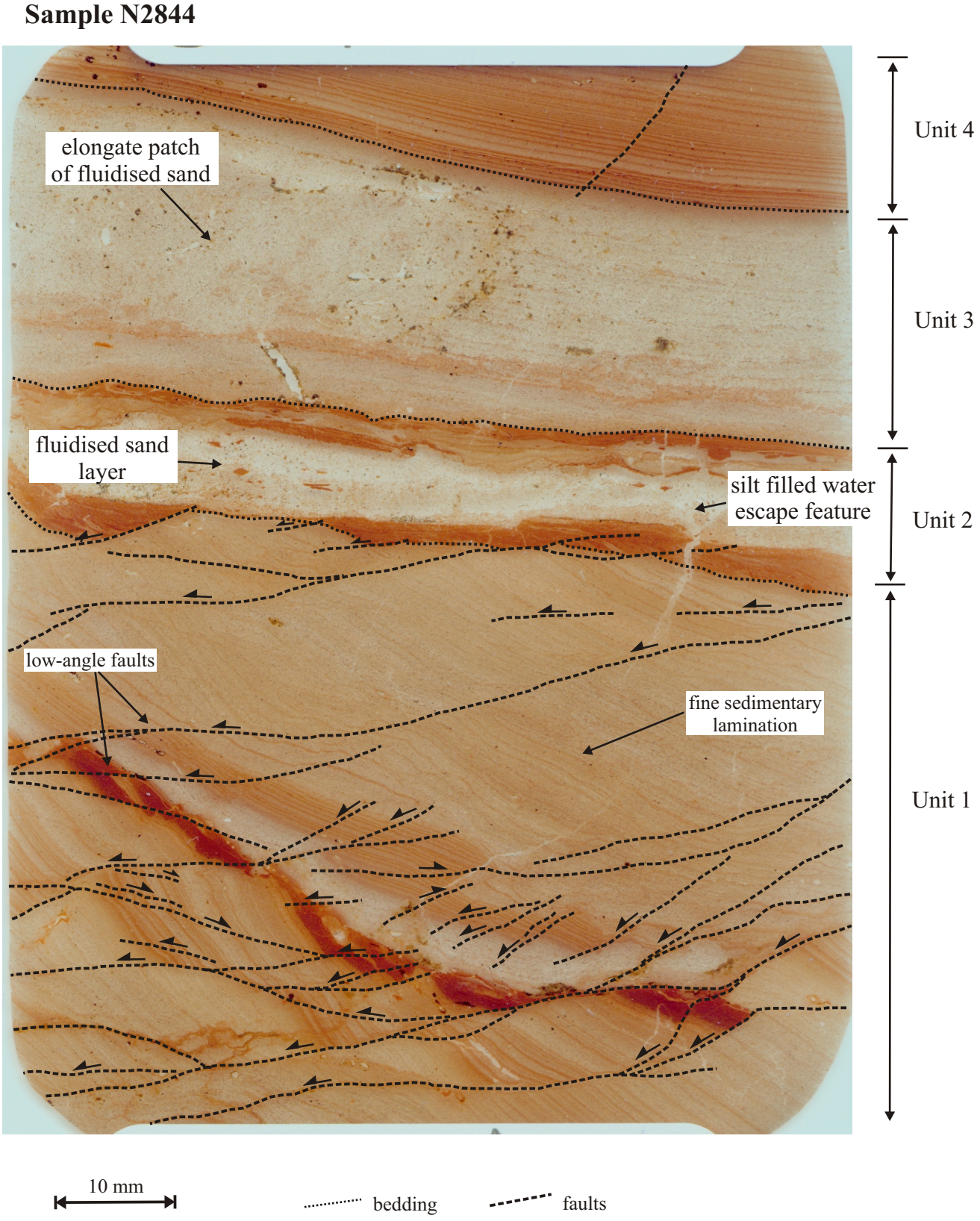

Fig. 6. Annotated scanned image of sample N2844.

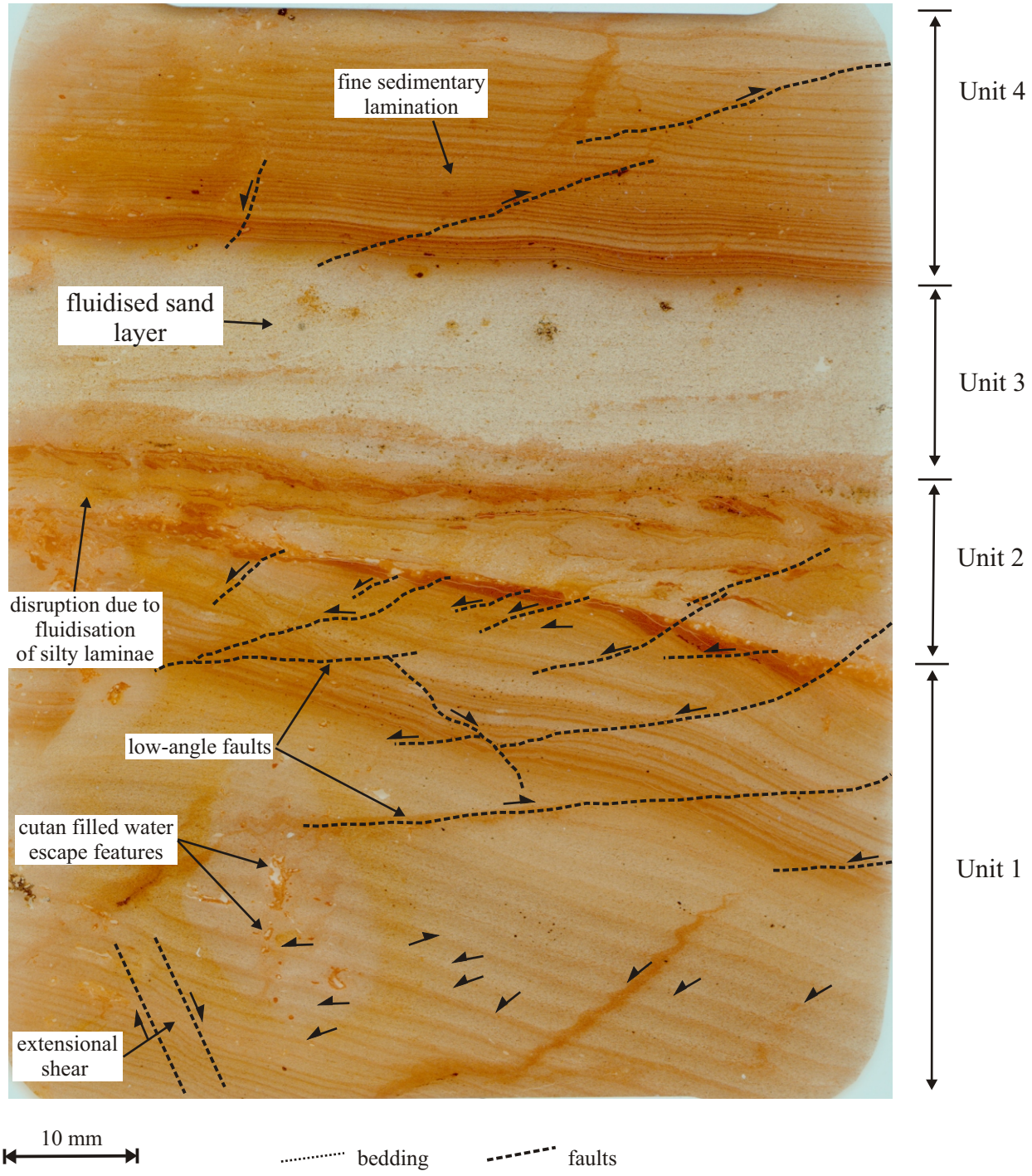

Fig. 7. Annotated scanned image of sample N2845.

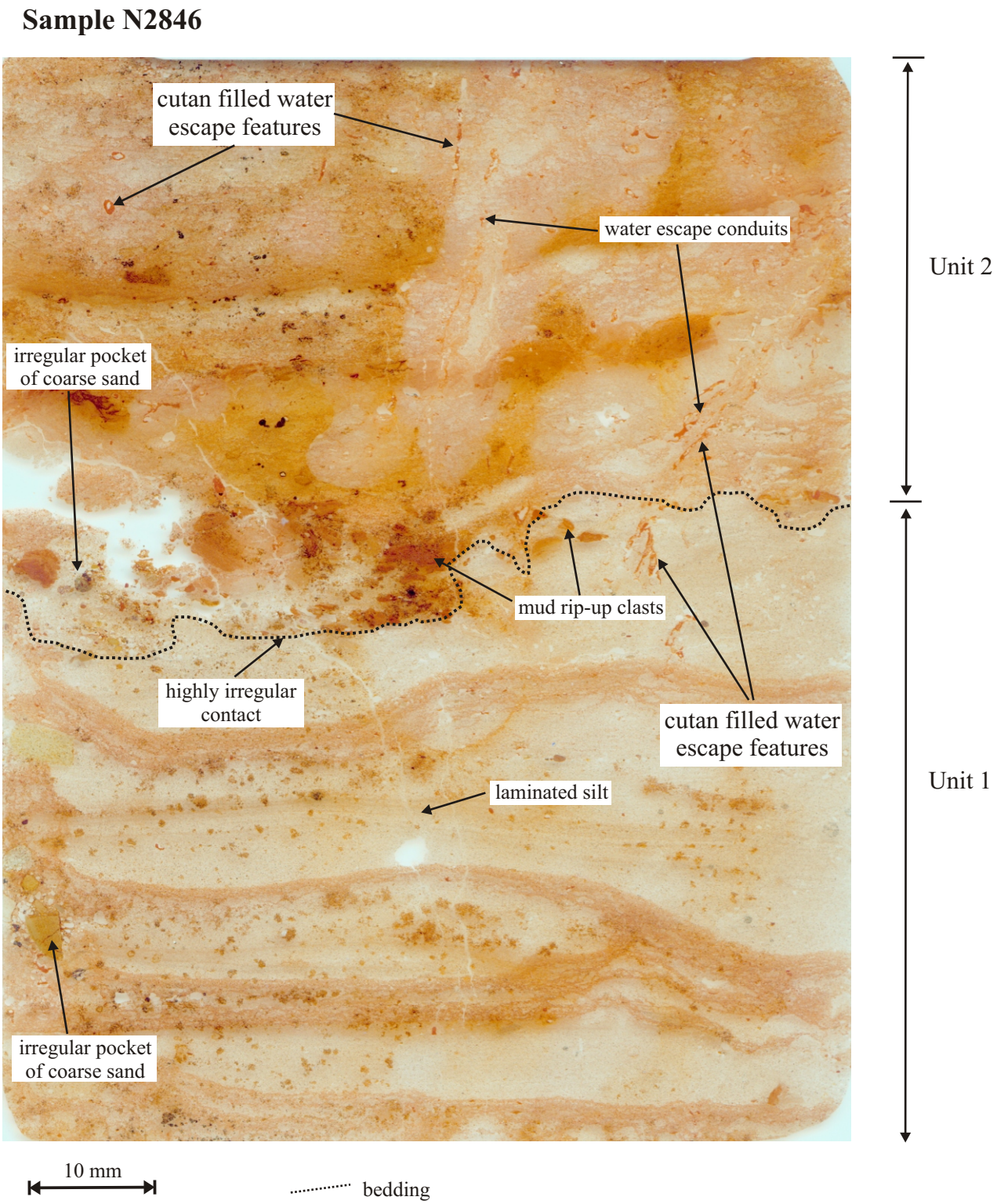

Fig. 8. Annotated scanned image of sample N2846.

Sample N2847

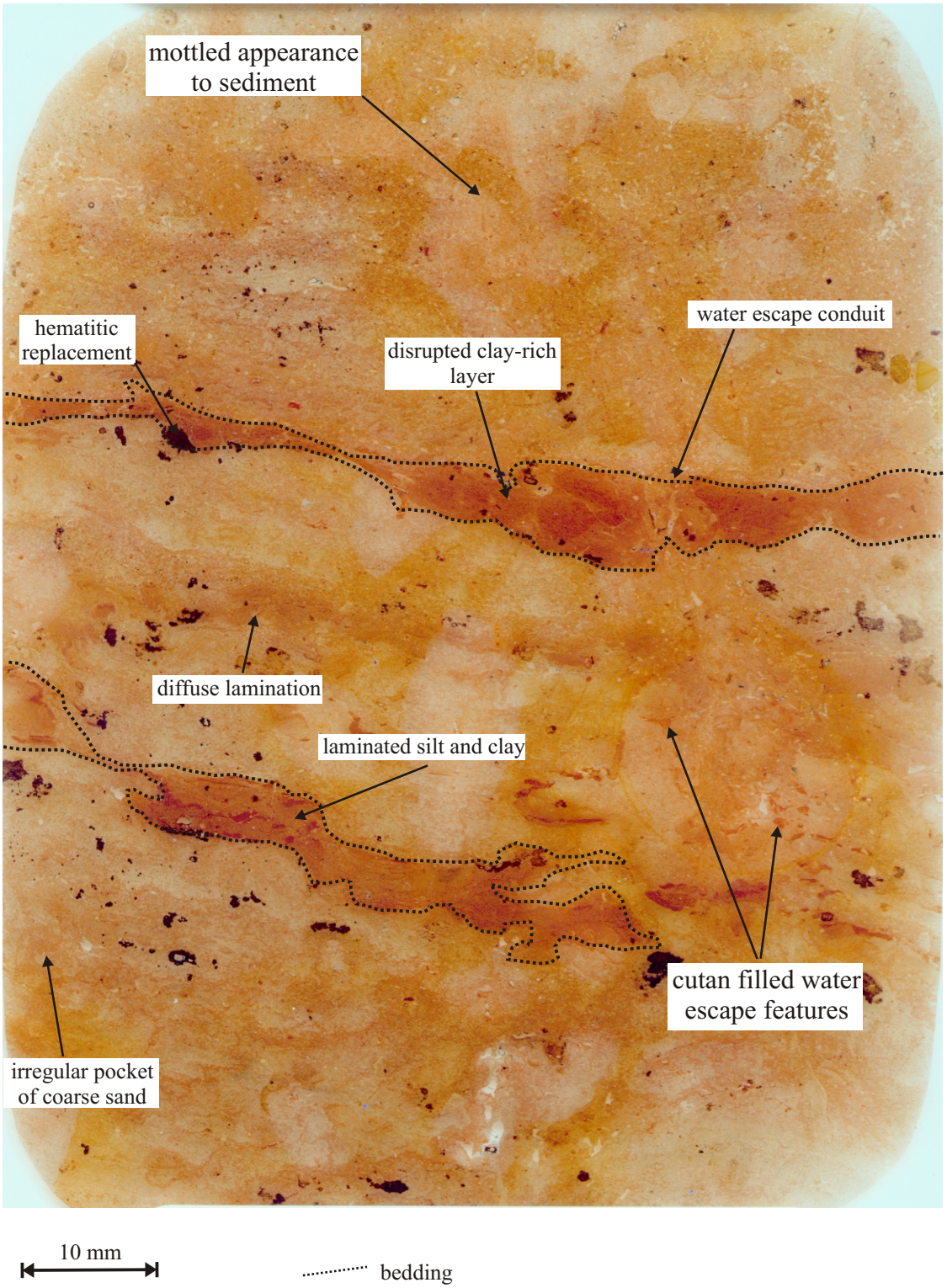

Fig. 9. Annotated scanned image of sample N2847.

Sample N2848

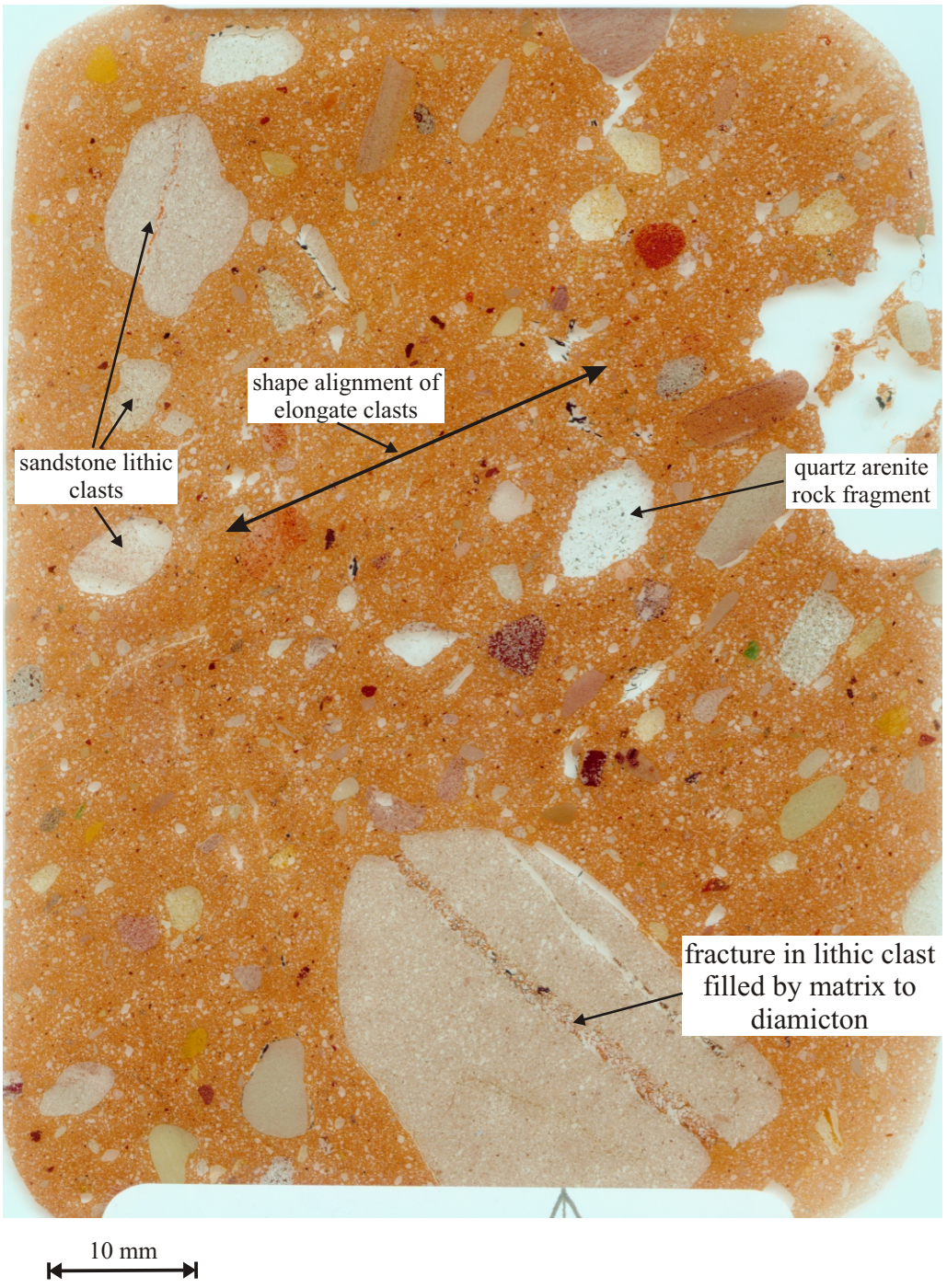

Fig. 10. Annotated scanned image of sample N2848.

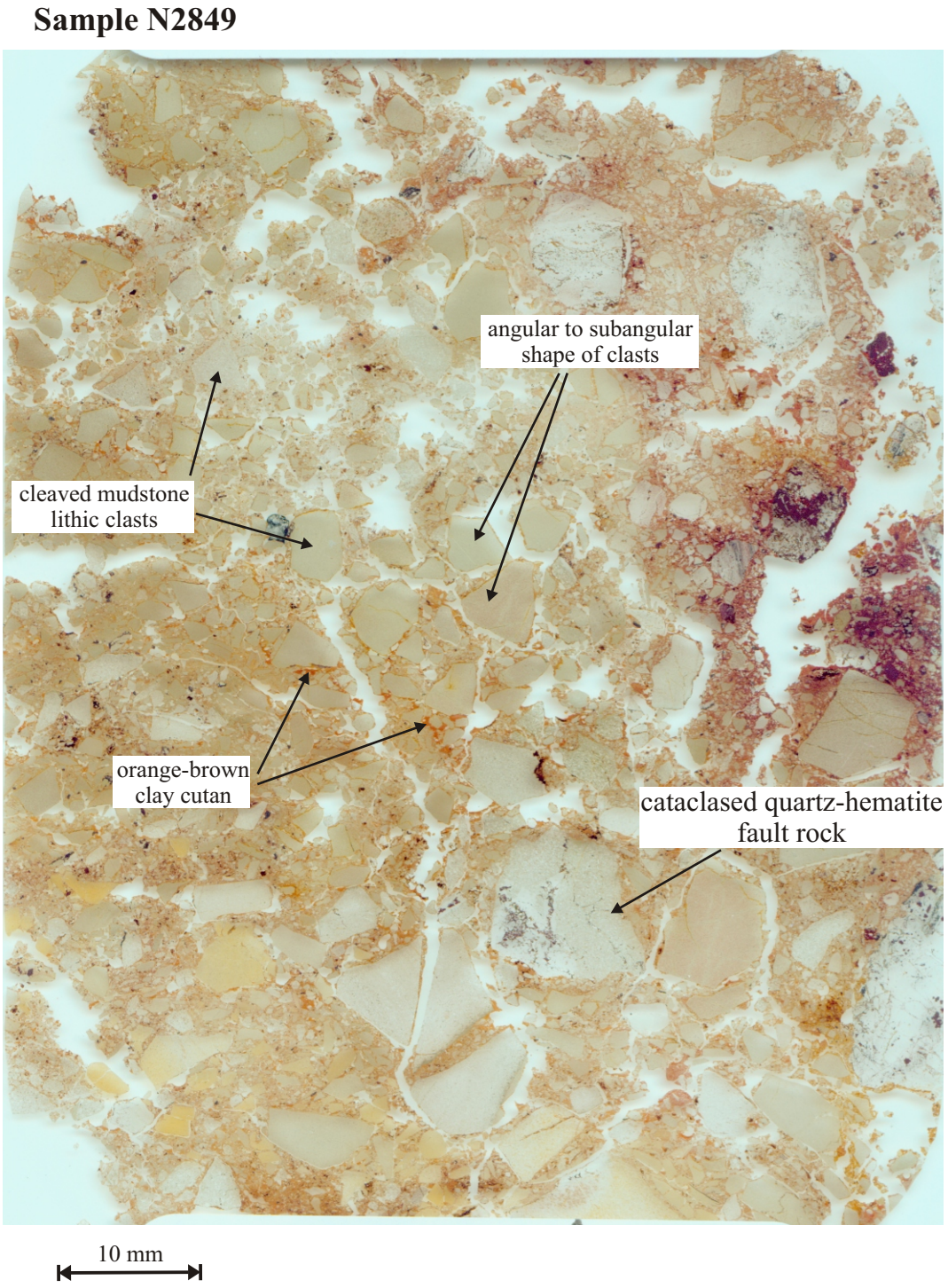

Fig. 11. Annotated scanned image of sample N2849.

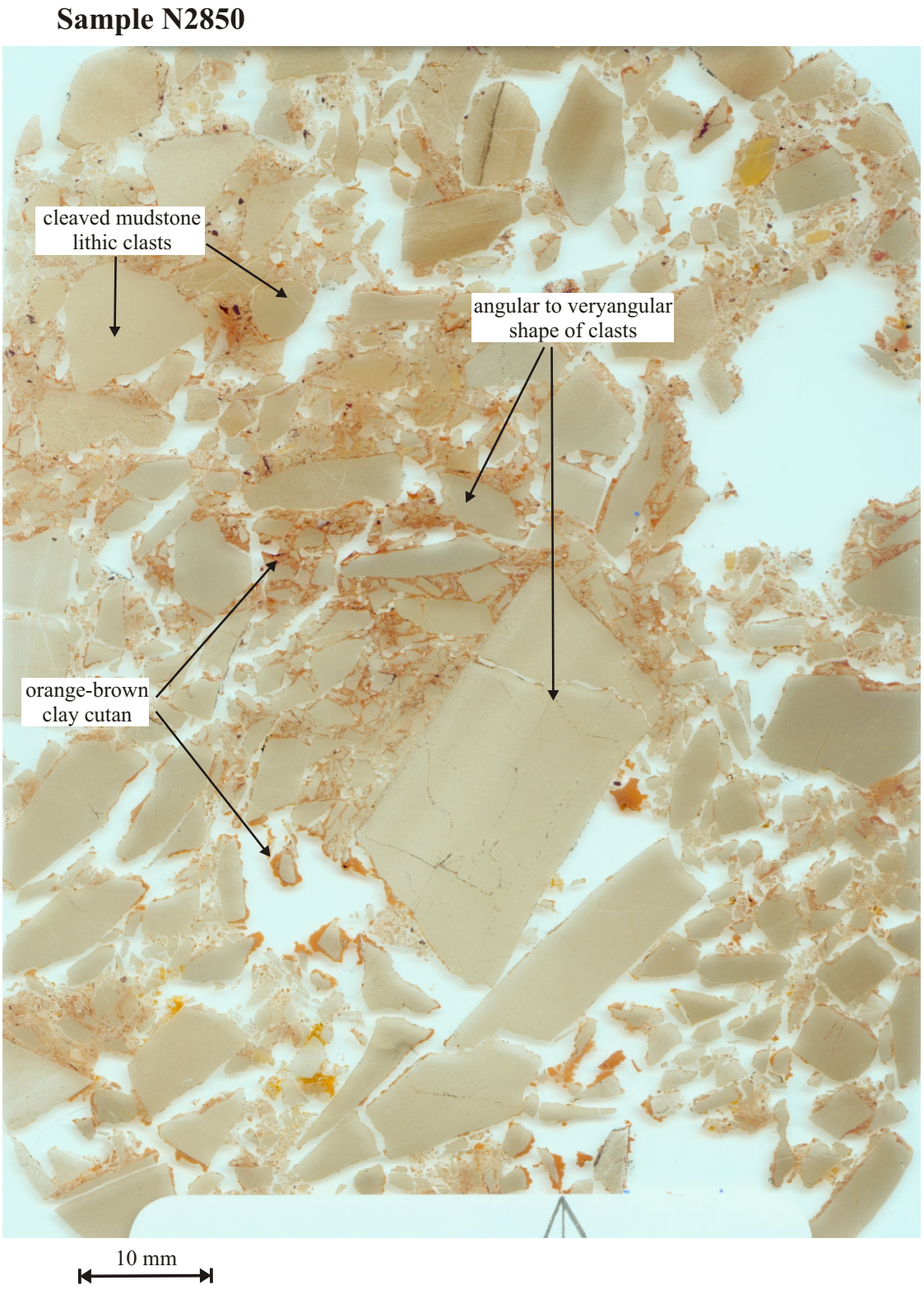

Fig. 12. Annotated scanned image of sample N2850.

Sample N2851

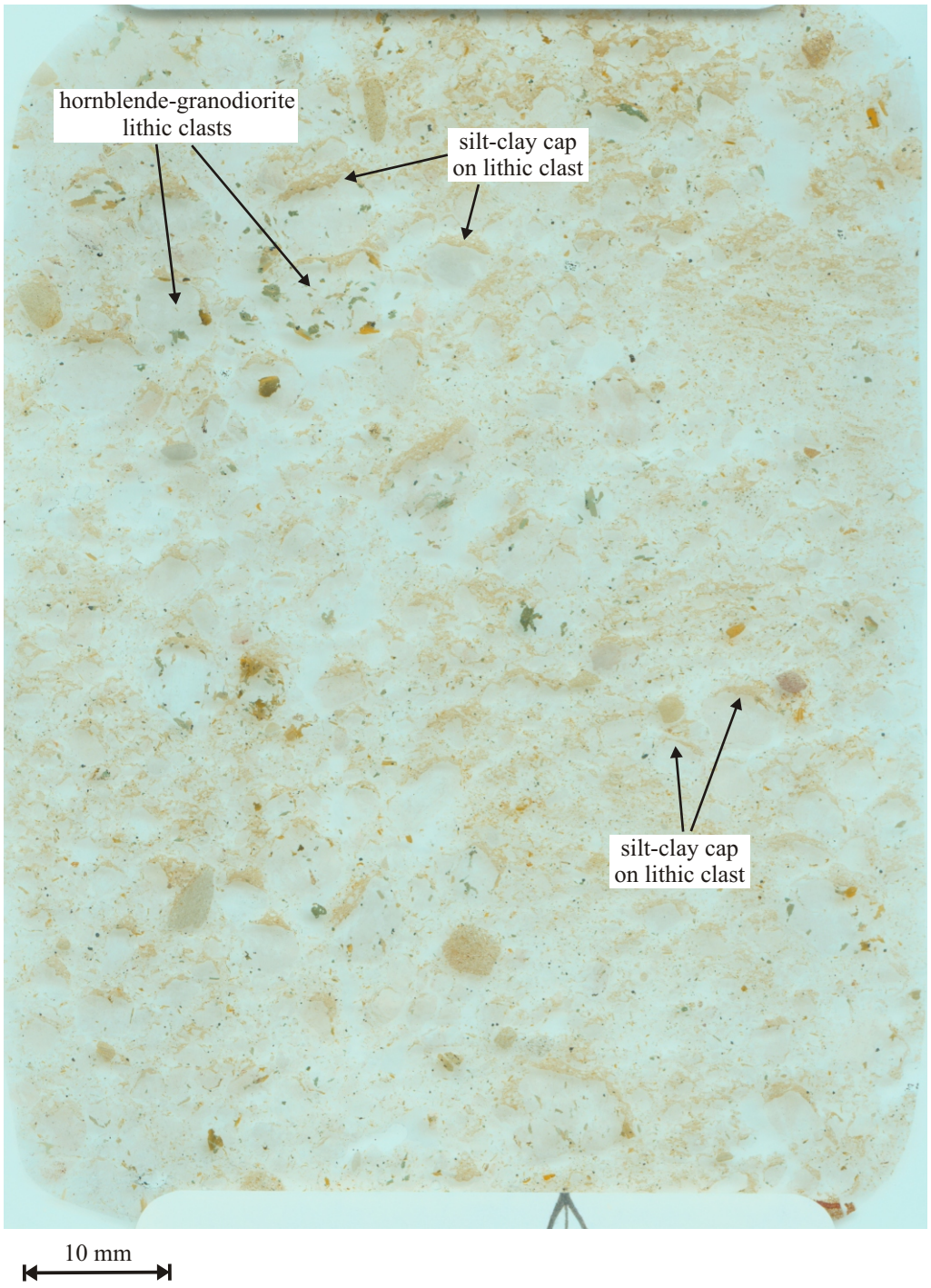

Fig. 13. Scanned image of sample N2851.

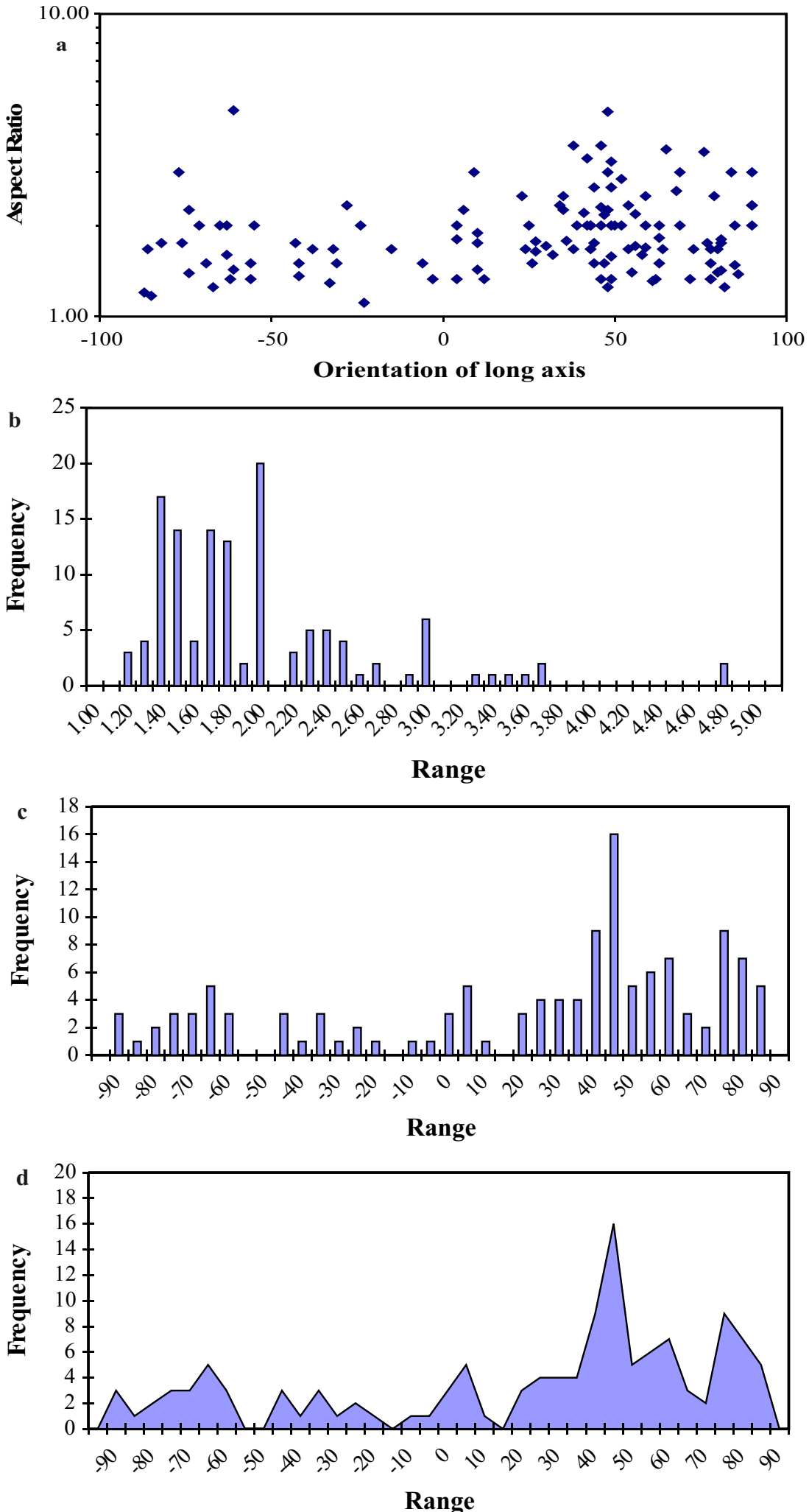

Fig. 14. Diagram showing clast orientation data for sample N2848. (a) plot of aspect ratio versus orientation of long axis. (b) histogram showing variation in clast aspect ratio. (c and d) plots showing variation in long axis orientation.

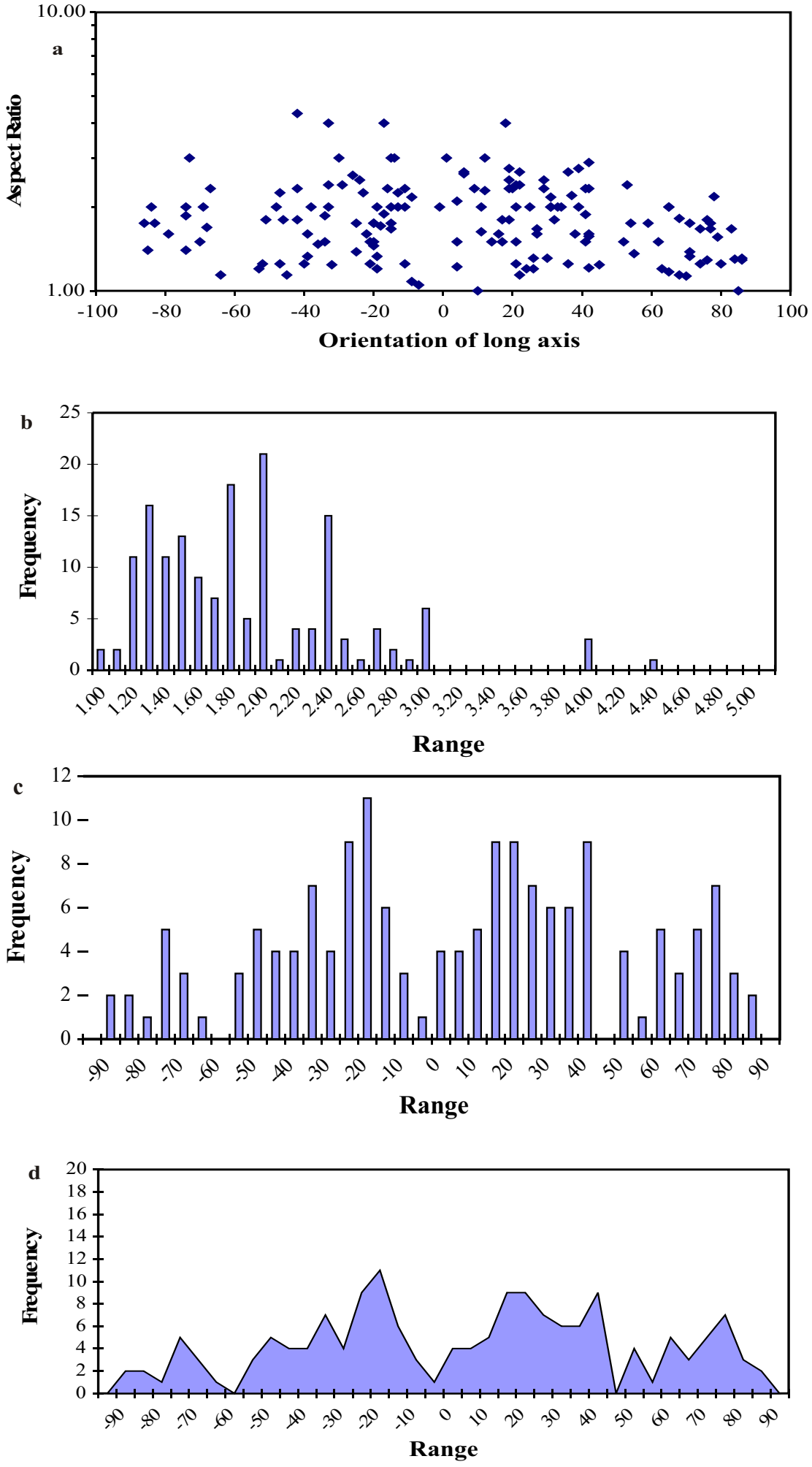

Fig. 15. Diagram showing clast orientation data for sample N2849. (a) plot of aspect ratio versus orientation of long axis. (b) histogram showing variation in clast aspect ratio. (c and d) plots showing variation in long axis orientation.

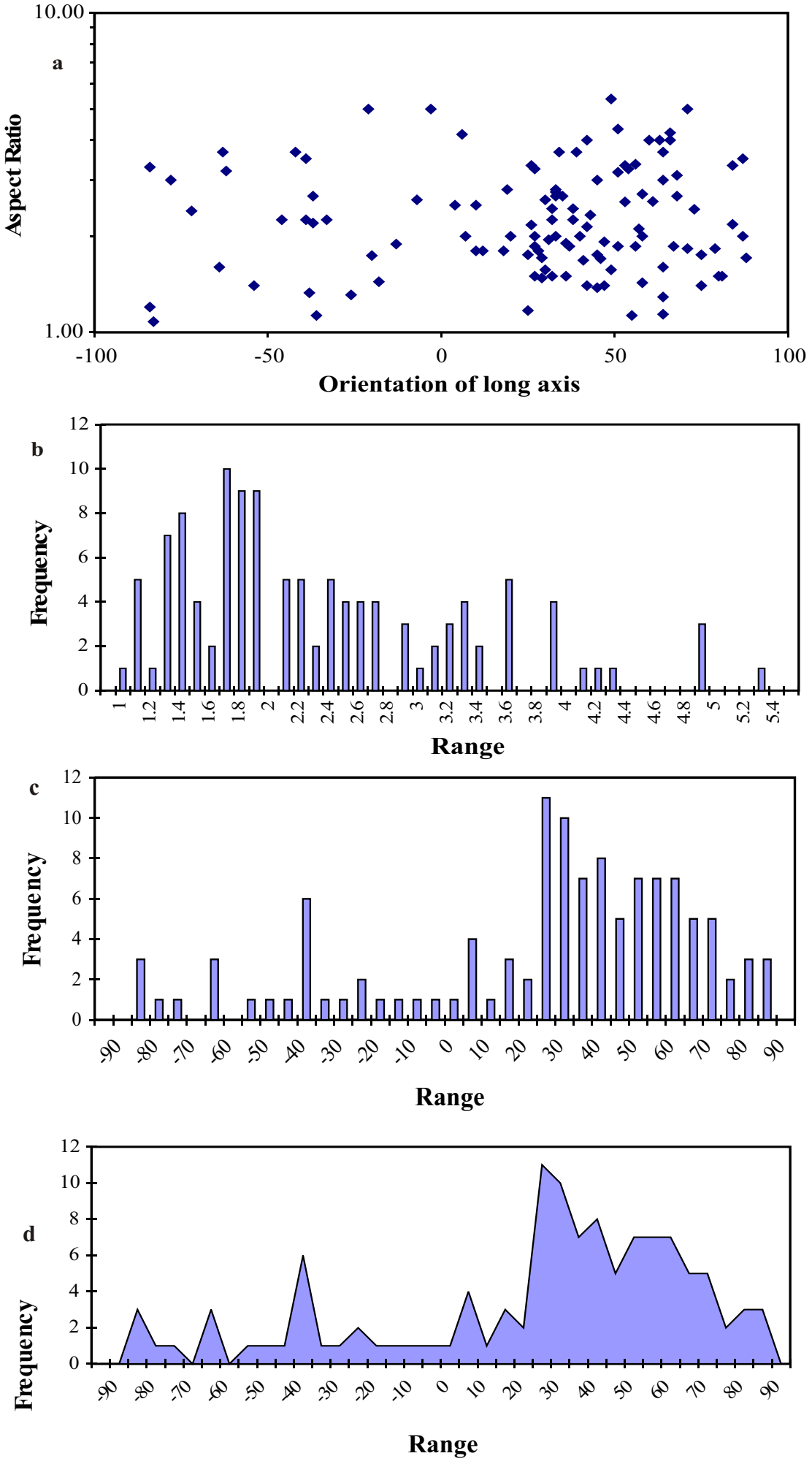

Fig. 16. Diagram showing clast orientation data for the lower part of sample N2850. (a) plot of aspect ratio versus orientation of long axis. (b) histogram showing variation in clast aspect ratio. (c and d) plots showing variation in long axis orientation.

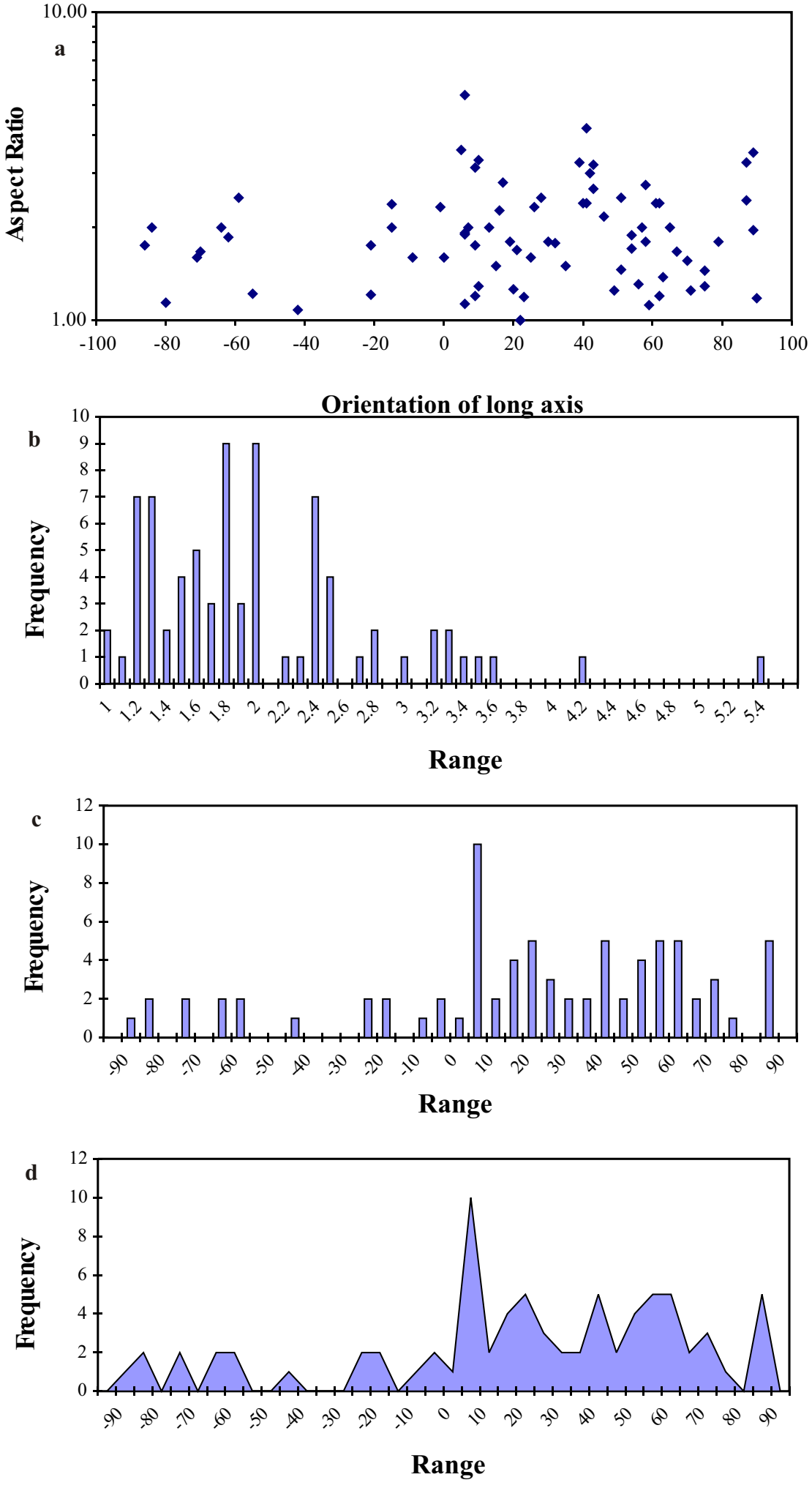

Fig. 17. Diagram showing clast orientation data for the upper part of sample N2850. (a) plot of aspect ratio versus orientation of long axis. (b) histogram showing variation in clast aspect ratio. (c and d) plots showing variation in long axis orientation.

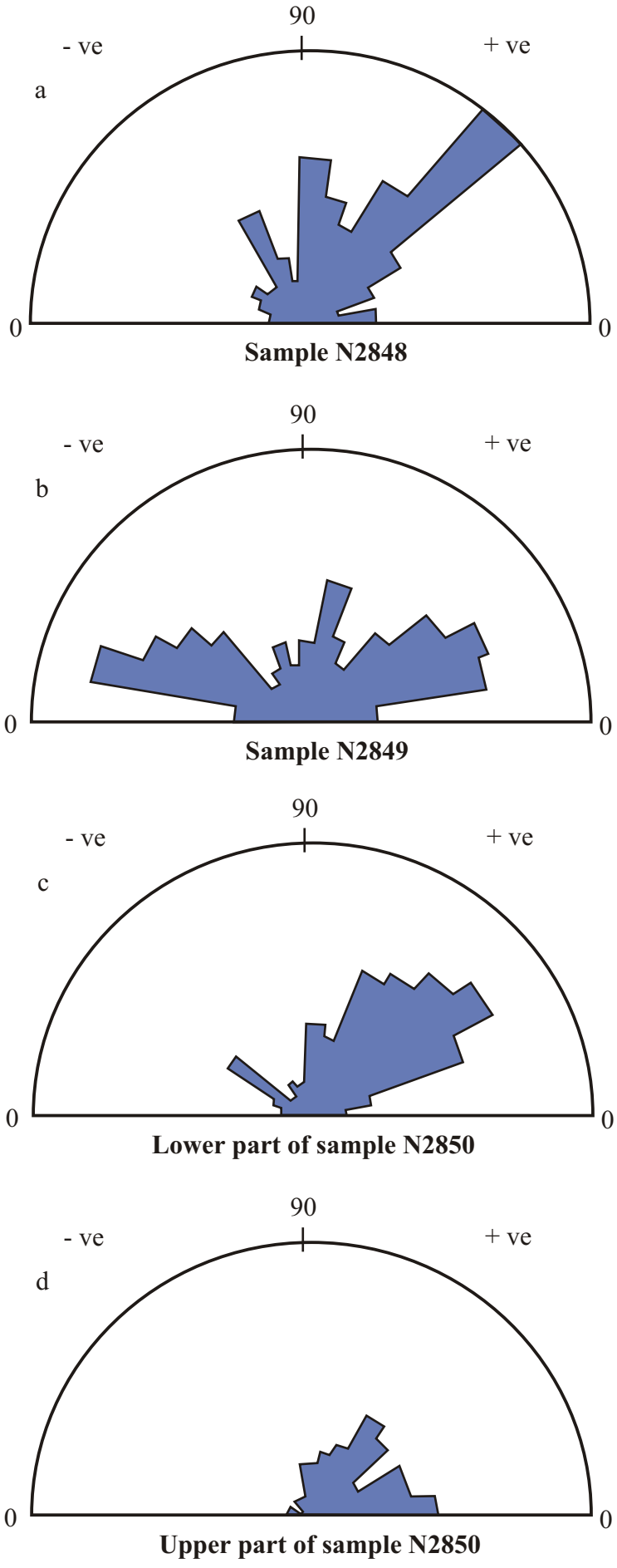

Fig. 18. Rose diagrams showing clast long axis orientation within: (a) Sample N2848; (b) Sample N2849; (c) lower part of sample N2850; and (d) upper part of Sample N2850.

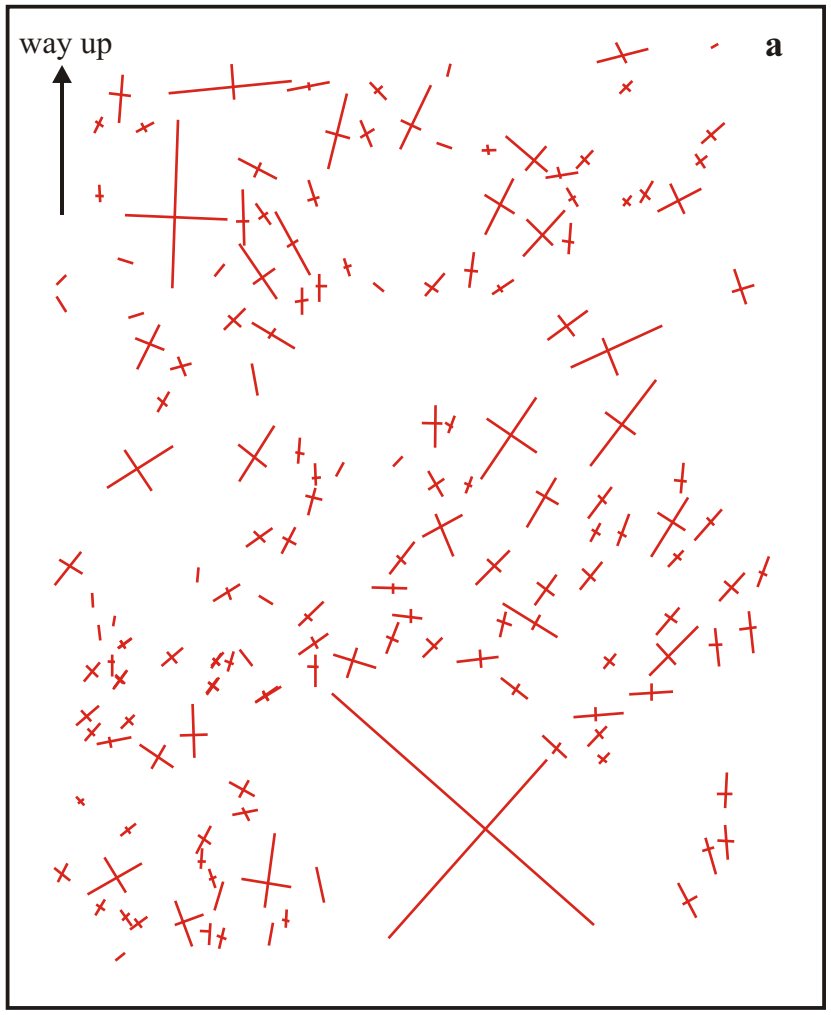

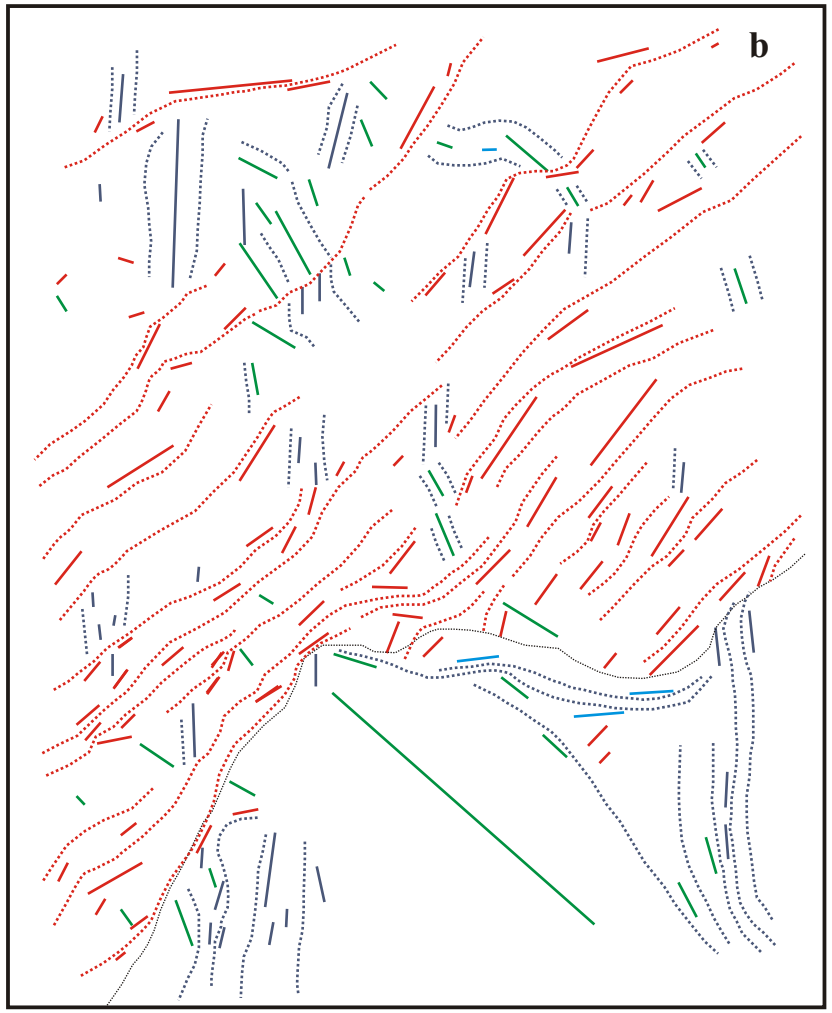

Fig. 19. (a) Diagram showing the orientation of the main axes of coarse sand to pebble sized clasts within Sample N2848. (b) Interpreted pattern of long axis orientation within sample N2848.

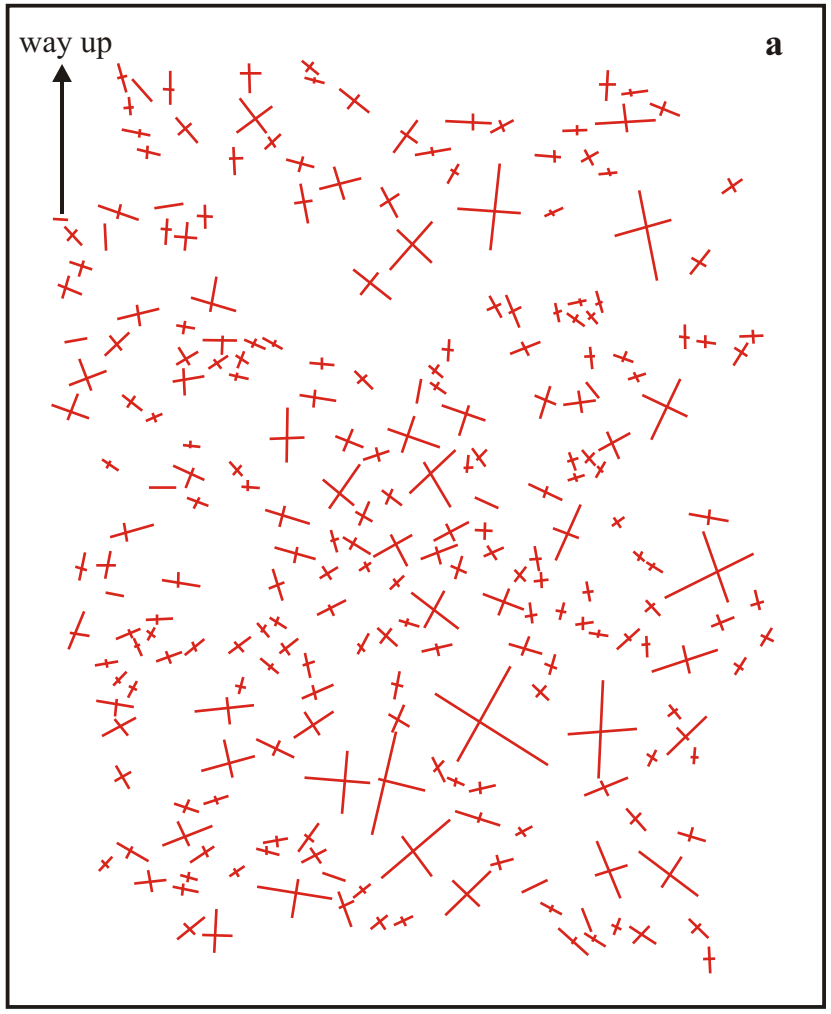

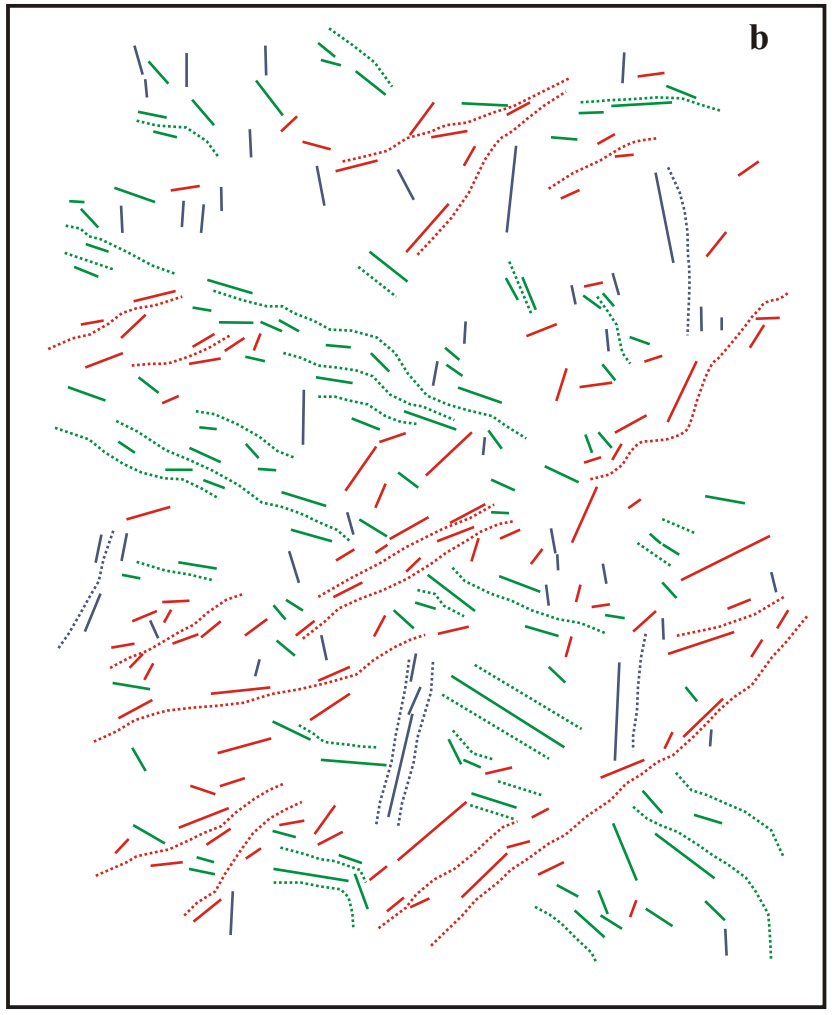

Sample N2849

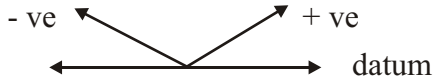

orientation of clast long axis

Fig. 20. (a) Diagram showing the orientation of the main axes of coarse sand to pebble sized clasts within Sample N2849. (b) Interpreted pattern of long axis orientation within sample N2849.

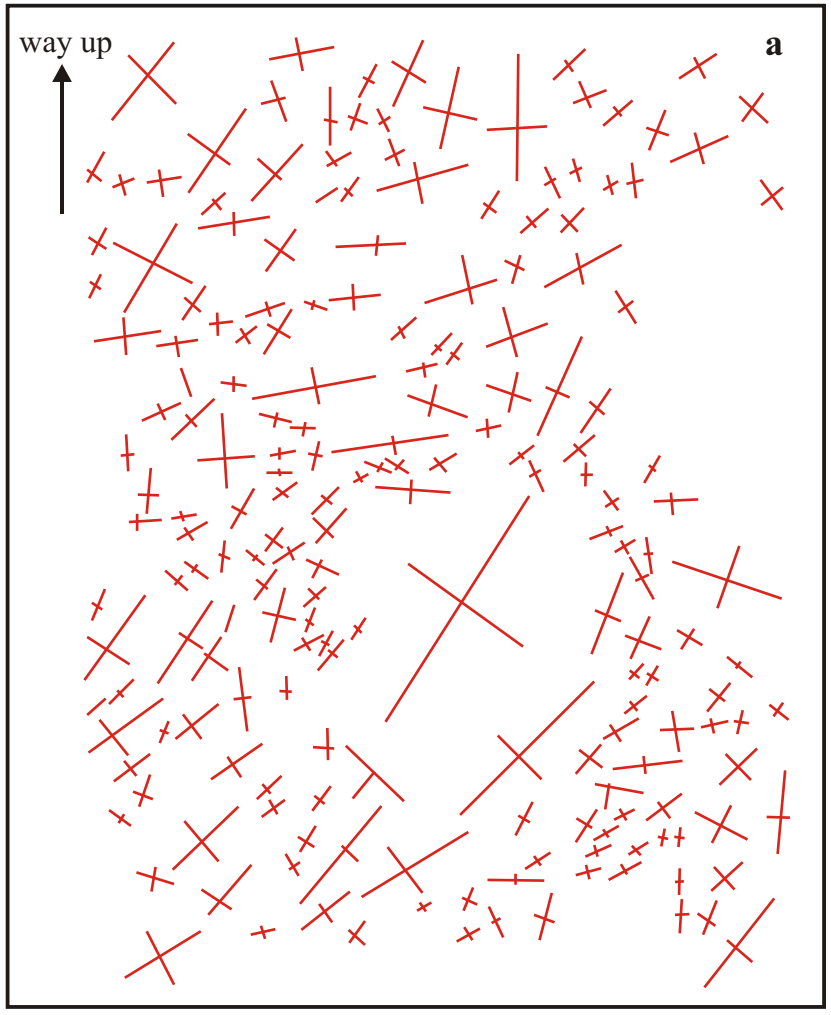

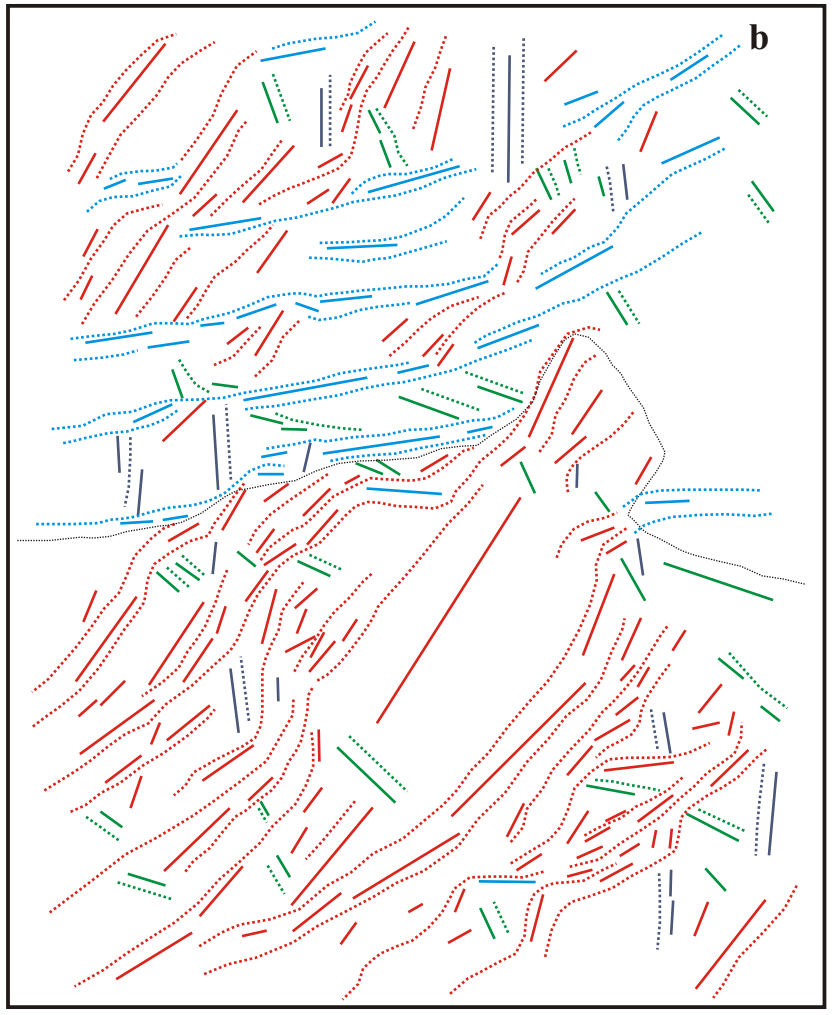

Fig. 21. (a) Diagram showing the orientation of the main axes of coarse sand to pebble sized clasts within Sample N2850. (b) Interpreted pattern of long axis orientation within sample N2850.

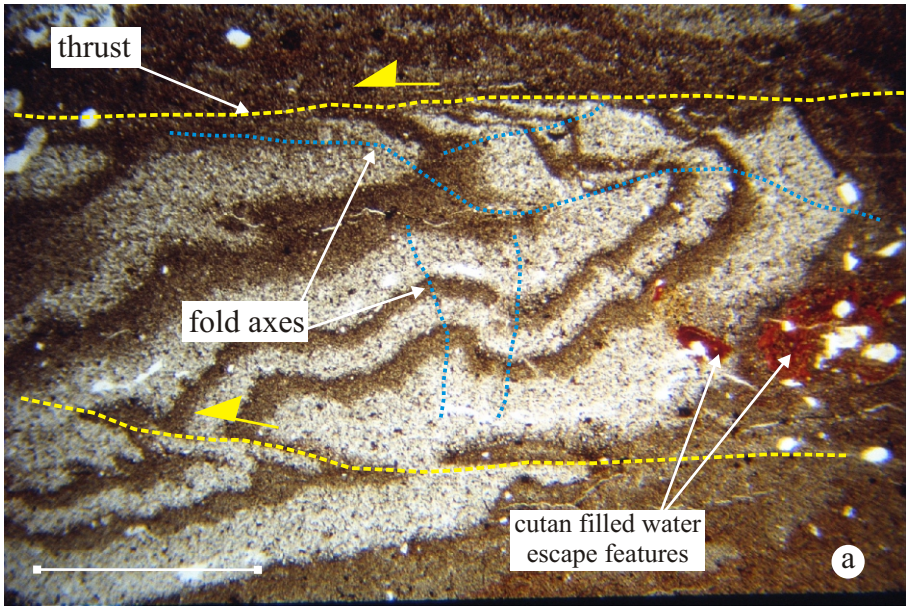

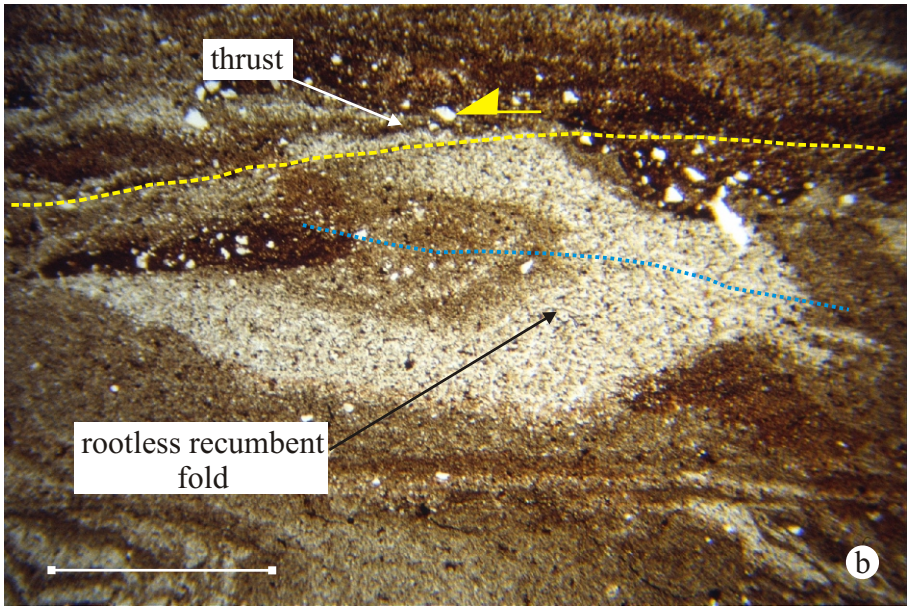

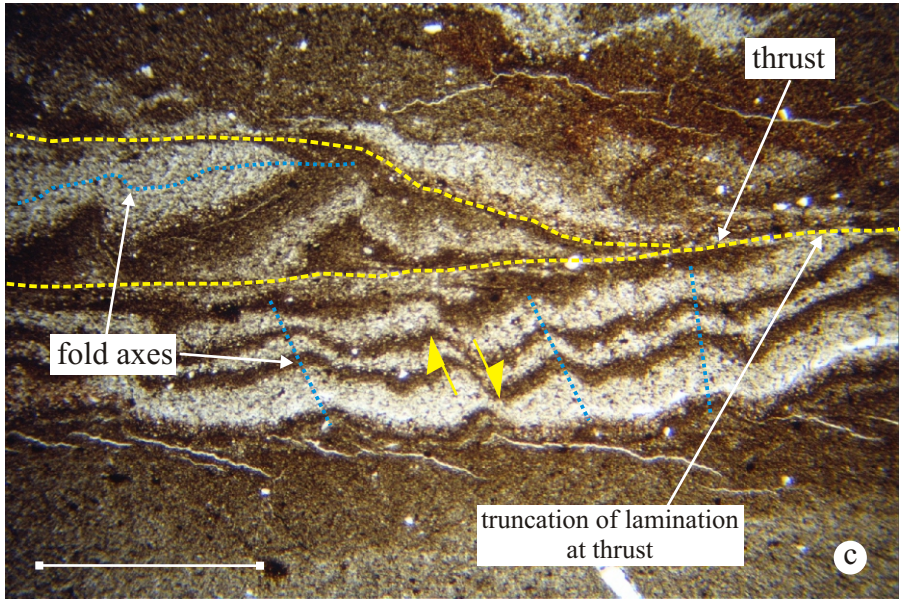

Plate 1. (a) Recumbent fold deforming laminated silt and clay. Overturned limb of fold is truncated by a small-scale thrust fault (Sample N2840, plane polarised light, scale bar = 4 mm). (b) Recumbent, rootless fold deforming silt within partially fluidised silt and clay (Sample N2840, plane polarised light, scale bar = 4 mm). (C) Disrupted laminated silt and clay deformed by small-scale crenulation-style folds and thrust faults (Sample N2840, plane polarised light, scale bar = 4 mm).

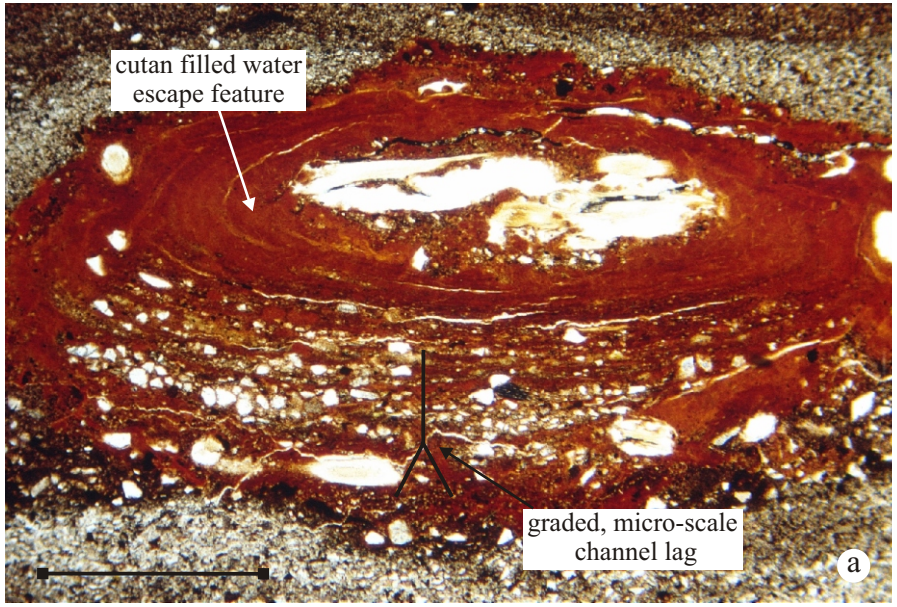

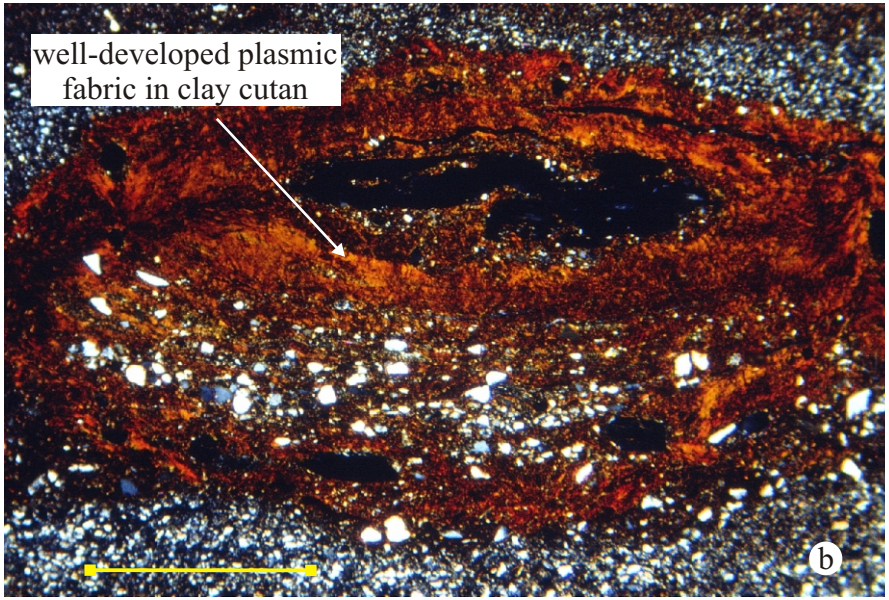

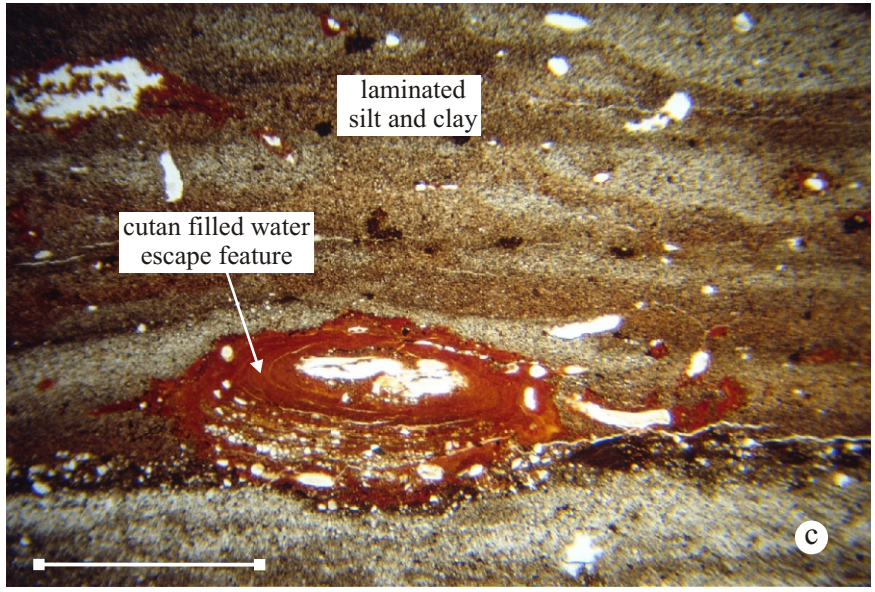

Plate 2. (a) Water escape feature filled by distinctive orange-brown clay cutan. Also note presence of graded micro-scale channel lag at the base of this feature (Sample N2840, plane polarised light, scale bar = 1 mm). (B) Water escape feature filled by clay cutan which possesses a well developed concentric plasmic fabric (Sample N2840, crossed polarised light, scale bar = 1 mm). (C) Lower magnification view of water escape conduit showing that it occurs immediately above a low permeability clay layer and is elongate parallel to bedding (Sample N2840, plane polarised light, scale bar = 4 mm).

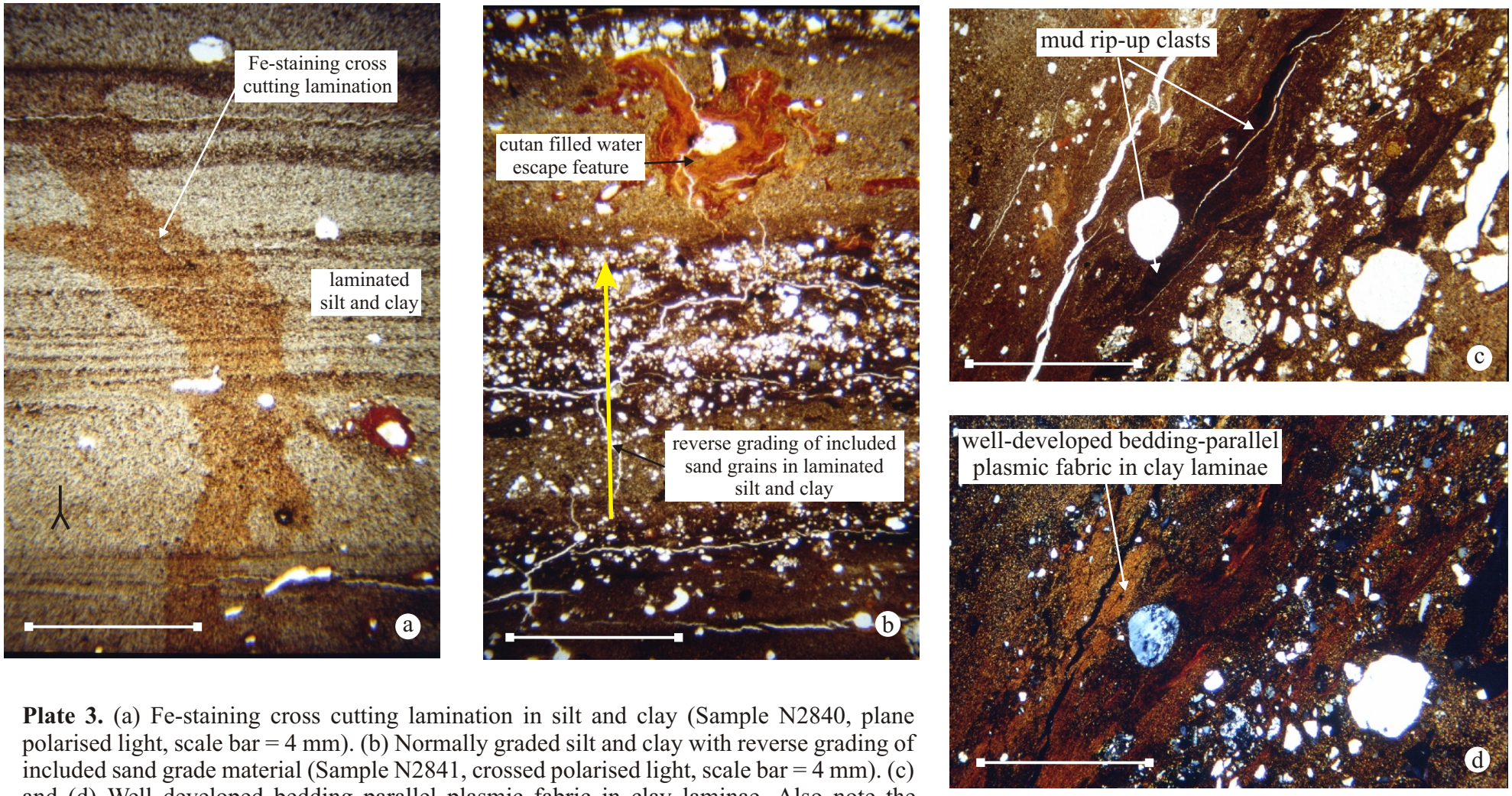

Plate 3. (a) Fe-staining cross cutting lamination in silt and clay (Sample N2840, plane polarised light, scale bar = 4 mm). (b) Normally graded silt and clay with reverse grading of included sand grade material (Sample N2841, crossed polarised light, scale bar = 4 mm). (c) and (d) Well developed bedding parallel plasmic fabric in clay laminae. Also note the presence of dark coloured mud-rip up clasts (Sample N2841, plane and crossed polarised light, scale bar = 4 mm).

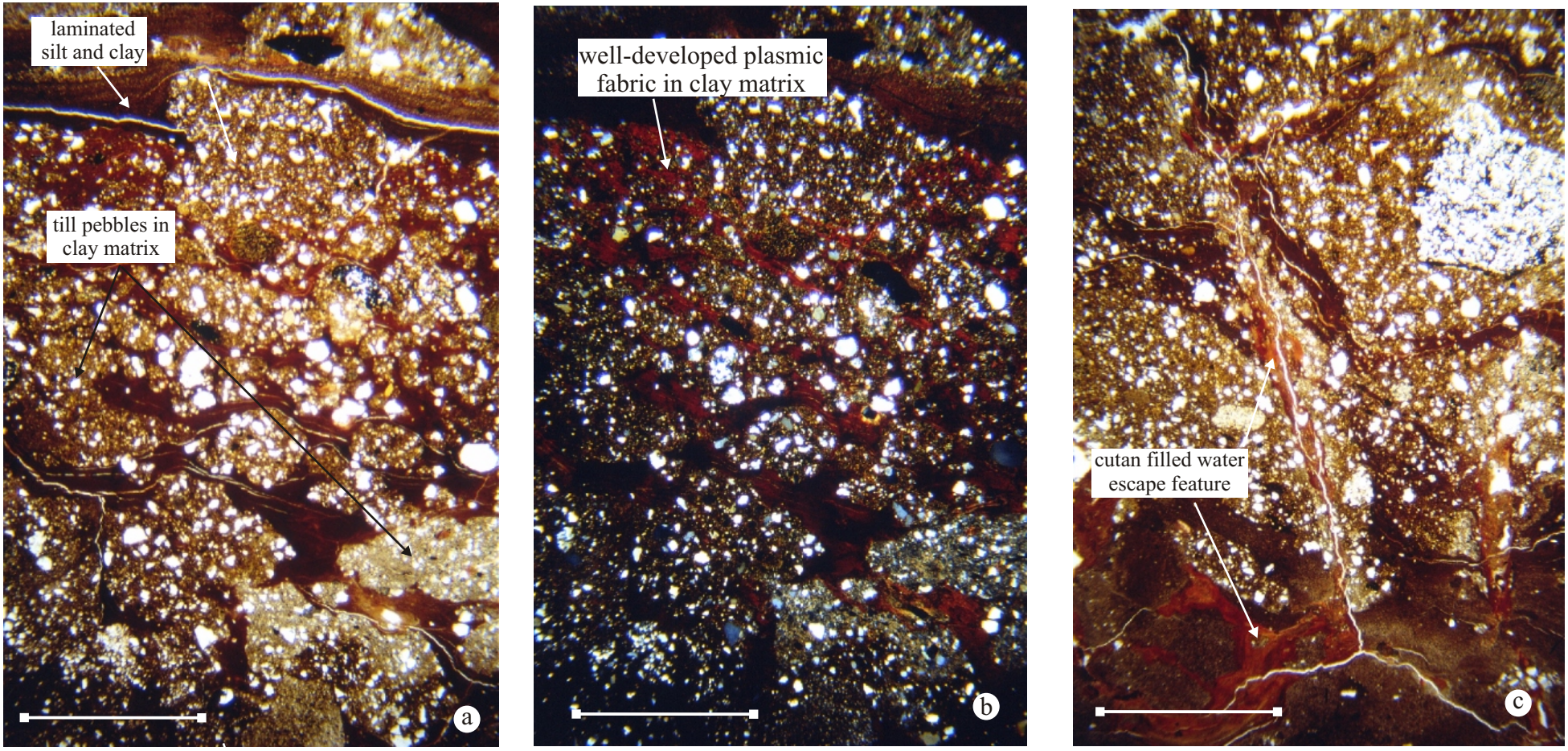

Plate 4. (a) Rounded to irregular till pebbles within a clay matrix (Sample N2842, plane polarised light, scale bar = 1 mm). (b) Rounded to irregular till pebbles within a clay matrix which possess a well developed plasmic fabric (Sample N2842, crossed polarised light, scale bar = 1 mm). (c) Lower magnification view of water escape conduit cross cutting diamicton layer rich in rounded till pebbles. Late-stage fluid flow concentrated into distinct pathways resulting in the deposition of orange-brown clay cutan (Sample N2842, plane polarised light, scale bar = 4 mm).

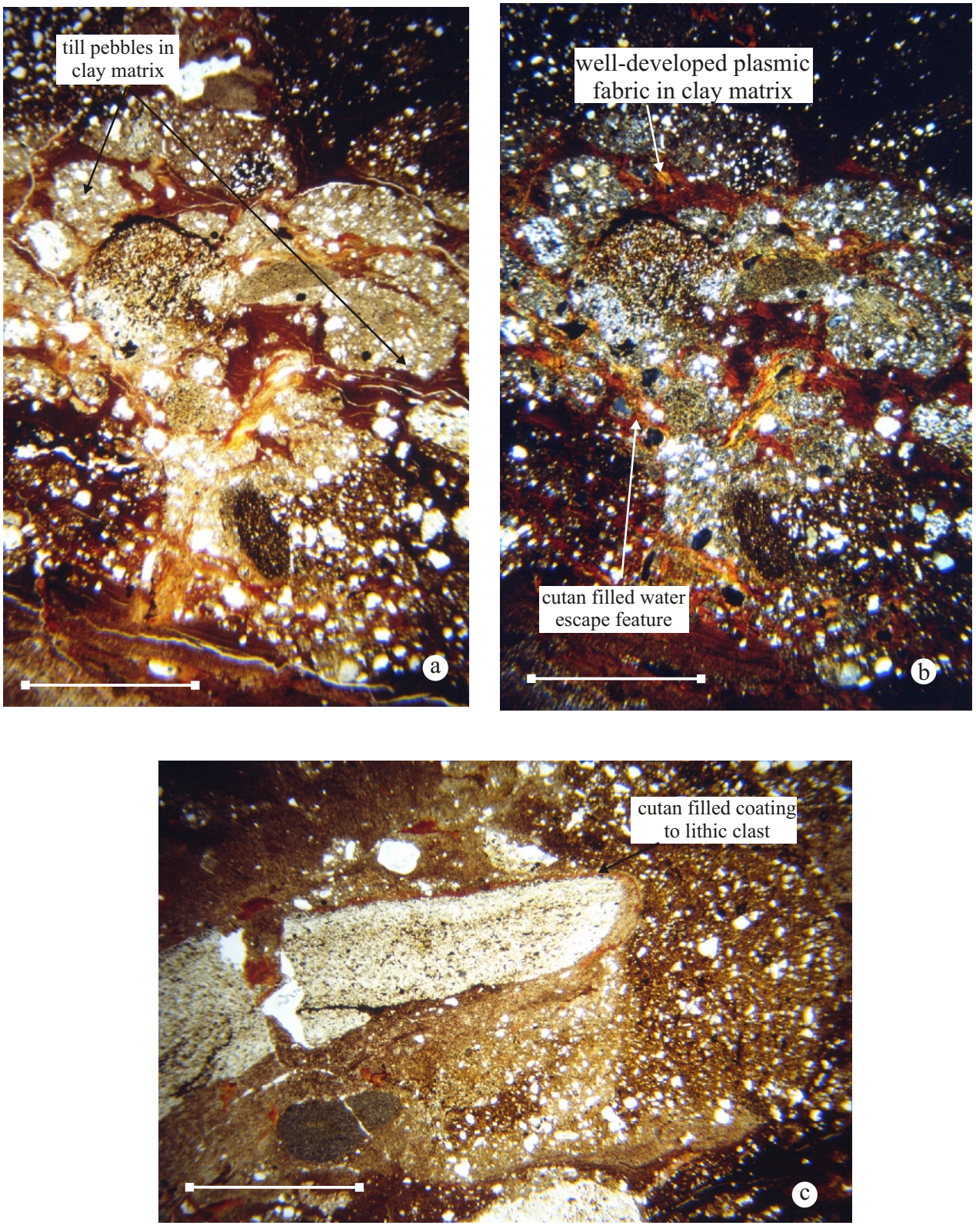

Plate 5. (a) Rounded to irregular till pebbles within a clay matrix. Also note presence of cutan filled late-stage water escape features within the matrix (Sample N2842, plane polarised light, scale bar = 4 mm). (b) Rounded to irregular till pebbles within a clay matrix which possess a well developed plasmic fabric. Also note presence of cutan filled late-stage water escape features within the matrix (Sample N2842, crossed polarised light, scale bar = 4 mm). (c) Fractured, elongate lithic clast enclosed within a clay cutan coating (Sample N2842, plane polarised light, scale bar = 4 mm).

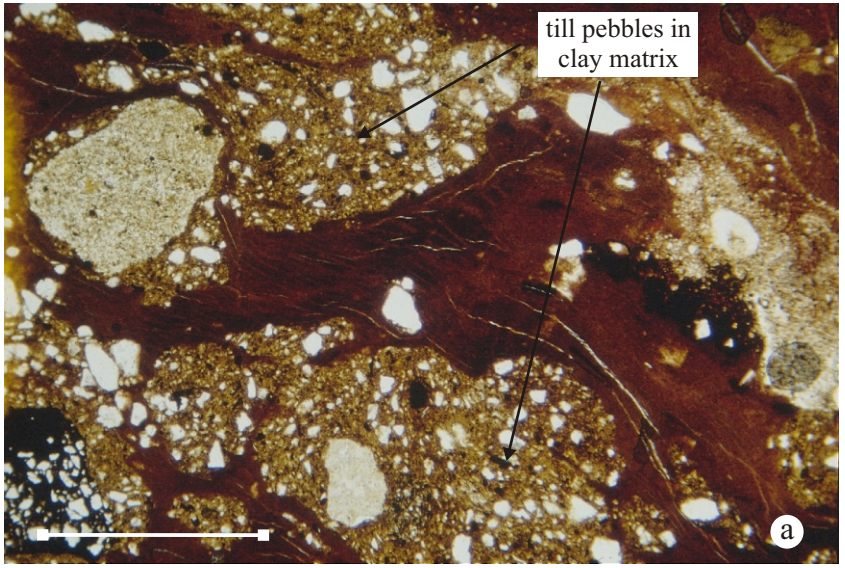

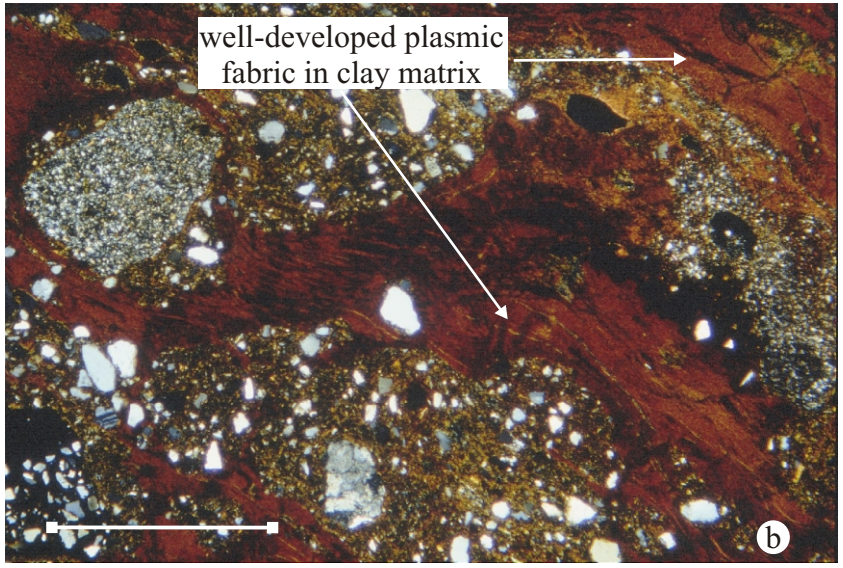

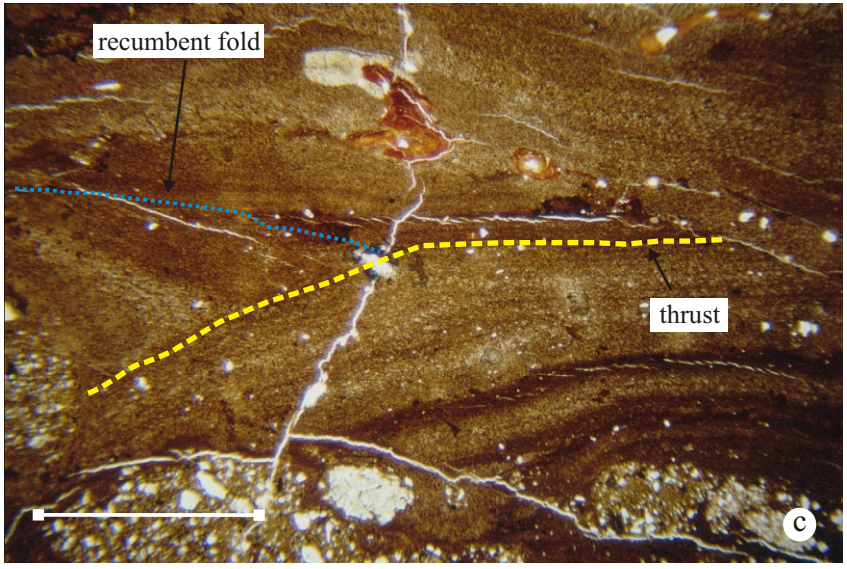

Plate 6. (a) Rounded to irregular till pebbles within a clay matrix (Sample N2842, plane polarised light, scale bar = 1 mm). (b) Rounded to irregular till pebbles within a clay matrix which possess a well developed plasmic fabric (Sample N2842, crossed polarised light, scale bar = 1 mm). (c) recumbent fold structure in hanging wall of thrust fault deforming laminated clay and silt (Sample N2842, plane polarised light, scale bar = 1 mm).

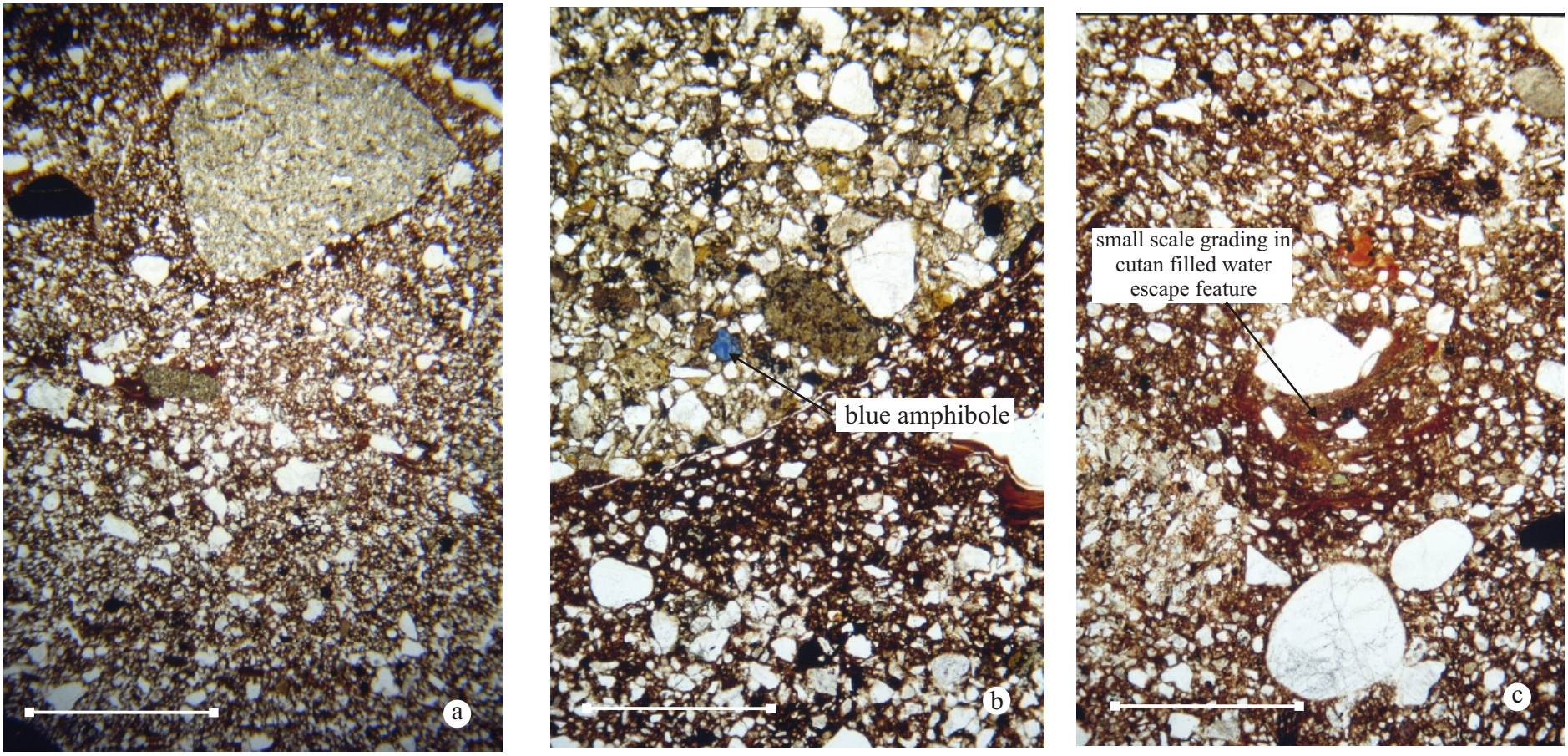

Plate 7. (a) sandy diamicton containing rounded lithic clasts. These lithic clasts locally represent broken fragments of larger pebbles (Sample N2843, plane polarised light, scale bar = 4 mm). (b) Rounded wacke sandstone rock fragment containing detrital blue amphibole (Sample N2843, crossed polarised light, scale bar = 1 mm). (c) Small-scale grading in cutan filled water escape feature (Sample N2843, plane polarised light, scale bar = 1 mm).

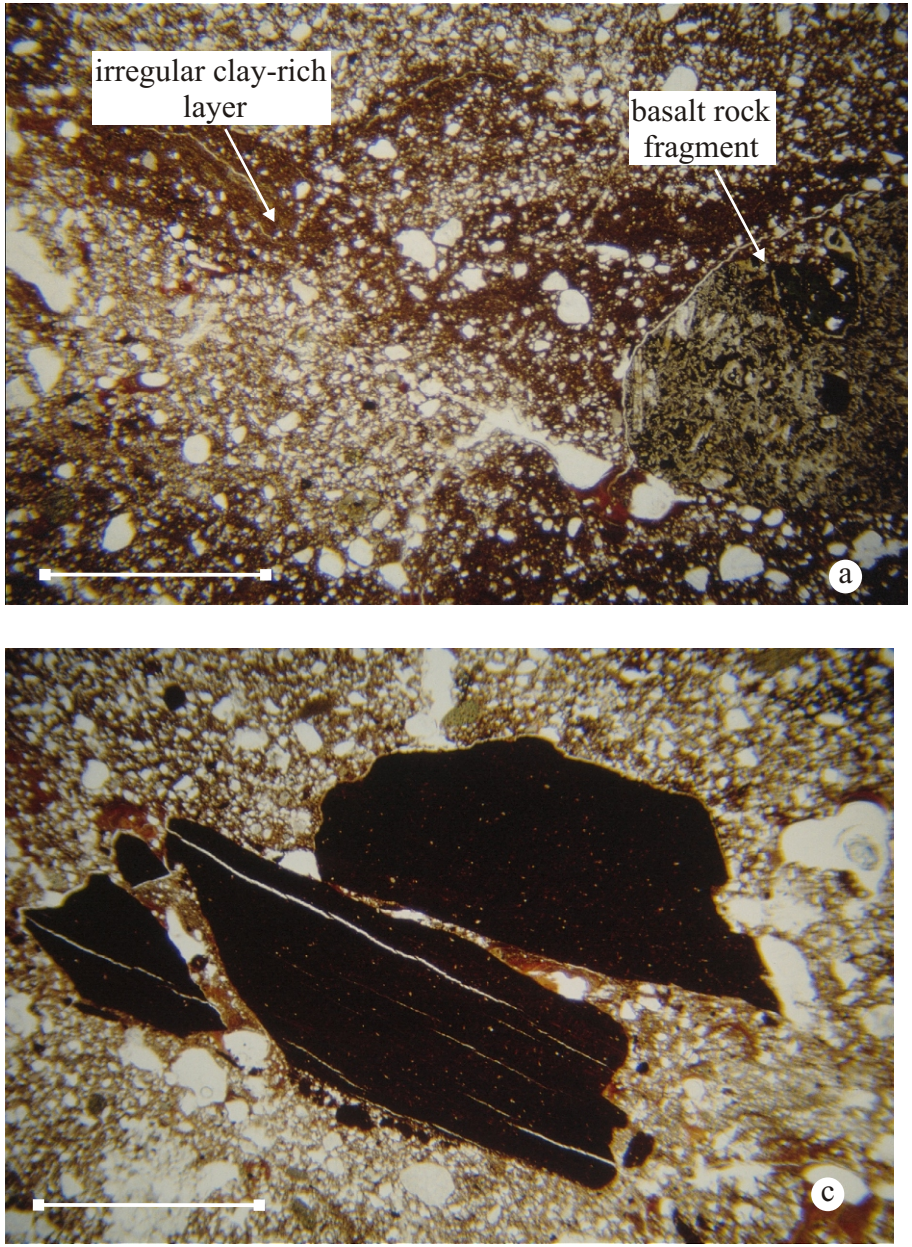

Plate 8. (a) irregular clay-rich layer within sandy diamicton. Also note rounded clast of altered olivine basalt (Sample N2843, plane polarised light, scale bar = 4 mm). (b) geopetal-like partial infill to water escape features (Sample N2843, plane polarised light, scale bar = 1 mm). (c) fractured mudstone lithic clast in sandy diamicton (Sample N2843, plane polarised light, scale bar = 1 mm).

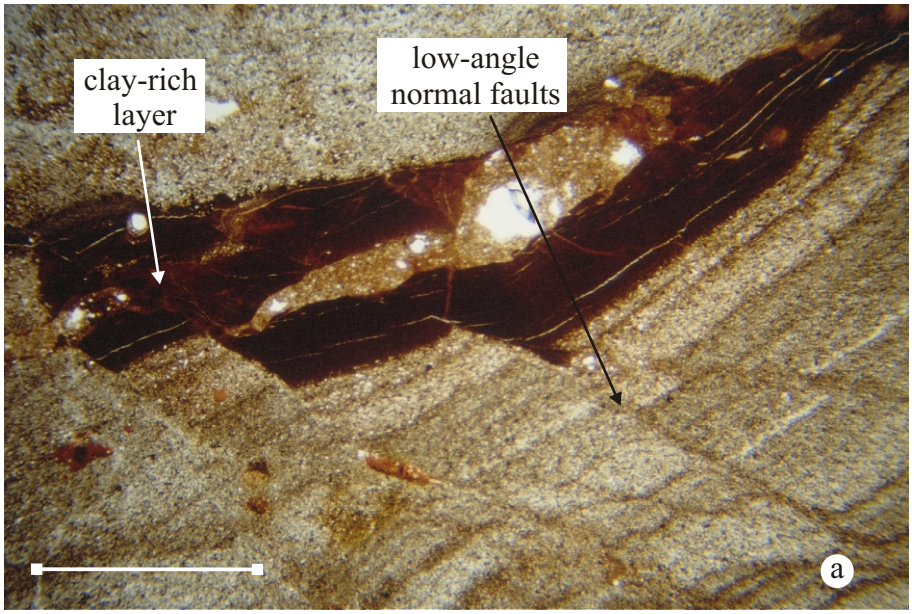

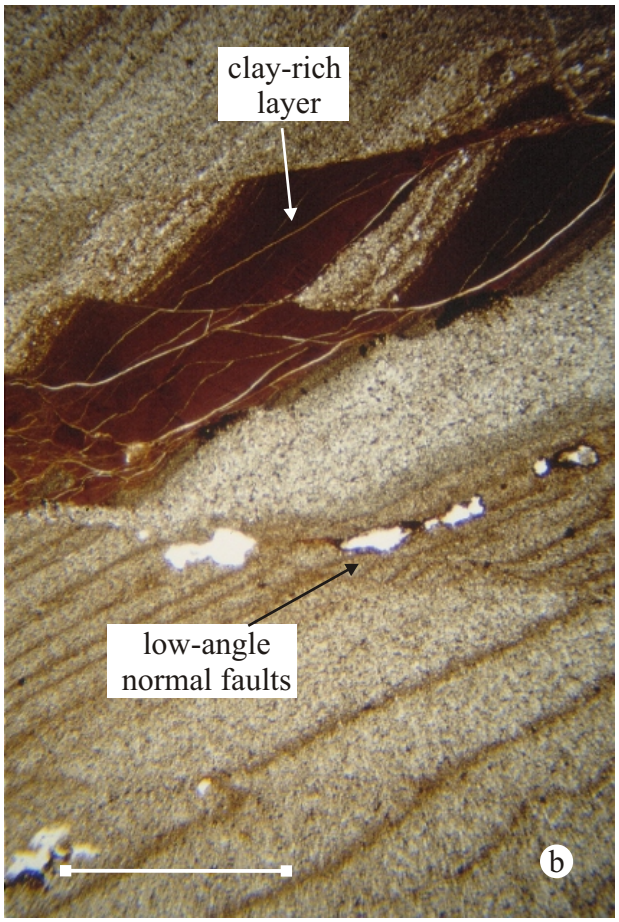

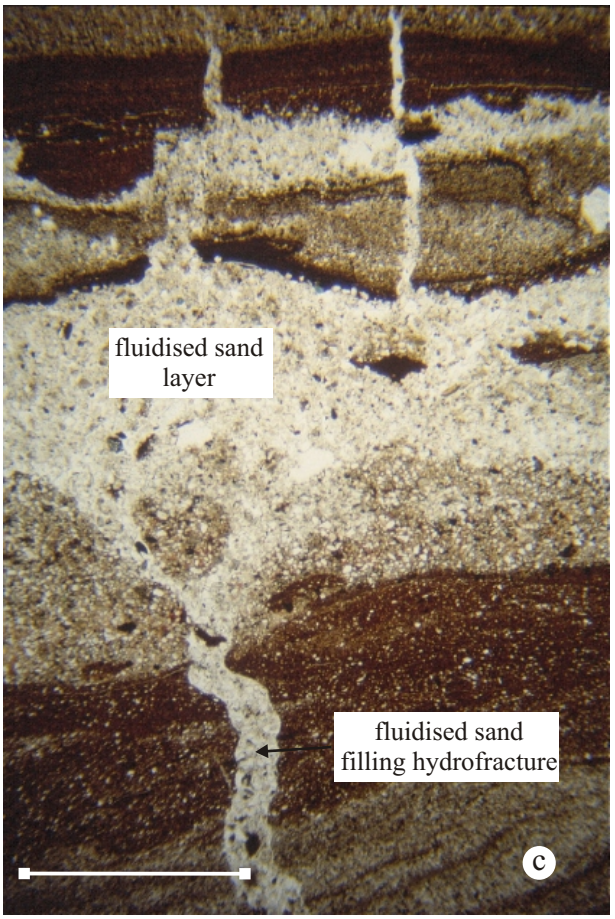

Plate 9. (a) low-angle faults deforming laminated silt and clay (Sample N2844, plane polarised light, scale bar = 4 mm). (b) low-angle faults deforming laminated silt and clay (Sample N2844, plane polarised light, scale bar = 4 mm). (c) fluidised sand forming discrete layer within laminated sediments. This layer is fed by a sand filled hydrofracture (Sample N2844, plane polarised light, scale bar = 4 mm).

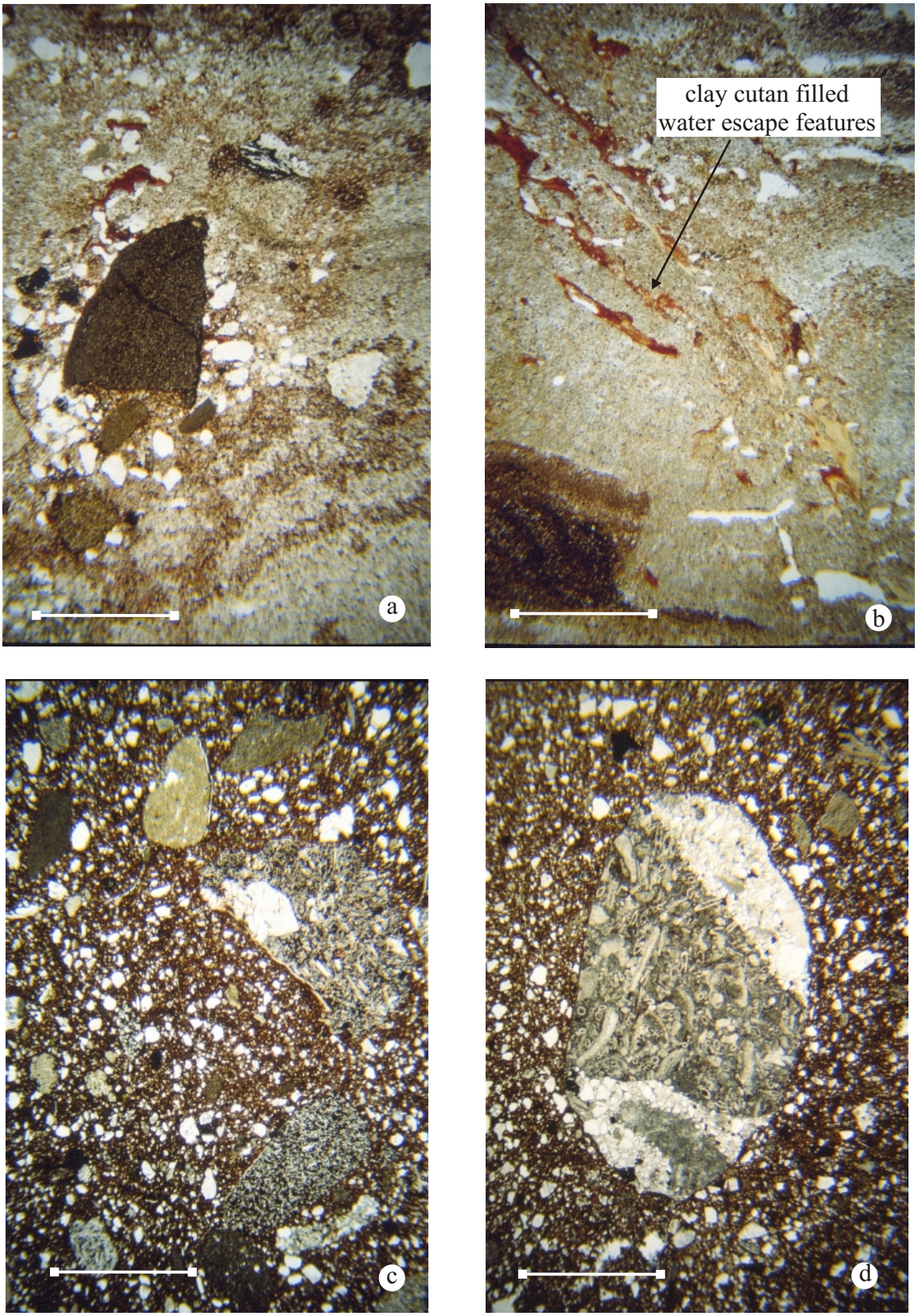

Plate 10. (a) patch of fluidised sand cross cutting laminated silt resulting in localised disruption of bedding (Sample N2846, plane polarised light, scale bar = 4 mm). (b) clay cutan filling late-stage water escape features (Sample N2846, plane polarised light, scale bar = 4 mm). (c) poorly sorted clast-rich diamicton (Sample N2848, plane polarised light, scale bar = 4 mm). (d) rounded bioclastic limestone clast in diamicton (Sample N2848, plane polarised light, scale bar = 4 mm).

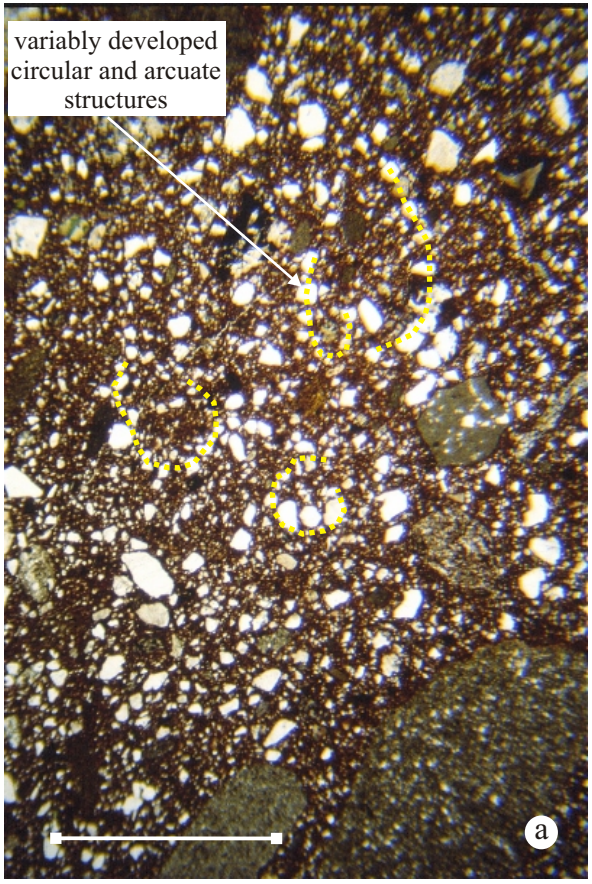

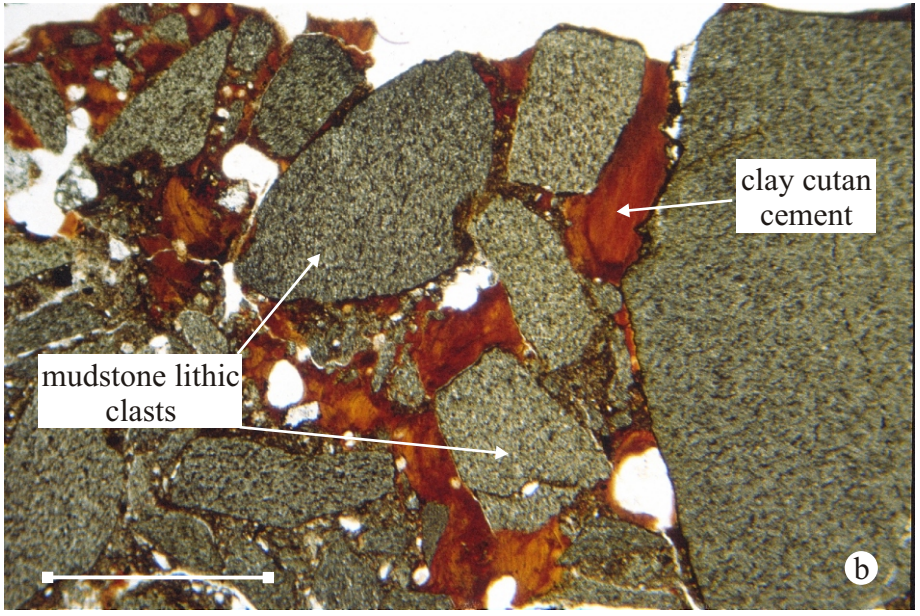

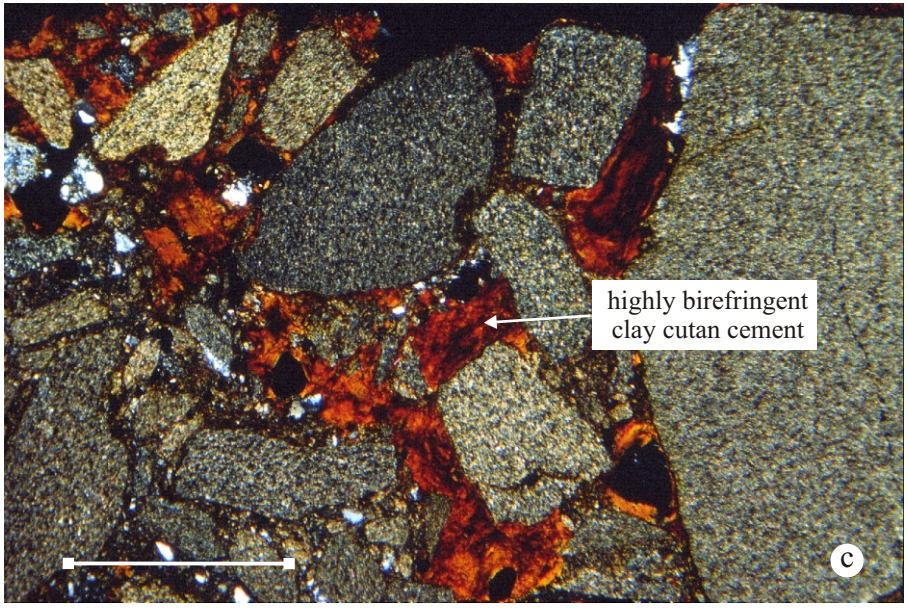

Plate 11. (a) variably developed circular and arcuate structures developed in matrix of diamicton (Sample N2848, plane polarised light, scale bar = 4 mm). (b) clay cutan cement in diamicton composed of angular to subangular mudstone rock fragments (Sample N2849, plane polarised light, scale bar = 4 mm). (c) highly birefringent clay cutan cement (Sample N2849, crossed polarised light, scale bar = 4 mm).

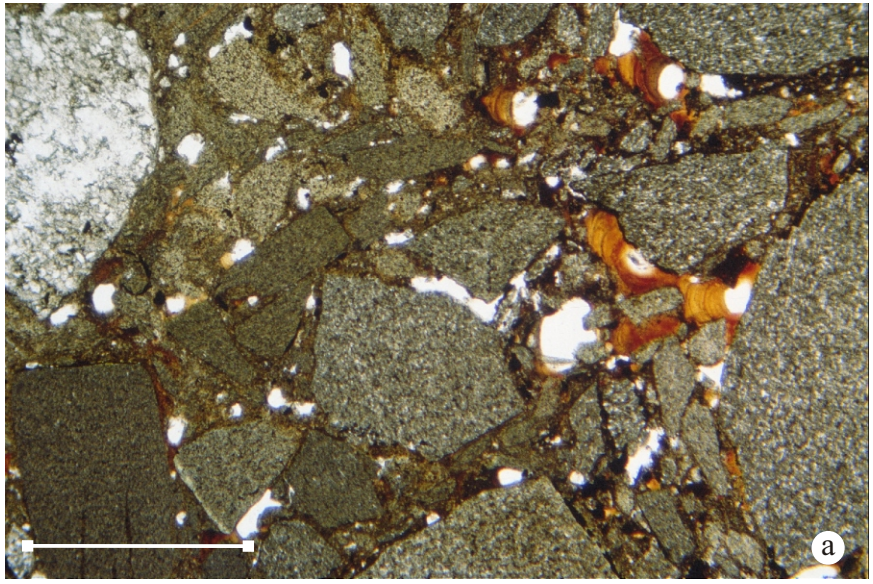

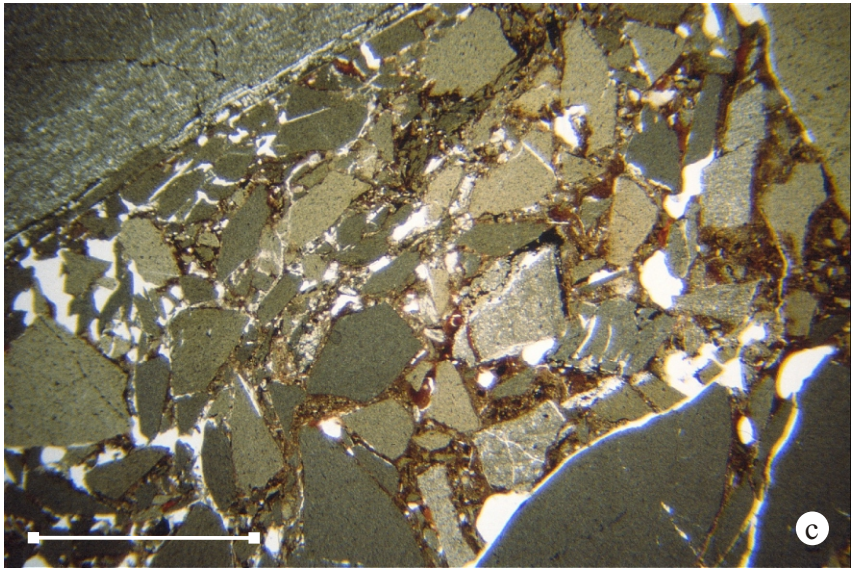

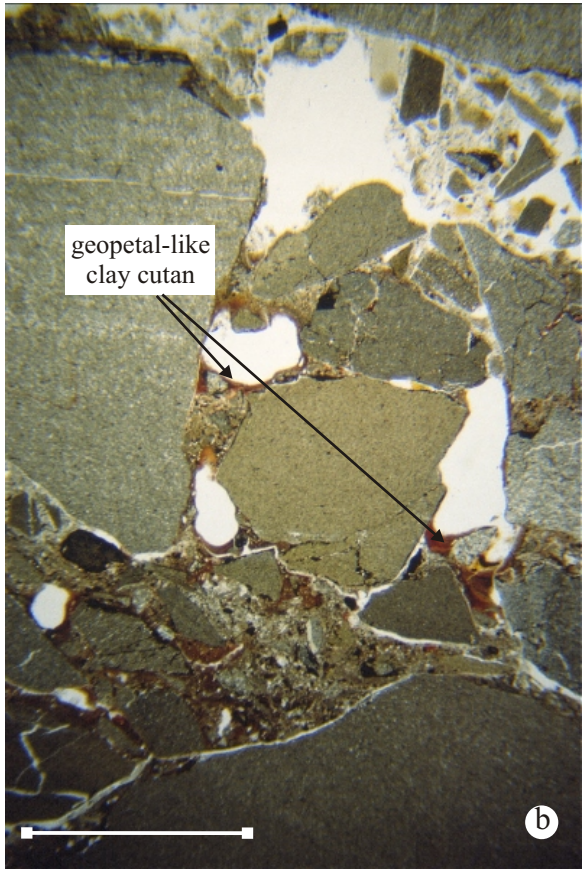

Plate 12. (a) lithic-rich diamicton in which the clasts are mainly composed of cleaved mudstone. Also note local development of clay cutan cement in areas lacking in matrix (Sample N2849, plane polarised light, scale bar = 4 mm). (b) geopetal-like clay cutan developed in pore spaced in lithic-rich diamicton (Sample N2850, plane polarised light, scale bar = 1 mm). (c) poorly sorted, lithic-rich diamicton (Sample N2850, plane polarised light, scale bar = 4 mm).

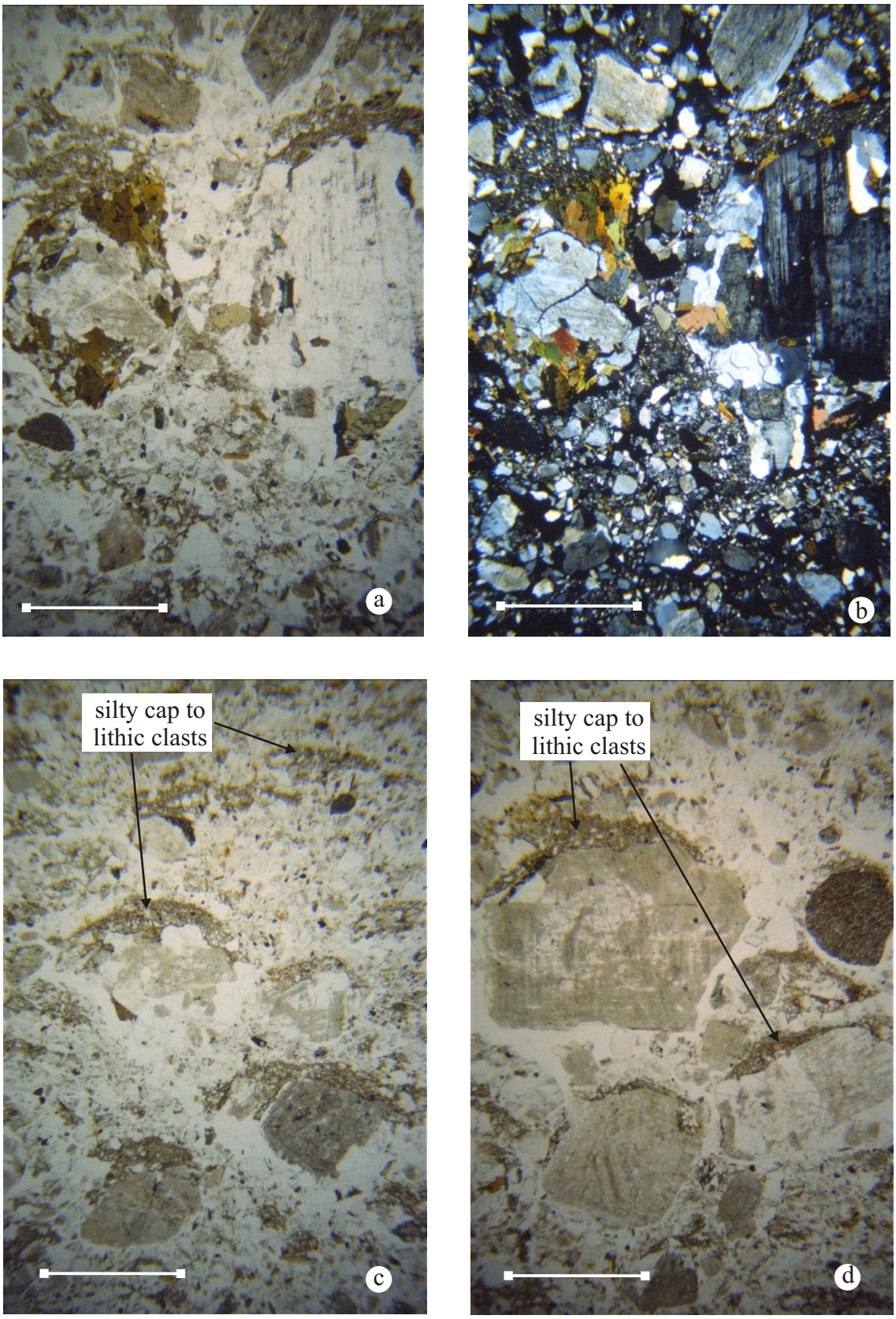

Plate 13. (a) and (b) poorly sorted gravelly diamicton composed almost entirely of material derived from the granitic to granodioritic Criffle-Dalbeattie granite intrusion (Sample N2851, plane and crossed polarised light, scale bar = 4 mm). (c) silty caps developed upon large lithic clasts (Sample N2851, plane polarised light, scale bar = 4 mm). (D) silty caps developed upon large lithic clasts (Sample N2851, plane polarised light, scale bar = 1 mm).